



# **Strength and Behavior of Reinforced Concrete Bridge Deck Slabs Overlaid with Ultra High- Performance Concrete**

A Thesis

Submitted to the Council of the Erbil Technical Engineering College at  
Erbil Polytechnic University in Partial Fulfillment of the Requirements  
for the Degree of Master of Science in Civil Engineering

By

**Siver Ibrahim Ismael**

B.Sc. in Technical Civil Engineering (2016)

Supervised by


**Dr. Ghafur H. Ahmed**

Erbil, Kurdistan

November 2022

## DECLARATION

I declare that the Master Thesis entitled: Strength and Behavior of Reinforced Concrete Bridge Deck Slabs Overlaid With Ultra-High Performance Concrete is my own original work, and hereby I certify that unless stated, all work contained within this thesis is my own independent research and has not been submitted for the award of any other degree at any institution, except where due acknowledgment is made in the text.

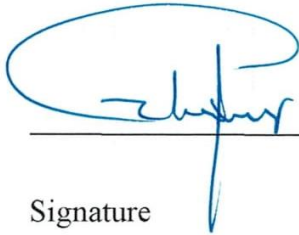
Signature: 

Student Name: Siver Ibrahim Ismael

Date: 19 / 1 / 2023

## SUPERVISOR CERTIFICATE

This thesis has been written under my supervision and has been submitted for the award of the degree of Master of Science in Civil Engineering with my approval as supervisor.



Signature

Dr. Ghafur H. Ahmed

Name

9.1.2023

Date

**I confirm that all requirements have been fulfilled.**

Signature:



Name: Asst. Prof. Dr. Bahman Omar Taha

Head of the Department of Technical Civil Engineering

Date: 10/01/2023

**I confirm that all requirements have been fulfilled.**

Signature:



Name: Asst. Lecture. Byad A. Ahmed

Postgraduate Office

Date: 10-1-2023

## EXAMINING COMMITTEE CERTIFICATION

We certify that we have read this thesis: Strength and Behavior of reinforced concrete bridge deck slabs overlaid with Ultra-High Performance Concrete and as an examining committee examined the student (Siver Ibrahim Ismael) in its content and what related to it. We approve that it meets the standards of a thesis in terms of scope and quality for the degree of Master in Civil Engineering.

Signature:

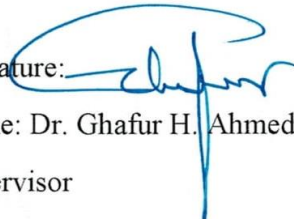


Name: Asst. Prof. Dr.  
Abdulhameed Abdullah Yaseen

Member

Date: 8/1/2023


Signature:



Name: Dr. Ghafur H. Ahmed  
Supervisor

Date: 9.1.2023

Signature:



Name: Prof. Dr. Sinan  
Abdulkhaleq Yaseen

Member

Date:

Signature:



Name: Prof. Dr. Ayad Zeki  
Saber Agha

Chairman

Date: 09-01-2023

Signature:



Name: Prof. Dr. Ayad Zeki Saber Agha  
Dean of Erbil Technical Engineering College

Date: 09-01-2023

## **DEDICATION**

To my beloved and first teachers, my parents, whose affections, love, encouragements, faithful prayers, and teaching me to trust in ALLAH, and believe in hard work, make me able to get such successful work.

To my both brothers and sisters, whose support, understanding, and believing me, make me proud of the work I do in my life.

My friend who encourages and supports me, and all the people in my life who touch my heart, I dedicate this research.

I am forever thankful

## LINGUISTIC REVIEW

I confirm that I have reviewed the thesis titled “Strength and Behavior of Reinforced Concrete Bridge Deck Slabs Overlaid with Ultra High-Performance Concrete (UHPC)” from the English linguistic point of view, and I can confirm that it is free of grammatical and spelling errors.



Signature

Date: September, 2022

## **ACKNOWLEDGEMENTS**

Praise be to Allah, the Gracious, the most Merciful, who has granted guidance and helped me to complete the present study. I would like to express my respect for my supervisor Dr. Ghafur H. Ahmed, for his appreciated guidance, suggestions, assessments, and support during my research efforts and coursework. I would like also to express my sincere appreciation, to the head and staff of the Erbil Polytechnic University-civil engineering department, and the staff of the structural laboratory of Salahaddin University, for their help and support during this work.

I would like to express my deepest gratitude to 77 Company, especially Mr. Hersh Xoshnaw the owner of the company, and their respected staff in general, as they opened the door of the company to accomplish my experimental work. I appreciate their support very much as they let me use their laboratory with all its components in the company, and provided me a special place to do my work. I will never forget this attitude and I wish them all the best.

Deep thanks to my best friends for their unforgettable help during experimental works, and testing, and all relatives who helped in the completion of this work, especially my aunt's son Mr. Hoshmand Q.L. who helped me in all experimental stages sincerely.

I have a special thanks to my parents and brothers for their continual support. Without them, I would have never returned to school and never succeeded.

Siver Ibrahim Ismael

September 4, 2022

## ABSTRACT

Ultra-High Performance Concrete (UHPC) has appeared in the past two decades. It is a relatively new type of concrete that exhibits mechanical properties that are far superior to conventional concrete. All around the world, many bridges have been built but are structurally deficient before reaching their design services. Because bridges are subject to high live loads due to traffic volume, they are usually overlaid with materials like NSC, bituminous, etc., which cause damage due to their weak resistance to tension force and permeability. Generally, deterioration starts with cracking on the top surface of bridge decks; over time, this damage goes through the substructures, and those structurally deficient bridges require a very high budget to replace. Applying a thin layer of UHPC on top of normal concrete bridge decks has been proposed as a potential treatment in a prior study. Because UHPC has a high compressive and tensile strengths, which mainly result from the addition of steel fibers that enhance durability and long-term stability properties.

In this study seventeen simply supported reinforced concrete flat plate slabs 1500x500x140 mm were casted and tested, loaded through two-line loads along the short span direction, to investigate the strength and behavior of reinforced concrete bridge deck slabs overlaid with UHPC.

The main variables studied in this investigation were:

- Overlay thickness 20-50 mm.
- Reinforced UHPC overlay with reinforcement ratio 0-1.31 %.
- Interface patterns rough, horizontal groove, vertical groove, cross-hatch groove, and diagonal groove.
- Substrate material compressive strength 20-40 MPa.



- Three types of material evaluated for overlay application NSC, HPC, and UHPC.
- The addition of a mechanical connector with a rough surface pattern evaluated zero until three rows of an anchor.

Results indicated that using UHPC overlay can double the ultimate strength carried by the composite slab compared with the HPC overlay. The thin layer of UHPC as the wearing surface increases the life of the existing structure and reduces the maintenance cost twice compared with HPC. Also, the addition of embedded rebar at the UHPC layer tends to conclude shear stress at the interface and normal stress at the UHPC overlay by about 30 %. Moreover, ultimate strength increases with an increase in the degree of interface roughness between two layers of concrete, and an adequate bond can be attained with all interface patterns. The ultimate strength increases with an increase in substrate material compressive strength due to adhesion and cohesion properties at the interface. For bridge deck slabs overlaid with UHPC the mode of failure is governed through the substrate while the adequate bond strength is provided by good surface preparation, otherwise, top concrete crush and splitting of the composite structure take place with HPC and NSC. Test results also indicated that the addition of a mechanical connectors with rough surface preparation leads to an increase strength by 50 %.

With the use UHPC overlay, the characteristics of the slab were entirely enhanced. The central deflection increased by about 50% compared with HPC. Overlay failure never happened with UHPC overlay. The concrete compressive and tensile strains are increased by a considerable amount (for the same load level). UHPC overlay with proper surface preparation leads to composite structure behaving monolithically and failure load goes through the substrate.

## CONTENTS

1	CHAPTER ONE.....	1
1.1	Introduction.....	1
1.2	Bridge Deck Slabs Definition.....	1
1.3	Bridge Deck Slabs Overlay.....	2
1.4	The Value of UHPC in Overlay.....	4
1.5	Thesis Objectives.....	7
2	CHAPTER TWO.....	8
2.1	Review of Literature.....	8
2.2	Bridge Deck Slabs Guidelines.....	8
2.2.1	AASHTO Design Guidelines for Bridge Deck Slabs.....	8
2.2.2	Minimum Thickness and Reinforcement of One-Way Solid Slabs.....	9
2.3	Bridge Deck Slabs Deterioration and Rehabilitation.....	11
2.3.1	Bridge Deck Slabs Deterioration.....	11
2.3.1.1	General Region and Mechanism of Failure.....	12
2.3.2	Bridge Deck Slabs Rehabilitation Strategies.....	13
2.4	A comprehensive explanation of UHPC.....	15
2.4.1	Definitions.....	15
2.4.2	Development Of UHPC.....	15
2.4.3	General Composition of UHPC.....	19
2.4.4	UHPC Families.....	21
2.4.5	Mechanical Properties of UHPC.....	22
2.4.5.1	Compressive Strength.....	22
2.4.5.2	Tensile Strength.....	25
2.4.5.3	Modulus of Elasticity.....	28
2.4.5.4	Poisson's Ratio.....	29
2.4.5.5	Coefficient of Thermal Expansion (CTE).....	30
2.4.5.6	Durability Properties Of UHPC.....	30
2.4.6	Long Term Stability Properties of UHPC.....	31

2.4.6.1	Creep.....	31
2.4.6.2	Shrinkage .....	32
2.4.7	Curing Regimes and Effects on the Properties of UHPC...33	
2.4.8	The Effect of Steel Fiber on the Mechanical Properties of UHPC .....	34
2.4.8.1	Compressive Strength.....	35
2.4.8.2	Tensile Strength.....	35
2.4.8.3	Bending Strength .....	35
2.4.8.4	Flowability.....	36
2.4.9	Advantages and Disadvantages Of UHPC .....	36
2.4.9.1	Advantages Of UHPC .....	36
2.4.9.2	Disadvantages Of UHPC.....	37
2.5	Bridge Deck Slabs Overlay with UHPC.....	37
2.5.1	Bridge Deck Slabs Overlay Guidelines.....	37
2.5.2	Overlay Thickness .....	38
2.5.3	Addition a Layer of Steel with an Overlay.....	38
2.5.4	Bond Strength of UHPC with Substrate.....	40
2.5.4.1	Surface Preparation.....	40
2.5.4.2	Mechanical Connectors .....	42
2.5.4.3	Epoxy Coating .....	44
2.6	Strengthening Methods .....	45
2.7	Summarization .....	52
3	CHAPTER THREE .....	53
3.1	Experimental Program .....	53
3.2	Concrete Compositions and Materials .....	53
3.2.1	Concrete Types .....	53
3.2.1.1	Normal Strength Concrete (NSC) .....	53
3.2.1.2	High Performance Concrete (HPC).....	54
3.2.1.3	Ultra-High Performance Concrete (UHPC) .....	54
3.2.2	Materials: .....	55
3.2.2.1	Cement.....	55

3.2.2.2	Silica Fume .....	56
3.2.2.3	Normal Sand .....	57
3.2.2.4	Fine Sand .....	58
3.2.2.5	Coarse Aggregate .....	58
3.2.2.6	Superplasticizer .....	59
3.2.2.7	Water.....	59
3.2.2.8	Steel Fiber.....	59
3.2.2.9	Steel Reinforcing Bar .....	60
3.3	Mix Details.....	60
3.3.1	Mix Proportions.....	60
3.3.2	Mixing Procedure .....	64
3.4	Selection of Bridge Deck Slab Specimen .....	66
3.5	Variables and Details .....	68
3.6	Slab Specimen Molds.....	71
3.7	Casting of Specimens.....	72
3.8	Curing Processes .....	73
3.9	Test Measurements and Instruments.....	74
3.9.1	Load Measurements.....	74
3.9.2	Deflection Measurements .....	75
3.9.3	Concrete Strain Measurements.....	76
3.10	Age of Concrete Specimens at Testing.....	77
3.11	Testing Procedure for Slab Specimens .....	78
3.12	Properties of Specimen’s Concrete Mixes.....	79
3.12.1	Compressive Strength.....	79
3.12.2	Splitting Tensile Strength .....	80
3.12.3	Flexural Strength .....	80
3.12.4	Bond Strength.....	80
3.12.5	Permeability Strength.....	82
4	CHAPTER FOUR .....	83
4.1	Results and Discussion .....	83
4.2	UHPC Properties and Comparisons.....	83

4.2.1	Compressive Strength.....	83
4.2.1.1	Trial Mixes .....	83
4.2.1.2	Control Mixes Used for Slabs .....	86
4.2.2	Splitting Tensile Strength.....	87
4.2.3	Flexural Strength .....	88
4.2.4	Bond Strength.....	89
4.2.5	Permeability.....	91
4.3	Control Specimens .....	92
4.4	Reinforced Concrete Flat Plate Specimens.....	92
4.4.1	UHPC Thickness .....	95
4.4.2	Reinforcement Ratio in UHPC Layer .....	96
4.4.3	Substrate Surface Patterns .....	98
4.4.4	Substrate NSC Compressive Strength.....	100
4.4.5	Overlay Compressive Strength.....	102
4.4.6	Mechanical Connectors .....	103
4.5	Load-Central Deflection Relationship .....	104
4.6	Load-Concrete Strains Relationships.....	110
4.6.1	Concrete Compressive Strains.....	111
4.6.2	Concrete Tensile Strains.....	112
4.7	Crack Patterns and Modes of Failure.....	112
5	CHAPTER FIVE .....	123
5.1	Statistical Analysis .....	123
5.2	Theoretical Analysis Design Equation .....	123
5.2.1	Design of Concrete Structures.....	123
5.3	Analysis of Proposed Empirical Equation .....	126
5.4	Regression Analysis.....	129
5.4.1	Comparison of Practical Results with Theoretical Analysis Design Equation and Prediction Equation Analysis.....	130
6	CHAPTER SIX.....	131
6.1	Conclusion .....	131
6.2	Recommendations.....	134

## LIST OF FIGURES

Figure 1.1: 3D view of NSC slab overlay with UHPC .....	4
Figure 1.2: Examples of bridge deck slabs deterioration .....	4
Figure 1.3: Basic constituents of UHPC.....	6
Figure 2.1: Slab section details.....	9
Figure 2.2: Strain distribution and net tensile strain in a solid one-way slab member.....	10
Figure 2.3: In the left-hand shows than UHPC overlay for protective and the right-hand shows the UHPC for protective and resistance.....	14
Figure 2.4: Basic shapes of steel fiber.....	20
Figure 2.5: Represent the tensile behavior of UHPC .....	26
Figure 2.6: Particle packing density, left hand for conventional concrete and right hand for UHPC.....	30
Figure 2.7: The effect of curing regimes on long-term creep .....	32
Figure 2.8: Ultimate bending resistance section analysis.....	39
Figure 2.9: Shear failure mechanism of bridge deck overlaid with R-UHPC.....	40
Figure 2.10: Lightly ground 0.05 mm (far left), grooved texture 0.90 mm (left), grooved-cross-hatch texture 1.60 mm (right), rough texture 2.80 mm (far right) .....	41
Figure 2.11: Mechanical behavior of a screw anchor under tensile (a) and shear (b) stresses .....	43
Figure 2.12: (a) Schematic illustration of the test specimen. (b) Test setup in Instron machine .....	45
Figure 2.13: Shear stud layout, Right-hand 3-stud, and left hand 6-stud.	48
Figure 3.1: Grading of Normal Sand with ASTM C33 limits.....	57
Figure 3.2: Grading of Gravels with ASTM C33 limits.....	59
Figure 3.3: Materials used: Cement, Sand, Silica fume, Grout, Superplasticizer admixture and Steel fiber.....	64
Figure 3.4: Prototype of Bridge Deck Slab System and Selected Specimen.....	67
Figure 3.5: Dimensions and Reinforcement of Typical Specimen .....	67
Figure 3.6: Steel layer embedded into the substrate concrete through the steel bolt and washer.....	69
Figure 3.7: Substrate surface textures: (a) Rough, (b) Horizontal, (c) Vertical, (d) Cross Hatch and (e) Diagonal Groove.....	69

Figure 3.8: Anchor bolt embedded into the substrate concrete, (Left: three rows at 228 mm) and (Right: two rows at 228 mm) .....	71
Figure 3.9: Slab mold used in this study .....	71
Figure 3.10: Casting substrate concrete.....	72
Figure 3.11: Casting overlay concrete .....	73
Figure 3.12: Water tank for slab specimens .....	74
Figure 3.13: Details of the testing machine (Salahuddin university laboratory).....	75
Figure 3.14: Dial gauge .....	76
Figure 3.15: Locations of concrete strain gauges in slab specimens .....	76
Figure 3.16: Strain gauge and data logger.....	77
Figure 3.17: Loading arrangement of the tested slabs.....	79
Figure 3.18: Half of cylinder filled with NSC at a 60-degree angle .....	81
Figure 3.19: Types of substrate texture: (a) Rough, (b) Horizontal groove, (c) Vertical groove, (d) Cross hatch and (e) Diagonal groove .....	82
Figure 4.1: Compressive Strength of Control Mixes vs. Age .....	87
Figure 4.2: Failure region for (a) Rough, (b) Diagonal, (c) Cross-Hatch, (d) Horizontal, and (e) Vertical .....	90
Figure 4.3: The result of water permeability testing; (a) NSC, (b) HPC and (c) UHPC .....	91
Figure 4.4: the observed failure load of the tested slabs .....	95
Figure 4.5: Ultimate failure load versus UHPC thickness, Group (1) .....	96
Figure 4.6: Ultimate failure load versus UHPC reinforcement ratio, Group (2).....	98
Figure 4.7: Ultimate failure load versus Substrate surface patterns, Group (3).....	100
Figure 4.8: Ultimate failure load versus substrate NSC Compressive strength, Group (4).....	101
Figure 4.9: Delamination in a part width of S20 slab .....	101
Figure 4.10: Ultimate failure load versus overlay compressive strength, Group (5).....	103
Figure 4.11: Failure mode of composite specimens: (a) Overlay $f_c'20\text{MPa}$ , (b) Overlay $f_c'80\text{MPa}$ and (c) Overlay $f_c'125\text{MPa}$ .....	103
Figure 4.12: Ultimate failure load versus mechanical connector, Group (6).....	104
Figure 4.13: Load-Central Deflection Relationship of Group (1), effect of overlay thickness .....	107
Figure 4.14: Load-Central Deflection Relationship of Group (2), the effect of UHPC reinforcement ratio .....	108

Figure 4.15: Load-Central Deflection Relationship of Group (3), the effect of different interface patterns .....	108
Figure 4.16: Load-Central Deflection Relationship of Group (4), the effect of different substrate compressive strength.....	109
Figure 4.17: Cracking in the composite specimens at the ultimate failure load and deflection.....	109
Figure 4.18: Load-Central Deflection Relationship of Group (5), the effect overlay compressive strength .....	110
Figure 4.19: Load-Central Deflection Relationship of Group (6), the effect of mechanical connector.....	110
Figure 4.20: Control mold Crack pattern .....	114
Figure 4.21: TH20 mold Crack pattern .....	115
Figure 4.22: TH40 mold Crack pattern .....	115
Figure 4.23: TH50 mold Crack pattern .....	116
Figure 4.24: R-UHPC5 mold Crack pattern.....	116
Figure 4.25: R-UHPC10 mold Crack pattern.....	117
Figure 4.26: R-UHPC15 mold Crack pattern.....	117
Figure 4.27: HG mold Crack pattern.....	118
Figure 4.28: VG mold Crack pattern.....	118
Figure 4.29: CH mold Crack pattern .....	119
Figure 4.30: DG mold Crack pattern.....	119
Figure 4.31: S21 mold Crack pattern .....	120
Figure 4.32: S40 mold Crack pattern .....	120
Figure 4.33: O30 mold Crack pattern.....	121
Figure 4.34: O80 mold Crack pattern.....	121
Figure 4.35: 2RA mold Crack pattern .....	122
Figure 4.36: 3RA mold Crack pattern .....	122
Figure 5.1: Ultimate failure moment data system .....	125
Figure 5.2: Comparison of ultimate and nominal moment of slabs .....	125
Figure 5.3: The comparison between this study's experimentation result and the proposed empirical equation.....	128
Figure 5.4: The comparison between the experimental results of some chosen slabs from Appendix B and the proposed empirical equation ...	129



## LIST OF TABLES

Table 2-1: Minimum thickness of solid one-way slabs.....	10
Table 2-2: Mechanism of interfacial debonding due to direct and indirect loads .....	13
Table 2-3: Composition of 80 MPa concrete compressive strength .....	16
Table 2-4: Ductal composition of UHPC .....	19
Table 2-5: The relation between elastic modulus and compressive strength.....	29
Table 2-6: Types of curing .....	33
Table 2-7: Coefficients $cr$ , $\mu$ , $K1$ , $K2$ and $\beta c$ in terms of interfacial roughness according to Model Code 2010 .....	43
Table 2-8: Summary of strengthening Bridge Deck slabs with an overlay .....	49
Table 3-1: Chemical Analysis of Cement .....	55
Table 3-2: Physical properties of the cement .....	56
Table 3-3: Physical properties of the Silica fume .....	56
Table 3-4: Chemical Analysis of Silica fume.....	57
Table 3-5: Grading of Aggregates with ASTM C33 Limits .....	58
Table 3-6: Properties of the Reinforcing Steel Bar .....	60
Table 3-7: Trial mixes for UHPC overlay .....	63
Table 3-8: Trial mixes for the substrate material .....	63
Table 3-9: Trial mixes for HPC overlay .....	64
Table 3-10: The Characteristics of the Tested Slabs.....	70
Table 4-1: Trial mixes for UHPC overlay .....	85
Table 4-2: Trial mixes for the substrate material (NSC).....	85
Table 4-3: Trial mixes for HPC overlay .....	86
Table 4-4: Control Mixes specifications .....	87
Table 4-5: Splitting Tensile Strength of Control Mixes (90 days).....	88
Table 4-6: Flexural Strength of Control Mixes (90 days) .....	89
Table 4-7: Average maximum failure load, shear stresses and normal stresses from slant-shear test .....	89
Table 4-8: Mechanical Properties of Control Specimens.....	93
Table 4-9: Test results of the slab specimens .....	94
Table 5-1: Proposed empirical equation data limits summary .....	128
Table 5-2: Comparison between practice results and designed equation .....	130

## NOTATIONS

Symbol	Meaning
$A_s$	Web (substrate) steel area, $mm^2$
$A_{sf}$	Flange (overlay) steel area, $mm^2$
$A_{st}$	longitudinal steel reinforcement, $mm^2$
$F_{Utd}$	UHPC Force, $kN$
$F_{ccd}$	Concrete Force, $kN$
$F_{sUd}$	UHPC's steel Force, $kN$
$F_{scd}$	Concrete's steel Force, $kN$
$G_{FU}$	High specific fracture energy
$K_1$	Interaction coefficient for tensile force activated in the connectors
$M_n$	The total nominal resisting moment, $N.mm$
$M_{n1}$	Flange (overlay) nominal moment, $N.mm$
$M_{n2}$	Web (substrate) nominal moment, $N.mm$
$M_u$	Ultimate failure moment, $N.mm$
$O_{Rr}$	Overlay Reinforcement Ratio %
$O_{f'c}$	Overlay UHPC compressive strength, $MPa$
$O_{th}$	Overlay UHPC thickness, $mm$
$P_{exp.}$	Experimental flexural load at failure, $kN$
$P_{pred.}$	Prediction flexural load at failure, $kN$
$S_{Rr}$	Substrate Reinforcement Ratio %
$S_{f'c}$	Substrate NSC Compressive strength, $MPa$
$S_{th}$	Substrate thickness, $mm$
$V_{RC}$	Ultimate Shear Resistance concrete, $kN$
$V_{RS}$	Ultimate Shear Resistance steel, $kN$
$V_{Ru}$	Ultimate Shear Resistance UHPC, $kN$
$V_f$	Volume of fiber in joint
$V_{nh}$	Nominal horizontal shear strength, $kN$
$V_u$	External shear strength, $kN$
$W_{Ut,max}$	maximum crack opening, $mm$
$c_r$	The coefficient for aggregate interlocking
$f_{Ute}$	Elastic limit strength, $MPa$
$f_{Utud}$	UHPC stress, $MPa$
$f'_c, f_{cyl.}$	Compressive strength of concrete cylinders, $MPa$
$f_{cd}$	Concrete stress, $MPa$

$f_{ck}$	Characteristic compressive strength of concrete
$f_{ct}$	Splitting tensile strength of concrete, <i>MPa</i>
$f_{cu}$	Compressive strength of concrete cubes, <i>MPa</i>
$f_r$	Flexural strength of concrete, <i>MPa</i>
$f_{sUd}$	UHPC's steel stress, <i>MPa</i>
$f_y$	Yield stress of steel reinforcement, <i>MPa</i>
$f_{yd}$	Design yield strength, <i>MPa</i>
$f_{yf}$	Yield strength of flange (overlay) steel, <i>MPa</i>
$f_{yw}$	Yield strength of web (substrate) steel, <i>MPa</i>
$h_f$	Height of flange (overlay layer depth), <i>mm</i>
$\beta_c$	Coefficient for the strength of the compression strut
$\epsilon_U$	strain-hardening domain, <i>mm/mm</i>
$\epsilon_c$	Concrete strain, <i>mm/mm</i>
$\epsilon_{ct}$	Creep Strain at that time
$\epsilon_{sc}$	Concrete's steel strain, <i>mm/mm</i>
$\epsilon_{su}$	UHPC's steel strain, <i>mm/mm</i>
$\epsilon_u$	UHPC strain, <i>mm/mm</i>
$\sigma_n$	Compressive stress in the joint due to external normal forces
$\tau_{Rd}$	Mechanical connection, <i>MPa</i>
$\tau_a$	Average shear stress, <i>MPa</i>
$\phi$	Strength reduction factor for shear 0.75
E	Modulus of Elasticity, <i>MPa</i>
$\mu$	Friction coefficient
$\rho$	The ratio of the reinforcing steel, %

## ABBREVIATIONS

<b>Symbol</b>	<b>Meaning</b>
2RA	Two rows of anchor at interface
3RA	Three rows of anchor at interface
CH	Cross Hatch interface pattern shape
COV	Coefficient of variation
DG	Diagonal Groove interface pattern shape
FRC	Fiber-reinforced concrete
HG	Horizontal Groove interface pattern shape
HPC	High Performance Concrete
HRWR	High Range Water Reducer
LMC	Latex Modified Concrete
LSDC	Low Slump Dense Concrete
LVDT	Linear Variable Differential Transformer
LWS	Light Weight Sand
MMC	Microsilica Modified Concrete
MMC-FA	Microsilica modified concrete with Fly ash
MSC	Microsilica Concrete
NSC	Natural Strength Concrete
O20	20 MPa overlay compressive strength
O80	80 MPa overlay compressive strength
r	Correlation coefficient
RCPT	Rapid Chloride Permeability Test
R-UHPC10	Reinforced UHPC with 5 mm rebar at 10 cm spaces in both direction
R-UHPC15	Reinforced UHPC with 5 mm rebar at 15 cm spaces in both direction
R-UHPC5	Reinforced UHPC with 5 mm rebar at 5 cm spaces in both direction
S21	21 MPa substrate NSC compressive strength
S40	40 MPa substrate NSC compressive strength
SD	Standard deviation
SST	Slant Shear Test
TH20	UHPC overlay thickness 20 mm
TH40	UHPC overlay thickness 40 mm
TH50	UHPC overlay thickness 50 mm
UHPC	Ultra-High Performance Concrete
VG	Vertical Groove interface pattern shape

# **1 CHAPTER ONE**

## **1.1 Introduction**

Many bridges or slabs have been constructed throughout the world, but before they receive design services, they are structurally deficient due to exposure to high live loads from heavy traffic. Additionally, it would be expensive to repair any structurally damaged bridges and would be urgently needed to create solutions that can be used safely and quickly in practice in addition to being inexpensive and durable. Bridge deck overlay technologies will eliminate the mentioned problems and increase the lifespan of bridges. There are many different types of material for overlay applications, but over the years, all studies have argued that UHPC is the best one and can address all of the concerns in the past. Bridge deck slabs deterioration frequently begins with cracking on the top surface; therefore, UHPC overlay is frequently used to increase the bridge's lifespan by protecting it from water and chemical entry and producing a strong wearing surface. A sufficient bearing capacity that is suitable for the loading of the bridge deck must also be provided by the overlay. When the UHPC overlay concrete reaches its maximum strength and resists crack propagation, these characteristics will be met. This chapter discusses bridge deck slabs and the materials that are used for overlays, along with the importance of UHPC for overlay compared with others.

## **1.2 Bridge Deck Slabs Definition**

The Bridge deck slab is one of the basic loads carrying components of a rectangular layout which is supported directly on the substructures or

perpendicular to the support component, the supporting components are made of steel or concrete as shown in Figure 1.1.

Deck slab is used as a base for the roadway, railway, pedestrian walkaway, and many other facilities. While designing a bridge, it is very important to give significant attention to decks to obtain good serviceability, safety, appearance, and many other properties because the deck slabs have an important role in providing the aesthetic appearance of the bridge. Furthermore, structurally it has the advantage that reducing deflection and resistance to the moment greatly. Also, the main challenges in T section bridges are the action of a shear force which cracks can develop in the web and flange due to the changes in cross-section. In addition, the durability of bridge deck slabs is depending on the slab thickness, reinforcement cover, and drainage system (Gunavathy and Indumathi, 2011).

### **1.3 Bridge Deck Slabs Overlay**

Decks have to be overlaid with a suitable material to obtain a wearing surface as presented in Figure 1.1 which protects against water or ions ingress that in result may let to corrosion of steel occur. Over a long decade there exist two basic types of overlay material an asphalt overlay and a thin polymer overlay. Although asphalt overlays are economical, their short life and continuous maintenance let the researchers think about another type of overlay material. Also, polymer overlays are effective in reducing corrosion but it isn't suited for small bridges with low traffic where maintenance work is more challenging. Furthermore, they may not be effective if chloride contamination is already present. That is why a thin bonded and desired slope UHPC overlay has been developed first in France

and solved all of the deficiencies that were present in other types of overlay (Graybeal et al., 2020, Wibowo and Sritharan, 2018).

Usually, the most common bridge deck deterioration occurs at cracking places that let penetrate water or ion down then causing corrosion of steel rebars. Further damage occurs due to freeze-thaw cycles and wheel dynamic loads. Figure 1.2 provides examples of bridge deck slab deterioration caused by the use of the wrong overlaying material, and the most common three regions of failure according to Hussein et al. (2016) opinion and also well-known globally are identified below:

- Failure at the bond line
- Failure in substrate
- Failure in overlay

It is important to consider proper substrate surface preparation while using UHPC to overlay bridge deck slabs. According to Muñoz and Ángel (2012) the bond strength effected by the following points, and the most of failure cases occur in the concrete substrate if enough bond strength is served by superior surface preparation:

- The interface angle significantly impacts a bond strength; a higher angle from the horizontal axis will result in increased bond strength, and sixty degrees will be adequate.
- Saturated conditions of substrate concrete increase bond strength but dry conditions negatively affect the bonding strength.
- The age of the bond affects its strength, from the direct tensile strength shows that the bonding strength at 10-11 days is greater than at 7 and 28 days given by ACI 318R-19 (2019).

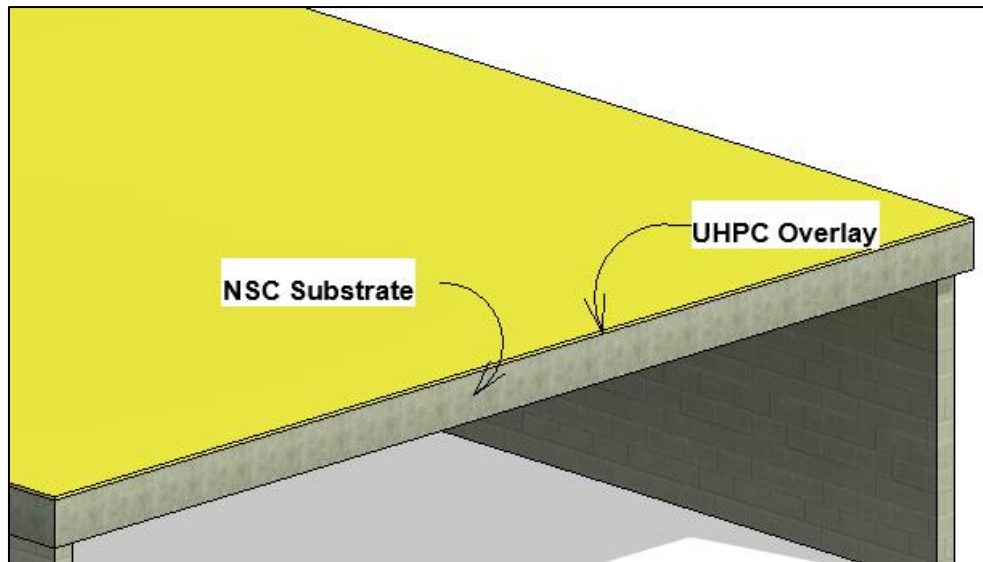


Figure 1.1: 3D view of NSC slab overlay with UHPC



Figure 1.2: Examples of bridge deck slabs deterioration

#### 1.4 The Value of UHPC in Overlay

With the advance in the knowledge, UHPC has developed and replaced all of the deficiencies that were present in other types of concrete. The properties of UHPC are greatly superior and surpassed all expectations compared to the properties of conventional concrete. In modern



construction, UHPC is favorable to construct beyond usual design permission. This new generation of concrete gives the ability to construct structural members with a longer span, lighter in weight, and larger in size. In addition, it can be used for an aesthetic appearance with a cast in irregular shapes or the high rise of a building due to its special workability (Wu et al., 2018, Bajaber and Hakeem, 2021).

The basic components of UHPC assist to obtain 100 MPa compressive strength at three days according to Stefaniuk (2020) which consist of; Portland cement, fine-grained sand, silica fume, superplasticizer, water, and steel fiber as presented in Figure 1.3:

The screened natural sand meeting sieve specifications is a basic load-carrying capacity material component of UHPC (Schmidt and Fehling, 2004). Ordinary Portland cement is a basic binder material in the UHPC with a ratio of twice the amount compared to the conventional concrete (Bajaber and Hakeem, 2021). The second basic binder is silica fume with 5-20 % to the weight of cement. It combines with a superplasticizer and provides dark color to concrete, and fills the voids. UHPC contains low w/c ratio compared to NSC, it is useful to increase density and reduce porosity but has influence on the workability negatively, that is why the addition of superplasticizer admixture is useful to plasticize concrete and increase workability (Mishra and Singh, 2019).

Schmidt and Fehling (2004) discussed that due to the low w/c ratio, high-temperature curing of more than 200 is necessary to hydrate the remaining cement particles and achieve more than 200 MPa of concrete compressive strength. The addition of steel fiber in concrete has a low effect on compressive strength rather than affects increasing tensile strength by providing resistance for the generation and propagation of crack (Mishra and Singh, 2019).

The following advantages make UHPC a desirable material for overlay application: (Haber et al., 2017)

- Very low permeability
- Very good freeze-thaw resistance
- Will completely replace conventional solutions
- Good bond to concrete
- Good abrasion resistance

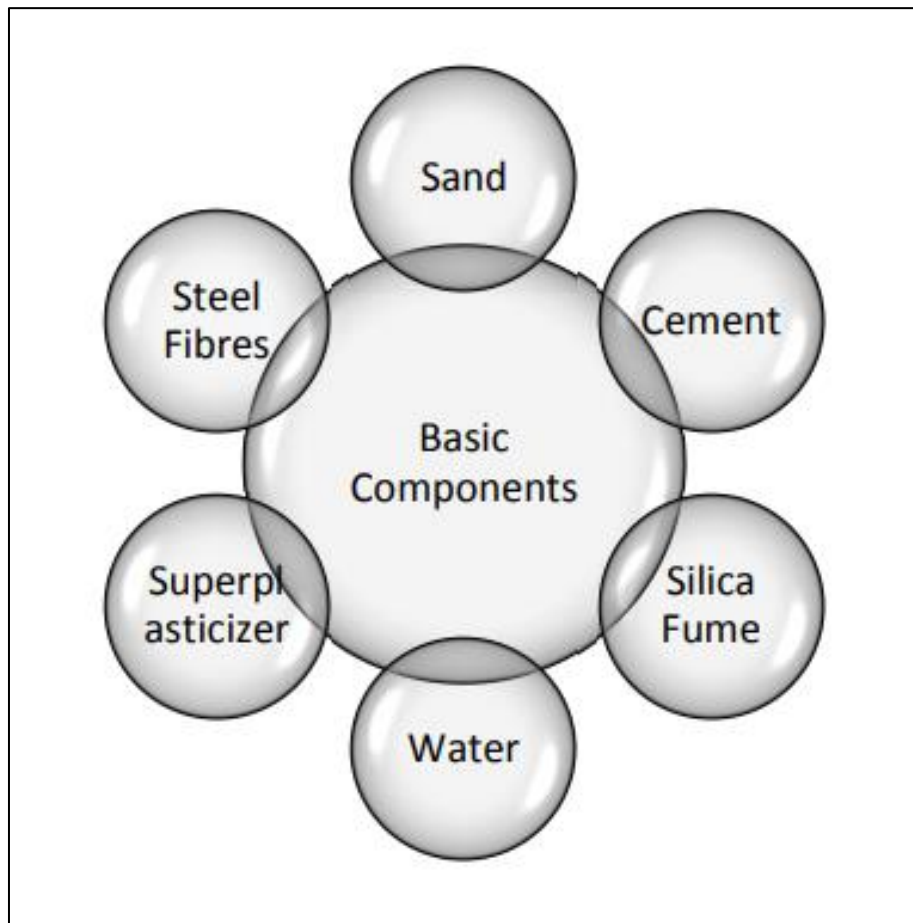


Figure 1.3: Basic constituents of UHPC

## 1.5 Thesis Objectives

The main objectives of this investigation are summarized in the following points:

- To carry out experimental investigation on the one-way slabs then overlay with UHPC. The investigation has planned to be done depending on the following variables; substrate material compressive strength, overlay material compressive strength, overlay thickness, different types of surface preparation, and shear stud to obtain bonding strength.
- Presenting unique properties of UHPC for bridge deck slabs overlay if compared with the conventional concrete.
- Characterizing the properties of UHPC. The benefits of using UHPC as an overlay for bridge deck slabs. Another purpose is to minimize the thickness of the overlay to reduce the dead load on the bridge structure.
- The main goal of this study is to determine the structural behavior of bridge deck slabs when overlaid with UHPC. Determining the failure mode from the experimental point of view, investigate whether the failure will occur in shear or bending.

## **2 CHAPTER TWO**

### **2.1 Review of Literature**

Recently a reinforced concrete bridge deck slab ‘cast in place or precast’ is an essential construction facility that serves society as a roadway for pedestrians, bikes, and vehicles. All around the world several materials were experimentally investigated to be used as an overlay material for bridge deck slabs but were structurally deficient before reaching their design service life. Selecting a suitable material for the overlay is require wide investigation because bridges are subject to high live load due to traffic volume. Usually, bridges are overlaid with some materials such as Natural Strength Concrete (NSC), Latex Modified Concrete (LMC), Silica Fume Modified Concrete (SFMC), Low Slump Dense Concrete (LSDC) and many others which cause failure due to weak resistance to tension force and due to many other deficient, until UHPC has been developed and solved entire problems that faced the bridge deck slabs overlay.

This chapter discusses the history and overview of other researchers about the bridge deck slabs with different materials which can be used for overlay, and the variables which other researchers focused on it to investigate the structural performance of bridge deck slabs according to ACI code permission.

### **2.2 Bridge Deck Slabs Guidelines**

#### **2.2.1 AASHTO Design Guidelines for Bridge Deck Slabs**

According to AASHTO (2017) bridge design guidelines, the following limits are considered for bridge deck slabs:

- The depth of the deck should be not less than 17.78 cm.

- One half of strip width not exceed 1.8 m.
- The edge of the deck shall be strengthened by a beam or other line components, also they have to be composite with the deck.
- The ratio of effective length to the design depth does not exceed 18.
- The limited bridge deck span with the direction of traffic is 4.5 m.
- The skew angle must not be exceeding 25 degrees and reinforcement must be placed in the direction of skew.
- Overhang beyond the centerline of the outside girder is at least five times the depth of the slabs and it has to be composite with supporting structural components.
- AASHTO permitted 5 cm cover on top and 2.5 cm cover on bottom with 10 cm reinforcement core as shown below in Figure 2.1.

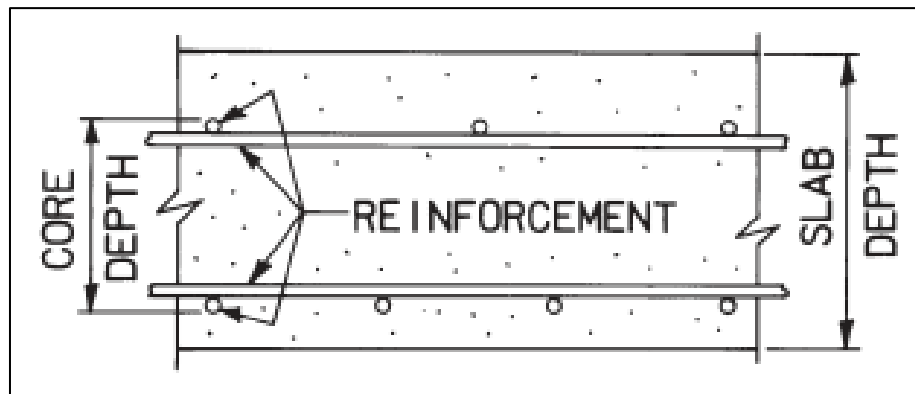


Figure 2.1: Slab section details

### 2.2.2 Minimum Thickness and Reinforcement of One-Way Solid Slabs

The minimum thickness of a solid one-way slab will vary according to support conditions as presented in Table 2-1. Immediately or time-dependent deflection has to be calculated before the member becomes

composite (ACI 318R-19, 2019). Also, the member shall be tension controlled as presented in Figure 2.2, (ACI 318R-19, 2019).

Table 2-1: Minimum thickness of solid one-way slabs

Support condition	Minimum h
Simply support	L/20
One end continuous	L/24
Both end continuous	L/28
Cantilever	L/10

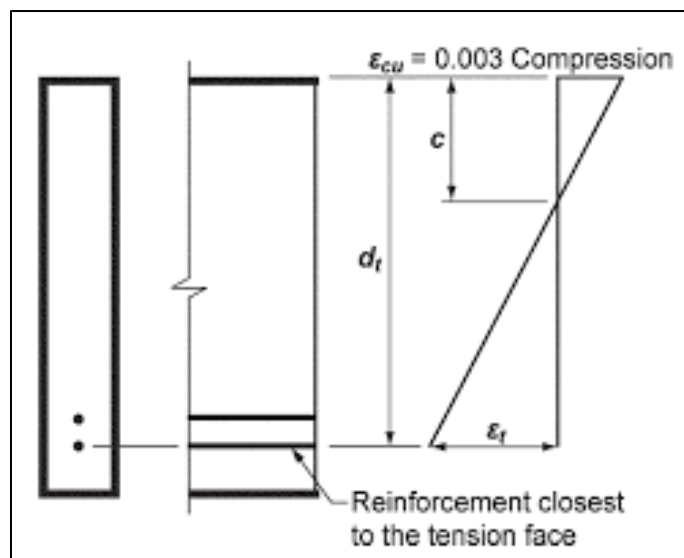


Figure 2.2: Strain distribution and net tensile strain in a solid one-way slab member

## **2.3 Bridge Deck Slabs Deterioration and Rehabilitation**

### **2.3.1 Bridge Deck Slabs Deterioration**

The common deterioration of bridge deck slabs consists of cracking, spalling, delamination, and corrosion of reinforcement. Various technique is used for maintenance like crack repair, sealing, and grouting, but they take 50-80 % of all bridge deck slabs expenditure. These techniques can prolong the life of a bridge but none has been approved to prevent further deterioration completely. After evaluating many materials for bridge deck slabs overlay, finally, UHPC has approved as the successful material for overlay. The first implementation of UHPC was in North America on Buchanan County Road D48 near Brandon-Iowa for a bridge that was built in the 1960s with the dimensions 31 m long, 9 m wide, and 5% superelevation, this bridge overlaid with UHPC which its mix properties developed by Lafarge Holcim with a lower slump to accommodate the sloping surface. The construction was performed by removing the old asphalt surface then grooving and spraying substrate material and adding a layer of reinforcement after that overlaying with 3.75 mm of UHPC in May 2016 (Sritharan et al., 2018, Wibowo and Sritharan, 2018).

The experimental investigations observed that the bridge deck slabs have to be overlaid with a suitable material by using a proper technique because this overlay is considered a source of failure. The failure in bridge deck slabs occurs from two essential mechanisms which consist of shear and flexural from two basic locations interface or substrate. Failure in shear occurs at the interface due to different strains between substrate and overlay materials and improper surface preparation is a reason for debonding which can be prohibited by adequate surface preparation for substrate material to transfer the load between overlay material and

substrate material properly, design for shear friction according to is important to avoid delamination. In addition, failure in flexural occurs at the tension zone of substrate material, another definition for bridge deck slabs overlay failure in flexural is “when the interfacial strength is higher than flexural stress” (Graybeal and Haber, 2018). Cracking is a visible problem on bridge deck slabs. Bridges are frequently subjected to high traffic loads, which cause top surface cracks and complete destruction of bridge deck slabs (Wibowo and Sritharan, 2018).

### **2.3.1.1 General Region and Mechanism of Failure**

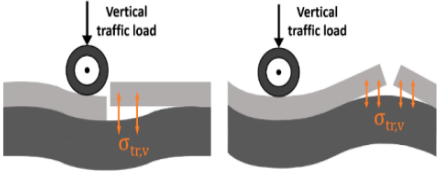
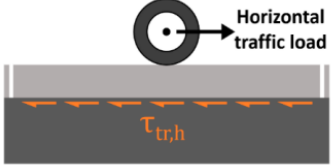
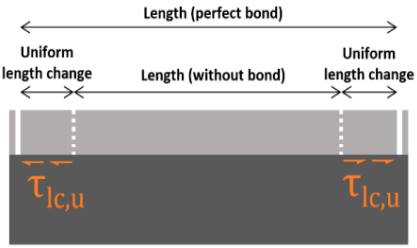
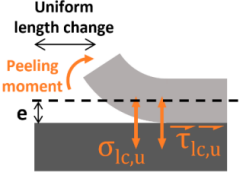
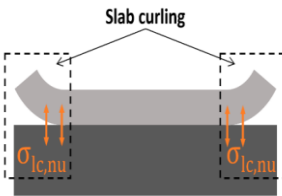
Bridge deck slabs overlay subject to compression and shear continuously due to traffic load, therefore the failure will occur. The basic four regions of failure experimentally identified in one of the studies: (Tayeh et al., 2012)

- Interfacial failure (a complete de-bonding at the transition zone).
- Interfacial failure and substrate cracking or minor substrate damage.
- Interfacial failure and substrate fracture.
- Complete substratum failure with a good interface.

The main mechanism of failure for bridge deck slabs is due to the interfacial stress by direct or indirect loads as shown Table 2-2: (López-Carreño et al., 2020)



Table 2-2: Mechanism of interfacial debonding due to direct and indirect loads

Type of load	Load	Stresses	Mechanisms
Direct	Traffic Vertical	Normal	
	Traffic Horizontal	Shear	
Indirect	Thermal exchange/Drying shrinkage/Autogenous shrinkage	Shear (due to uniform component)	
		Normal (peeling due to uniform length change)	
		Normal (due to non-uniform length change)	

### 2.3.2 Bridge Deck Slabs Rehabilitation Strategies

Recently many bridges have been damaged before reaching their design service life. There are two kinds of strategies that have been available to solve this problem; the first one is replacing the partial deck with a new one which has the disadvantage that time-dependent performance and cost. the second strategy consists of sealer or cracks repair. Sealer and crack

repair have the advantage of low maintenance cost but it also has the disadvantage of short life (Krauss et al., 2009). Replacing procedure is mainly performed for overlay material, the performance includes of; remove the old overlay material then preparing a good surface preparation for the old substrate material after that overlaying the substrate material with a suitable material which is investigated experimentally. Furthermore, the overlay material has to be easily removed because bridge deck slabs are exposed to damage due to contact with live load continuously. One of the effective maintenance methods that are used recently is consist of maintaining the existing structures by adding a layer of steel with an overlay in a transverse direction to improve the behaviors of structure in bending moment capacity and shear resistance, it also resists the widening of a crack in the existing structure. This method is called protective and resistance which requires overlay thickness between 40-80 mm and 25-40 mm for protective only as shown in Figure 2.3 (Brühwiler and Shen, 2017).

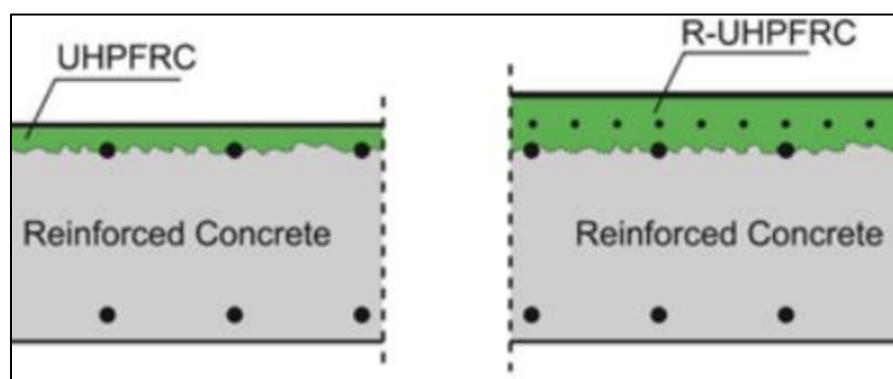


Figure 2.3: In the left-hand shows than UHPC overlay for protective and the right-hand shows the UHPC for protective and resistance

## **2.4 A comprehensive explanation of UHPC**

### **2.4.1 Definitions**

UHPC is one of the successful cement-based composite materials which accurately designed for many purposes in building construction significantly for overlay bridge deck slabs. UHPC properties of sufficient bond with substrate material and ability to resist cracking due to existing discontinuous steel fibers made it a desirable material for bridge deck slabs overlay. The unique dense matrix of UHPC resists the penetration of chloride ions to the base material which associates with the corrosion of substrate steel bars.

According to the Federal Highway Administration (FHWA), the UHPC has at least 150 MPa compressive strength and 5 MPa tensile strength, but this definition isn't used universally because Canadian Standard Association defined that UHPC has at least 120 MPa compressive strength at 28 days (Tadros et al., 2019).

### **2.4.2 Development Of UHPC**

Different types of materials have been developed all around the world for overlaying bridge deck slabs. Each type of overlay material has a particular advantage and disadvantage. Various types of failures and delamination have been observed which makes researchers continue to investigate a better kind of overlay that can solve almost all bridge deck slab problems.

It had been many years for researchers make experiments to find a new kind of concrete to provide very high compressive strength. Depending on

the following components 80 MPa concrete compressive strength at 28 days have obtained for dense mortar: -

Table 2-3: Composition of 80 MPa concrete compressive strength

<b>Material</b>	<b>Weight by gram</b>
Fine sand	1350
Cement	544
Silica fume	100
Superplasticizer	12.2
w/c (0.25) %	136

The hidden fact provided that silica fume is a very effective content in mortar by filling the voids between cement and other particles but this composition isn't containing steel fiber which represents that it hasn't adequate resistance to tension forces (Larrard, 1989). With the nonstop development of concrete technologies, 236 MPa concrete compressive strength has been obtained depending on the following key components sand, cement, water, silica fume, water and superplasticizer with 4 days curing at 90 °C (Larrard and Sedran, 1993).

The efforts had continued to obtain high and higher strength but almost all mix designs had the problem of ductility, then the main principle of UHPC depending on the attempts of previous researchers obtained by Richard and Cheyrezy (1994), which called Reactive Powder Concrete (RPC) with compressive strength between 200-800 MPa. Also, the problem of ductility was solved with the addition of steel fiber into the matrix which provided fracture energies up to 40 KJm<sup>-2</sup>. A dense matrix of UHPC is achieved with the following components: -

- Eliminate coarse aggregate and replaced it with fine sand with a maximum size of 600  $\mu\text{m}$ .
- Fine quartz sand aggregate 150-600  $\mu\text{m}$ .
- Cement with the largest particle size 80-100  $\mu\text{m}$ .
- Crushed quartz 10  $\mu\text{m}$ .
- Silica fume, fume/cement is 0.18 %.
- Ductility of matrix solved by adding 1.5-3 % of steel fiber by volume into the matrix and preferred dimensions aspect ratio 86

Resplendino (2012) reported that the first recommendation of UHPC was first in France (Française de Génie Civil (AFGC) 2002), then several bridges were built and overlaid with UHPC. Later in 2009 several papers updated this recommendation until the commercial production of UHPC first opened in North America which is known as ductal. Most papers and investigations are depending on the ductal composition.

Luo (2002) compared the following types of overlays for bridge deck application: -

- Low w/c ratio concrete
- Asphalt concrete with membrane
- High performance concrete
- Fly-ash modified concrete
- Silica-fume modified concrete
- Polymer concrete
- Latex-modified concrete (LMC)

Luo (2002) in a direct shear test evidenced that the failure mode of all concrete types is through the interface except the LMC is through the substrate it is because air content of LMC is very low, therefore admired that the LMC is a suitable material for overlay. Also, suggested that latex-modified slurry can be used as bonding slurry for all other types of overlay

but from another point of view LMC is a very sensitive material for reaction to climate change.

Various types of materials for overlay are discussed intensively by Krauss et al. (2009) stating that the most common one is asphalt concrete. The advantages of each overlay are presented particularly. Generally, they have the property of low initial cost but the following disadvantages made them undesirable materials for overlaying bridge deck slabs, although some maintenance techniques can prolong the life of overlay like a sealer. It doesn't work well with cracked surfaces; crack repairs can solve this problem but even it doesn't work well with penetrated crack depths: -

- Poor bond with the substrate material
- Long curing time and traffic issue
- The short life of overlaying
- Increase dead load due to its high thickness
- Sensitivity to weather
- Top surface cracking and permeability of water or ions into the base

Usually, the traditional bituminous pavement is subject to degradation therefore waterproofing technique plays an important role to decrease the amount of maintenance. Pasetto and Giacomello (2014) evaluated the effect of polymer binder with aggregate to increase the durability of the structure that used two types of resins and several types of aggregate, which was performed based on laboratory tests of skid resistance, permeability, and tensile. The weak point identified in this study includes that aggregate cannot be immersed completely into the resin which let it to produce void and stress. The bituminous pavement requires maintenance continuously, for example, seal coating has to be performed at least once time for every three years.

### 2.4.3 General Composition of UHPC

The composition principle of UHPC gradually emerged in several countries since 1986, each country has developed a special design guideline with a different requirement for the characterization of materials, the countries include Germany, Switzerland, Australia, Canada, Spain, Japan, and America (Larsen and Thorstensen, 2020). The first commercial production of UHPC first opened in North America that known as ductal, ductal is a trade-named, pre-bagged UHPC product sold by Lafarge Cement Company which its ingredients and percentages are clarified in a Table 2-4 (Tadros and PE).

Table 2-4: Ductal composition of UHPC

<b>Material</b>	<b>kg/m<sup>3</sup></b>	<b>Percentage by Weight</b>
Portland Cement	712	28.5
Fine Sand	1,020	40.8
Silica Fume	231	9.3
Ground Quartz	211	8.4
HRWR	30.7	1.2
Accelerator	30.0	1.2
Steel Fibers	156	6.2
Water	109	4.4
Total Weight	2500	

*HRWR: High Range Water Reducer*

Almost all researchers are depending on the ductal compositions for their studies. The compositions of UHPC are the same as NSC except eliminate coarse aggregate to obtain a dense matrix and reduce a void ratio. In another hand eliminating coarse aggregate is important because the coarse aggregate influences reducing bond strength. Also, the following materials were added to the UHPC mix, each material added for a particular purpose:

- Steel fiber: Fiber is used to improve tensile strength. Concrete is a brittle material therefore fiber is used to reduce the brittleness of cementitious material. It has a great influence on cracking behavior through control extending of crack. Almost all studies presented that the shape, length, and volume of fiber in UHPC affect its tensile and flexural strength. New science presented that until 3% ( $V_f$ ) volume of fiber, has an effect on increasing strength but more than this value reduces workability because it increases friction between fiber and concrete matrix. In addition, the highest tensile strength was obtained with 13 mm of fiber length compared to 9 mm and 20 mm for same radius. Moreover, last investigations identified that the combination of all shapes of fiber together has an unbelievable influence on increasing strength and the basic shapes of fiber presented in Figure 2.4 (Larsen and Thorstensen, 2020).

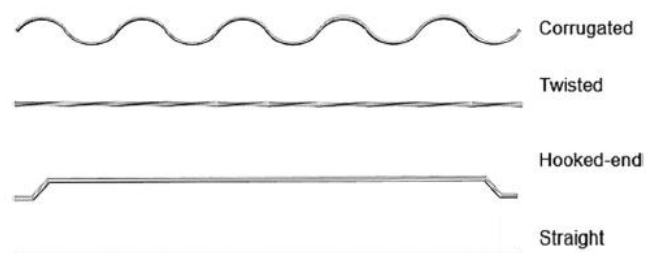


Figure 2.4: Basic shapes of steel fiber



- Silica fume: The addition of silica fume to concrete is very important because small particles of silica fume fill voids between cement particles and increase bond strength which affects reducing permeability and increasing durability (Aldred et al., 2006).
- HRWR: This admixture also called superplasticizer or water reducer is used to the viscosity of concrete, increase density and reduce shrinkage cracking (Schmidt and Fehling, 2004).
- Ground quartz: It is a hard and durable material that has incredible resistance to crack due to traffic load (Yang et al., 2000).
- Accelerator: The use of an accelerator is desirable it depends on the time for completion of the project. it is used for project types that faced a load of traffic to accelerate the chemical reaction and setting time (Su et al., 2022).
- Low W/C ratio: Investigation gives the advice to use a low w/c ratio to reduce porosity (Choi, 2016).

#### **2.4.4 UHPC Families**

Several types of concrete mixtures can be considered in the family of UHPC. One of the families of UHPC called Reactive Powder Concrete (RPC) developed with a compressive strength between 200-800 MPa, the mix design of dense concrete experimented which the resist permeability of ions into the concrete and solved the problem of ductility with the addition of steel fiber into the matrix (Richard and Cheyrezy, 1994). Another cement-based mineral is called Ultra High Strength Concrete (UHSC). The homogeneous matrix of UHSC was obtained with eliminate coarse aggregate and substituted with sand. Also, packing density increased by using complementary grain size distribution of powder particles by eliminating the transition zone between sand and powder

(Aïtcin, 2016). The commercial production of UHPC known as ductal Lafarge North America (2009), that produced 100 MPa compressive strength at 12-36 hours using a w/c ratio less than 0.25% and 2% of steel fiber by volume. Another family of UHPC is HRUHPC (Heavy Reinforced Ultra High-Performance Concrete) whose tensile strength is 90 percent higher than UHPC (Buitelaar, 2004).

Ahmed et al. (2021) depended on the following materials cement, silica fume, fine and coarse aggregates, water, and superplasticizer to produce High-Performance Highly-Viscous Concrete (HPVC) that obtained around 126 MPa of concrete compressive strength at 180 days with having the property of excellent workability flowability and durability. The excellent property optimized in this study is economic assistance using this results in various applications but this mixed design cannot be used in some types of structure that may face a high level of tension force like bridge deck slab overlay because this matrix is weak in ductility.

#### **2.4.5 Mechanical Properties of UHPC**

The following mechanical properties made UHPC unique material for overlaying bridge deck slabs: -

##### **2.4.5.1 Compressive Strength**

The first dependable property of UHPC is compressive strength. This property will change with time that is why it is called time-dependent property. Many factors affect the compressive strength of UHPC which consist of the type of curing, shape of the specimen, size of specimen, size, shape, and volume of steel fiber, mix compositions, casting direction, loading rate, age of concrete with many others (Ahmed, 2009):

## **1. Curing Regimes and Age of Samples**

Types of curing have a great influence on compressive strength, four types of curing are evaluated which consist steam treatment, delayed steam treatment, tempered and untreated environment. Graybeal (2006) presented that the UHPC can gain strength and stiffness quickly at an early age, for specimens without any treatment; 10 MPa of compressive strength was observed within 24 hours then after three days increased to 69 MPa. At results found that for untreated curing regimes gain of strength has continued for at least one month after casting but for controlled curing regimes a very little change in strength was observed after heat treatment.

Furthermore, Heinz and Ludwig (2004) identified that the compressive strength of UHPC will increase with an increase in hydration. cement hydration depends on the heat treatment, the degrees of heat have to be above 90 °C for at least 2-6 days.

## **2. Shape of Specimens**

The geometry of the specimen affects strength, the higher value of strength can be obtained with a cube rather than a cylinder because shorter aspect ratio and the proportionally larger lateral confinement provided by the machine platens (Graybeal, 2006).

## **3. Size of Specimens**

The smaller cubes and cylinders tended to exhibit larger standard deviations because heterogeneities in the concrete would likely remain in a uniform size range but would be proportionally larger in smaller specimens (Graybeal, 2006).

#### **4. Size, Shape, and Volume of Steel Fiber**

To find out the effect of fiber volume on compressive strength different volumes of fiber were experimented, Wu et al. (2016) concluded that with 3% of fiber volume can obtain the highest compressive strength because the stress between fiber and matrix will reduce with an increase of fiber content and it delays the formation and propagation of cracks. Furthermore, 3% hooked end and corrugated steel fibers increased the compressive strengths by 48% and 59% at 28 days compared to straight steel fiber. The increase of fiber content decreased stress between fiber and matrix which in result increased compressive strength and the highest strength obtained with hooked ends shape. In addition, recent studies emphasize that contribution of all types of fiber will provide an attractive result.

#### **5. Mix Compositions**

Kim et al. (2019) determined that the compressive strength of concrete is greatly related to silica fume content but it has the disadvantage that decreasing slump flow which is why the addition of a superplasticizer is required. Sun (2004) produced two groups of overlay material, the first group contain limestone and the second group contain gravel. The 61 MPa maximum compressive strength has been obtained with the group which contains limestone because the researcher observed that the compressive strength with gravel is lower compared with limestone due to the angularity of limestone.

## **6. Casting Direction**

The effect of casting direction isn't significant on compressive strength because the effect is less than 2% when loading perpendicular or parallel with casting direction (Stiel et al., 2004).

## **7. Loading Rate**

The effect of loading rate presented that the loading rate range between 0.24-1.7 MPa/second affects the UHPC compressive strength by less than 3.5 % (Kazemi and Lubell, 2012).

### **2.4.5.2 Tensile Strength**

The tensile behavior of UHPC is divided into three parts as presented in Figure 2.5. The first part is elastic strength which has a limit between 7 to 11 MPa. Then in the second part, the strain hardening begins under the effect of steel fiber that tensile strength reached 9 to 15 MPa. The third part is strain softening, this study observed that the maximum crack is equal to the half-length of steel fiber. In addition, observed that the strain hardening property can be obtained only with at least 3% of fiber volume which depends on the aspect ratio, orientation, and content volume of fiber. The pull out of steel occurred after the test which greatly related to the UHPC's fracture energy that characteristically ranging from 20 to 30  $\text{KJ}/\text{m}^2$  and it depending on the fiber matrix, orientation and bond (Brühwiler and Denarié, 2018).

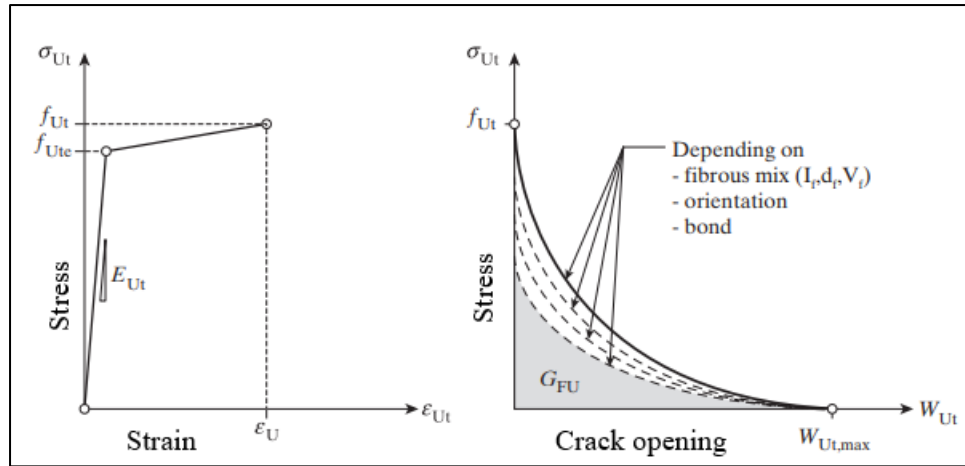


Figure 2.5: Represent the tensile behavior of UHPC

Where:

$f_{Ut}$  : Tensile strength

$f_{Ute}$ : Elastic limit strength

$\epsilon_{Ut}$  : Tensile strain

$\epsilon_U$ : strain-hardening domain

$W_{Ut}$ : Crack opening

$W_{Ut,max}$ : maximum crack opening

$G_{FU}$ : High specific fracture energy

The outstanding tensile properties of UHPC are measured with tensile tests which are clarified below:

### 1. Direct Tension

According to ASTM C1583, this test is used to determine failure stress under pure tension which gives a close result to the true tensile strength. The direct tension setup consists of an inner and outer plate system with epoxy adhesive, tension load will be applied on both sides of the concrete

cylinder specimen. Generally, for bridge deck slabs overlay application this test is used to determine the bond strength between two types of concrete, the composite structure of NSC-UHPC with different interface patterns evaluated by Newton and Weldon (2018) which identified that acceptable bond strength isn't achieved for all NSC surface texture depth with direct tension test due to pure in tension. The below equation can be used to determine direct tension strength:

$$T = \frac{P}{A_c} \quad \text{Equation 2-1}$$

where:

T = tensile strength

P = ultimate load

A<sub>c</sub> = cross-sectional area of the specimen

$$A_c = \frac{\pi}{4} D^2 \quad \text{Equation 2-2}$$

D: Diameter of cylinder

Furthermore, Graybeal and Haber (2018)'s experimental study overlaid bridge deck slabs with two types of material UHPC and LMC. After field inspection, the delamination has believed to exist which is why the direct tension pull-off test was concluded for some points which observed that tensile strength of materials and interfacial bond between two layers of concrete influence results. This test observed that unique bond strength obtained with UHPC even in some places that aren't prepared priority because the tensile strength of UHPC is 33% more than LMC.

## **2. Splitting Tensile Strength ( $f_{ct}$ )**

According to ASTM C496, the splitting tensile test can be obtained by applying compression force along the length of the concrete cylinder by a universal testing machine with applying plywood and supplement bar on both sides of the specimen. For UHPC overlay on NSC, this test can carry out by casting half of the specimen in long direction with NSC, after 28 days have to be overlaid with UHPC. The substrate textures can enhance the indirect tensile strength which Tayeh et al. (2012) concluded that the highest bonding strength can attain with the sandblasting technique.

Al-Basha et al. (2019) were experimented the cylinder and prism mold for splitting tensile test to determine the effect of surface preparation on bond strength, in result showed that the cylinder specimen isn't correlated properly with different types of surface preparation.

### **2.4.5.3 Modulus of Elasticity**

Modulus of elasticity of concrete is the measurement of the stiffness of the concrete which is a good indicator of strength. At a higher value of modulus of elasticity, the concrete can withstand higher stress and become brittle. The experimental test for determining the modulus of elasticity of the concrete is known as a compression test on the cylindrical concrete sample. Tayeh et al. (2012) acknowledged that the UHPFC would have a higher elastic modulus than the NSC. Graybeal (2006) study measured the modulus of elasticity and strain based on the Linear Variable Differential Transformer (LVDT) load reading and deformation measurement which shown that the values are changed depending on the types of curing

The relation of modulus of elasticity is proportional to compressive strength as can be shown in Table 2-5. With 250 °C high-temperature heat



treatment the value of compressive strength increased, proportionally the value of modulus increased from 57 to 70 GPa Richard and Cheyrezy (1994) but the addition of steel fibers in UHPC didn't have a great influence on elastic modulus. For example, only a 7 % increase in the elastic modulus was observed with the addition of 2 % by mixture volume of steel fibers (Bonneau et al., 1996).

Table 2-5: The relation between elastic modulus and compressive strength

References	Modulus of Elasticity
(ACI 363R-92, 1997)	$E=3300\sqrt{f'_c}+6.9$
(Ma and Schneider, 2002)	$E=16,364\ln f'_c-34,828$
(Sritharan et al., 2003)	$E=4150\sqrt{f'_c}$
(Ma et al., 2004)	$19000\sqrt[3]{\frac{f'_c}{10}}$
(Graybeal, 2007)	$3840\sqrt{f'_c}$

Where:

$f'_c$ : concrete compressive strength (MPa)

E : Modulus of Elasticity (GPa)

#### 2.4.5.4 Poisson's Ratio

According to AASHTO (2017) the value of the Poisson ratio was 0.2 for normal-weight concrete with compressive strength up to 100 MPa.

$$\text{Poisson Ratio } "v" = \frac{\text{lateral strain}}{\text{longitudinal strain}} \quad \text{Equation 2-3}$$

#### 2.4.5.5 Coefficient of Thermal Expansion (CTE)

CTE was measured according to AASHTO test specification, TP60-00 by measuring the change in length of the concrete cylinder. This test is influenced by concrete saturation, saturation of UHPC is very low due to its low permeability. CTE of UHPC is around  $15 \times 10^{-6}$  mm/mm/°C, it is higher than the normal value of  $10 \times 10^{-6}$  mm/mm/°C which belongs to high cement content in UHPC because the CTE of cement is between 11-16 mm/mm/°C (Graybeal, 2006).

#### 2.4.5.6 Durability Properties Of UHPC

UHPC improves durability greatly due to its dense matrix. the dense matrix obtained with porous material that fills voids between particles, the porous materials have to be carefully designed to optimize the microstructures. The new technology in term of the state of arts have been published after the UHPC have become dependable construction material in the last decades, Du et al. (2021) discussed that impermeability of UHPC belong to regular particle packing density compared to conventional concrete as represented below:

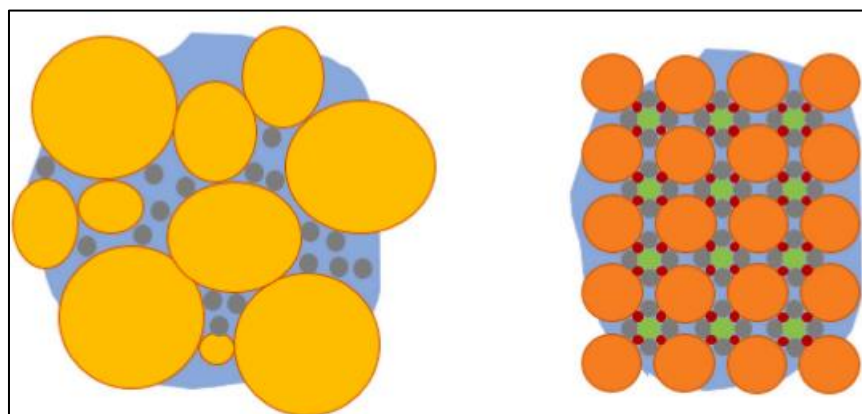


Figure 2.6: Particle packing density, left hand for conventional concrete and right hand for UHPC

Also, the existence of steel fiber reduces the width of crack which make reduce the permeability of any ion into the substrate which don't let to corrosion of steel bars to occur, and as a result durability increase (Du et al., 2021).

For this purpose, Tayeh et al. (2012) used the Rapid Chloride Permeability Test (RCPT) to check permeability. the RCPT is performed by monitoring the amount of electrical current that passes through a sample 50 mm thick by 100 mm in diameter in 6 hours. This sample is typically cut like a slice of a core or cylinder. A voltage of 60V DC is maintained across the ends of the sample throughout the test. Due to the high density of UHPC the permeability of water and ions into the UHPC is negligible (Al-Basha et al., 2019). Also, Habel (2004) measured the air permeability of UHPFRC with the Torrent test at the age of 80 days depending on the hypothesis that moisture exchange is very small. Due to the dense matrix, the very low air permeability was happened around  $k_T < 0.003 \cdot 10^{-16} m^2$  then with some resolution reached  $k_T = 0.001 \cdot 10^{-16} m^2$ .

## **2.4.6 Long Term Stability Properties of UHPC**

### **2.4.6.1 Creep**

Creep is a change in the shape of concrete under sustained load that consist of early age and long term creep testing. Graybeal (2006) experimented early age creeps testing according to ASTM C39 and long-term creep testing according to ASTM C512 which investigates the dimensional stability and conducted that curing regimes had a great influence on the results. As presented in the Figure 2.7 low creep results were obtained with steam curing due to more rapid and more complete self-

desiccation of the UHPC, and the equation 2-4 below is used to satisfy the results: (Graybeal, 2006)

$$\epsilon_{ct} = \frac{t^{0.6}}{A+t^{0.6}} B \quad \text{Equation 2-4}$$

Where:

t: is the time in days since load initiation

$\epsilon_{ct}$ : is the creep strain at that time

A and B: are variables

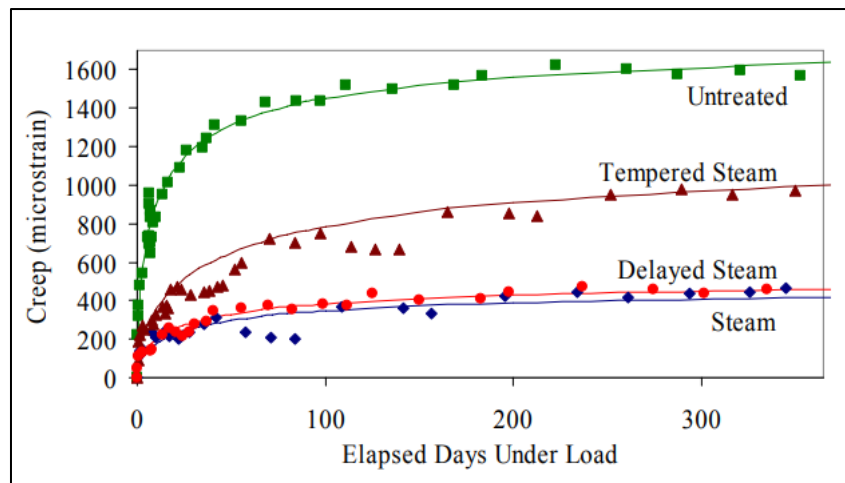


Figure 2.7: The effect of curing regimes on long-term creep

#### 2.4.6.2 Shrinkage

Investigating the effect of shrinkage for UHPC overlay on bridge deck slabs is important because early age shrinkage causes stress on the bonding strength. Sadek et al. (2019) has found that the types of curing and the thickness of NSC and UHPC affect the shrinkage. Also, concluded that 55% of early age shrinkage occurs at plastic state at early 10 hours which hasn't any effect on the bonding strength, and long-term shrinkage has identified that low fluctuation in strain occurs in a controlled environment, but jump in strain occur due to changing of environment.

Furthermore, more shrinkage will occur with thicker slab thickness and lower reinforcement ratio. Due to the high binder ratio and low w/c ratio of UHPC the autogenous shrinkage may occur which have effect on the bonding strength. At early 24-48 hours this effect is large but after setting this effect will reduce due to the dense matrix of UHPC (Tayeh et al., 2012).

In Al-Basha et al. (2019)'s study early age shrinkage was 1500  $\mu\epsilon$  after 24 hours and long-term shrinkage was 475  $\mu\epsilon$  at 28 days. Furthermore, the application of pressure throughout the setting about 6-12 hours eliminates chemical shrinkage and microcracking through the matrix, also this pressure application removes exceeded water and reduces air bubbles. After the setting of concrete, heat curing helps hydrate the remaining minerals (Tadros et al., 2019).

#### 2.4.7 Curing Regimes and Effects on the Properties of UHPC

The following curing regimes were presented in Esmaeili and Kasaei (2016) study that discussed about the effect of different curing regimes on the properties of UHPC, accelerated curing regimes improve UHPC properties significantly compared to 28 days of water curing:

Table 2-6: Types of curing

Designation	Curing regimes
WC-7	Water-cured for 7 days
AC-7	Air-cured for 7 days
WC-28	Water-cured for 28 days
AC-28	Air-cured for 28 days
HC	Heat-cured at 90°C (194°F) for 48 hours
AWC	Accelerated water-cured at 90°C (194°F) for 48 hours
AUC	Autoclaved at 2 MPa (290 psi) pressure, 210°C (410°F) for 5 hours

Heat treatment has the following effects: (Graybeal, 2006)

- Increase UHPC compressive strength by 50%.
- Increase the Modulus of elasticity by 25%.
- Decrease creep coefficient by 175%.
- Eliminate long-term shrinkage.
- Decrease permeability to a negligible level.
- Enhance abrasion resistance.

#### **2.4.8 The Effect of Steel Fiber on the Mechanical Properties of UHPC**

To avoid chemical reactions between iron and other compositions like aluminum in UHPC the coating of steel fiber with copper or nickel is recommended by (Mandal et al., 2008). Generally, the load will be transferred from matrix to fiber, this transferring can be improved from 39 to 124 MPa with a copper coating.

A rhetorical discussion presented mathematical background about Fiber Reinforced Concrete (FRC), Zollo (1996) selected fiber types and properties, also presented four types of fiber according to (ACI) Committee 544; steel, synthetic, glass, and natural fiber. This study served as an expression to count the number of fibers in a unit volume as presented in equation 2-5 and discussed that fiber with a low modulus of material can be placed in a fiber concentration to improve fracture toughness:

$$FC = \frac{7.5 \times DRT \times 10^{-4}}{l \times d^2 \times SG} \quad \text{Equation 2-5}$$

Where:

FC - fiber count

l - fiber length (in mm)

d - fiber equivalent diameter (in mm)

SG - specific gravity of the fiber material

DRT - fiber dosage rate ( $\text{N/m}^3$ )

#### **2.4.8.1 Compressive Strength**

Several studies investigated the effect of steel fiber on compressive strength which Larsen and Thorstensen (2020) reported that steel fiber has a little effect on compressive strength. There exist several factors that have an influence on it for example test specimens. For cylinder specimens, the inclusion effect of steel fiber is negligible rather and this effect can be visible on large cubes with more than 3% of steel fiber.

#### **2.4.8.2 Tensile Strength**

The inclusion of steel fiber increases the tensile strength of UHPC but with a limited state, over this limit may have an opposite effect due to fiber agglomeration and entrapped (Larsen and Thorstensen, 2020). Depending on the ductal production of UHPC 9 MPa tensile strength was obtained at 28 days with 0.2% of steel fiber air (Larsen and Thorstensen, 2020).

#### **2.4.8.3 Bending Strength**

To discuss the effect of steel fiber on bending strength Kim et al. (2019) used para-aramid fibers and found that bending strength depends on the fiber diameter, length, and twist of fiber. It concluded that the highest strength was obtained with 13 mm length and 0.2 mm diameter of fiber but the effect of length is neglected for twisted fiber. A low volume of deformed fiber can improve flexural strength rather than straight (Larsen and Thorstensen, 2020). Wu et al. (2016) presented that the fiber content has a little effect on the deflection curve at pre cracking stage, the effect

considered at post cracking stage due to the high sustain of cracks at this stage, also found that 2% of the straight fiber is incorporated to sustain post crack.

#### **2.4.8.4 Flowability**

Fiber with volume fractions 0.1%, 2%, and 3% and fiber shapes straight, corrugated, and hooked end have a large effect on flowability. Flowability decreased with increased fiber volume due to increase specific surface area. Also, hooked end fiber provided the lowest flowability because it increases friction between fiber and aggregate mainly (Wu et al., 2016).

#### **2.4.9 Advantages and Disadvantages Of UHPC**

##### **2.4.9.1 Advantages Of UHPC**

McDonagh and Foden (2016) concluded the following advantages of UHPC:

- Ductility is the ability to sustenance tensile loads even after initial cracking.
- Ultra-high compressive strength up to 200 MPa.
- Extreme durability; low water to cementitious material
- Self-consolidating and highly moldable mixtures.
- High-quality surfaces
- Flexural/tensile strength up to 40 MPa through fiber reinforcement
- Thinner sections; longer spans; lighter weight.
- New graceful product geometries.
- Chloride impermeability.
- Abrasion and fire resistance.



- No steel reinforcing bar cages.
- Minimal creep and shrinkage after curing

#### **2.4.9.2 Disadvantages Of UHPC**

While using UHPC for the entire bridge deck slabs overlay might have resulted in a more durable system but it would be difficult to justify the cost (McDonagh and Foden, 2016).

The attempts of researchers had approved that the application of UHPC overlay can reduce 50-80 % cost of repair and maintenance except for high initial cost, as the first application of UHPC in North America had done, also identified that this application can prolong the life of bridge deck slabs and reduce the cost of maintenance (Sritharan et al., 2018).

Depending on the commercial production of UHPC in North America that known as ductal, UHPC requires at least 3000\$ per cubic meter (Tadros and PE) . It is why various transportation agencies are currently working together to create UHPC at a lower cost than ductal (Tadros et al., 2019).

### **2.5 Bridge Deck Slabs Overlay with UHPC**

#### **2.5.1 Bridge Deck Slabs Overlay Guidelines**

A composite slab has to resist load as a unit because at any interconnected concrete elements tension will occur at the contacted surface, horizontal shear transfer properly while transverse reinforcement is provided or surface preparation specified in a construction document. A composite concrete member at all locations along the contact surface has to satisfy horizontal shear transfer according to the equation 2-6 (ACI 318R-19, 2019):

$$\phi V_{nh} \geq V_u \quad \text{Equation 2-6}$$

Where:

$V_{nh}$  : Nominal horizontal shear strength

$\phi$  : Strength reduction factor for shear 0.75

$V_u$  : External shear strength

### 2.5.2 Overlay Thickness

The thickness of UHPC has a great influence on increasing dead load and deformation. Likewise, rising in temperature is higher at an early age due to more thickness of UHPC. Graybeal and Haber (2018) discussed that traditionally the overlay thickness was between 51-152 mm with a dead load between 1.4-3.6  $kN/m^2$ , after the development of UHPC the overlay thickness decreased 25-51 mm which decreased dead load to 0.57-1.2  $kN/m^2$  because thin overlay with UHPC can improve in durability, strength and all other properties.

### 2.5.3 Addition a Layer of Steel with an Overlay

Brühwiler and Denarié (2018) suggested that addition a layer of steel in the transverse direction at interface especially for old structures to complement the UHPC to R-UHPC, to improve the tensile strength, deformation capacity, and strain hardening behavior. In addition, explained that small bar diameter and spacing can prohibit the fiber orientation.

When a layer of steel is added with UHPC the 4% higher strain can be obtained compared with strain yielding of steel rebar. Also, the addition of a layer of steel rebar with UHPC subsidizes the resistance by reducing the

height of the compression zone and increasing static height (Brühwiler and Bastien-Masse, 2015).

Brühwiler and Shen (2017) investigated structural behavior of slab with the addition of a layer of steel in terms of bending moment and shear resistance. The addition of layer R-UHPC will increase the height of the compression zone in resistance for bending but UHPFRC cannot be fully exploited because the substrate concrete will crush before the top layer reach its strength, plane section analysis for bending resistance is clarified below:

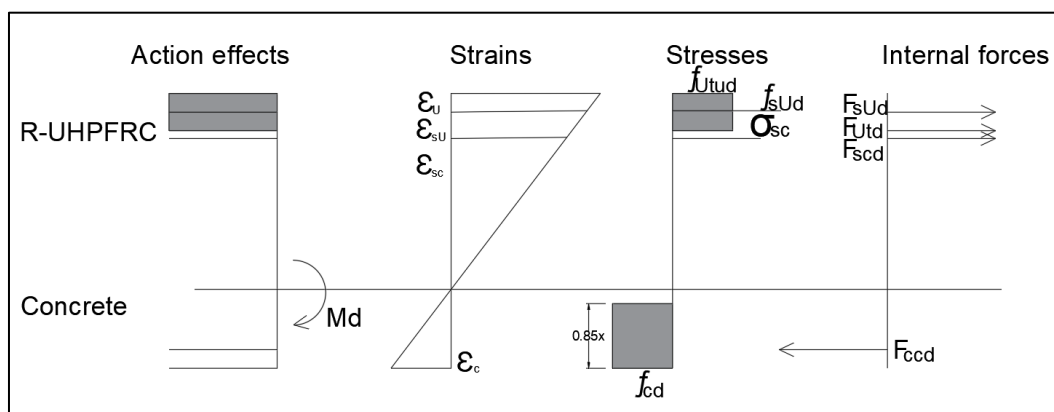


Figure 2.8: Ultimate bending resistance section analysis

Furthermore, the mechanism of shear failure is consisting of the combination of all crushing of substrate material, yielding of reinforcement steel, and two hinges bending of R-UHPFRC as identified in Figure 2.9: (Brühwiler and Shen, 2017)

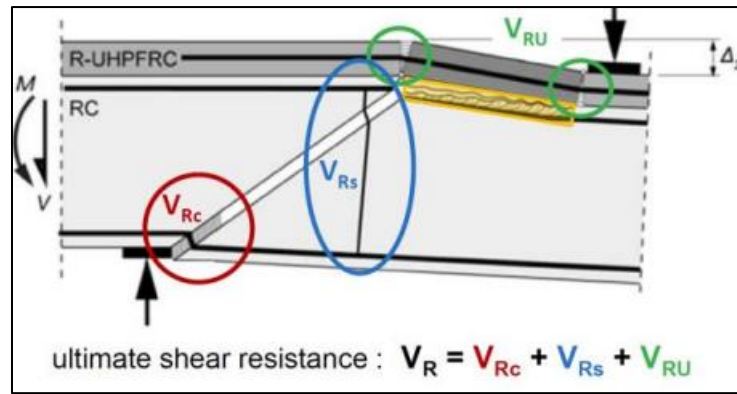


Figure 2.9: Shear failure mechanism of bridge deck overlaid with R-UHPC

#### 2.5.4 Bond Strength of UHPC with Substrate

According to the ASTM C882 standard the Slant Shear test method is used to determine the bonding strength. In this test, the cylinder specimen is subject to both compression and shear to evaluate the bonding strength between two inclined layers. Usually, epoxy coating and different types of surface preparation for substrate material are used to obtain an adequate bond with overlay material. Feng et al. (2021) approved that bridge deck slabs overlaid with UHPC can reduce or eliminate the problems which face the structure, but the weak point is related to the interface bond between two kinds of concrete which can be solved with surface preparation for old structures or with using shear stud and epoxy.

##### 2.5.4.1 Surface Preparation

Al-Basha et al. (2019), Tayeh et al. (2012) carried out experimental studies to investigate the effect of different types of substrate surface texture in terms of bond and shear strength with UHPC overlay, a slant shear strength testing setup was used to determine the bond strength because bond strength highly depends on the texture of the substrate material. Lightly ground, rough, and four types of grooved texture were

used to determine the bond strength as shown in Figure 2.10. the results provided that the deeper interlock of surface preparation can provide a better bond strength. These researches identified that rough texture can provide the highest bond strength, the results have been found depend on the experimental program only because it is difficult to determine the effect of bonding strength in terms of an analytical model and theoretical analysis.

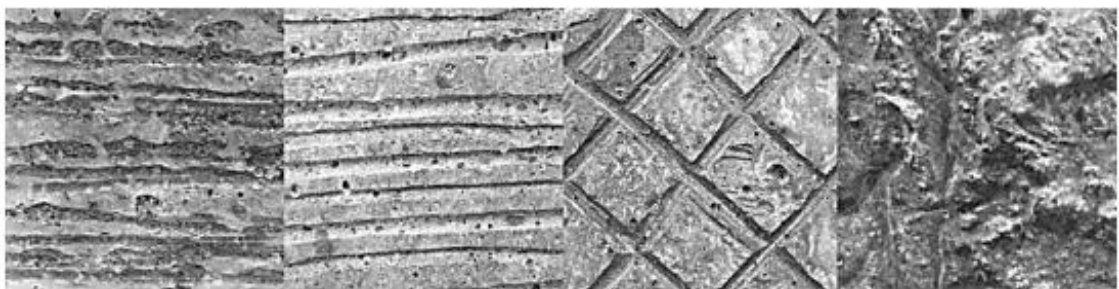


Figure 2.10: Lightly ground 0.05 mm (far left), grooved texture 0.90 mm (left), grooved-cross-hatch texture 1.60 mm (right), rough texture 2.80 mm (far right)

It is clear that surface preparation types have a great influence on bonding strength, Graybeal and Haber (2018) evaluated two essential types of surface preparation as presented below:

- Scarification: It is the technique of using a cutter to remove approximately between 6-19 mm of the substrate material.
- Hydrodemolition: In this method, high pressure of around 310 MPa has to be used with a water jet to remove the required depth of substrate material.

The result of the pull-out tension test noticed that the failure occurred in the substrate not in the bonding surface when the substrate surface was prepared by sand blast method (Brühwiler and Shen, 2017). In addition, the results recorded that different types of surface preparation can enhance 31-102 % of bond strength (Tayeh et al., 2012).

### 2.5.4.2 Mechanical Connectors

To obtain monolithic structural behavior of bridge deck slabs overlay after cracking, connection mechanisms have to be designed correctly. The connector has to resist both tension and shear as shown in Figure 2.11. The main principle of connection belongs to steel rebars and fiber in concrete. The interface strength design can be obtained with the equation 2-7 (López-Carreño et al., 2020):

$$\tau_{Rd} = 0.4 [c_r \cdot f_{ck}^{1/3} + \mu \cdot (\sigma_n + K_1 \cdot \rho \cdot f_{yd}) + K_2 \cdot \rho \cdot \sqrt{f_{yd} f_{cd}}] \leq 0.4 \cdot \beta_c \cdot v \cdot f_{cd}$$

Equation 2-7

Where:

$\tau_{Rd}$ : Mechanical connection in MPa.

$\beta_c$ : Coefficient for the strength of the compression strut.

$v = 0.55 \left(\frac{30}{f_{ck}}\right)^{1/3} \leq 0.55$ : Reduction factor for the strength of the diagonal strut.

$f_{cd}$ : The design value of concrete compressive strength of the weakest layer.

$c_r$ : Coefficient for aggregate interlocking.

$f_{ck}$ : Characteristic compressive strength of concrete.

$\mu$ : Friction coefficient

$\sigma_n$ : Compressive stress in the joint due to external normal forces.

$K_1$ : Interaction coefficient for tensile force activated in the connectors.

$K_2$ : Interaction coefficient for flexural resistance of the connectors.

$\rho$ : The ratio of the reinforcing steel crossing the interface.

$f_{yd}$ : Design yield strength

$R_t$ : This value can be experimentally obtained with the sand path method

Table 2-7: Coefficients  $c_r$ ,  $\mu$ ,  $K_1$ ,  $K_2$  and  $\beta_c$  in terms of interfacial roughness according to Model Code 2010

Surface Roughness	$c_r$	$K_1$	$K_2$	$\beta_c$	$\mu$	
					$f_{ck} \geq 20$	$f_{ck} \geq 35$
Very Rough (e.g., high pressure water blasted, indented) $R_t \geq 3.0$ mm	0.2	0.5	0.9	0.5	0.8	1
Rough (e.g., sand blasted, high pressure water blasted, etc.) $R_t \geq 1.5$ mm	0.1	0.5	0.9	0.5	0.7	
Smooth (e.g., untreated, slightly roughened.) $R_t < 1.5$ mm	0	0.5	1.1	0.4	0.6	
Very Smooth (e.g., cast against steel formwork) $R_t$ not measurable	0	0	1.5	0.3	0.5	

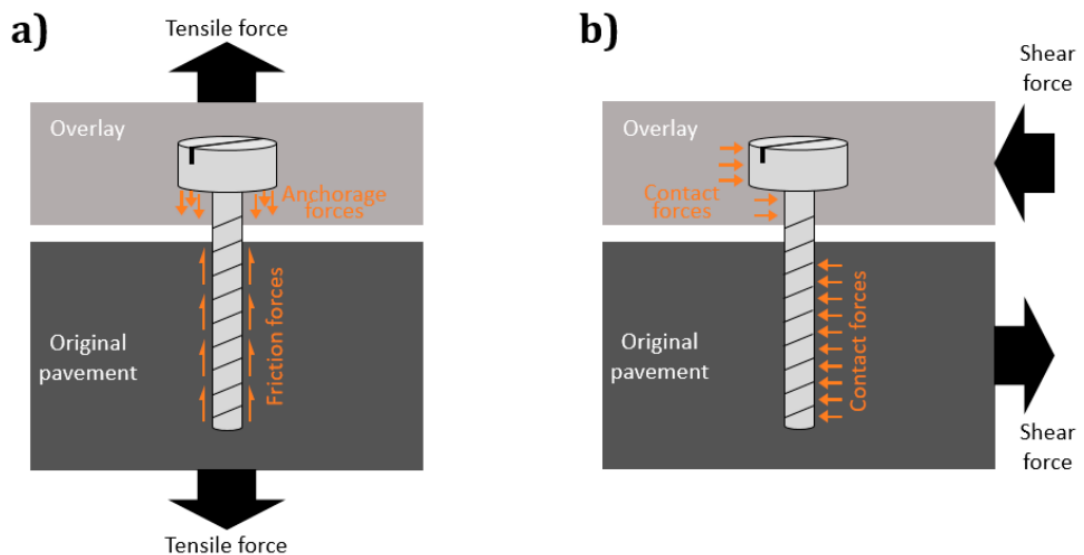


Figure 2.11: Mechanical behavior of a screw anchor under tensile (a) and shear (b) stresses

### 2.5.4.3 Epoxy Coating

Another mechanism that is used to obtain bonding strength between two layers of concrete is epoxy coating. Mohsen A. Issa et al. (2007) evaluated mixture design for two types of high-performance concrete accurately; LMC and MSC in terms of surface preparation, mixing, and curing. And compared two types of bond strength epoxy coating and water-jet blasting with grooved preparation which presented that actual bond strength cannot be reached through using the epoxy coating due to cold weather problems but grooved preparation will not cause any damage.

A new test method is developed by Chilwesa et al. (2017) to evaluate the bonding strength between new and old concrete which setup is shown in Figure 2.12, and a linear displacement voltage transducer is placed at each contact surface to measure slip between two layers of concrete. The substrate surface roughness and overlay strength had a great influence on reducing slip. Also, to be sure that test specimens are fixed properly in the machine, average shear stress can be estimated with the equation 2-8:

$$\tau_a = \frac{P}{2A} \quad \text{Equation 2-8}$$

Where

$\tau_a$ : Average shear stress

$P$ : Applied load

$A$ : Interface contact area



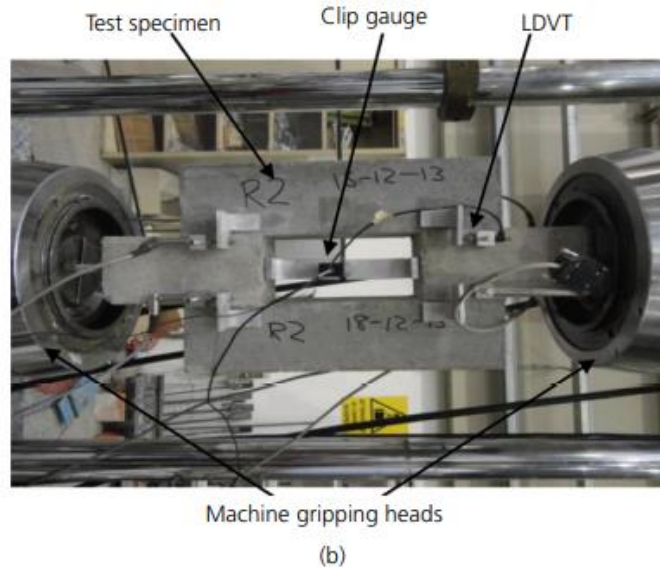
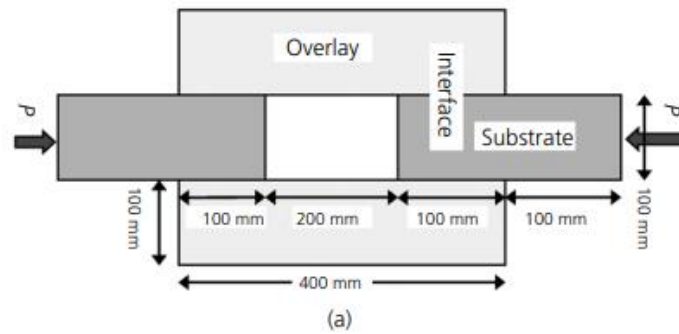


Figure 2.12: (a) Schematic illustration of the test specimen. (b) Test setup in Instron machine

## 2.6 Strengthening Methods

In the last decades, many investigators published their reports about bridge deck slabs overlaid with UHPC. The basic goal of all studies is to determine the failure mode of bridge overlay structure because determining the failure reason is important to resolve all deficiencies and prolong the life of a bridge.

Graybeal and Haber (2018) discussed that failure mode may occur in the substrate material, overlay material, or interface, therefore two types of substrate material were evaluated concrete and UHPC with two types of overlay material UHPC and LMC and two types of surface preparation scarification and hydro demolition which failure mode of each evaluation

presented in Table 2-8. Moreover, it was noted that good bond was still obtained even in locations where the deck concrete had not been roughened before the UHPC overlay was applied; nevertheless, this is reliant on the superior characteristics of UHPC, which has good bond strength and is not a recommended method.

In Aaleti et al. (2013)'s study 2.7 m length by 0.8 m width and 203 mm thickness of NSC as a prototype of one-way bridge deck slabs is molded with different in texture depth from 2 mm to 6 mm to evaluate the bond strength. Then compressive strength of 32 MPa of NSC and 107 MPa of UHPC was used. Then overlaid with 38 mm thickness of UHPC. After 28 days the performance of the composite section was evaluated under flexural and shear loading. In the result observed that no slip was produced in the interface until the specimen failed in shear. Then the shear crack didn't penetrate through the UHPC rather than the shear horizontally propagated and tried to delaminate both layers. The interface roughness depth and bond strength are correlated, and the rougher texture causes the composite structure to withstand more failure load.

In Wibowo and Sritharan (2018)'s education three samples of two-way slabs were cast 2.5 m by 2.5 m and 20 cm thickness with rough surface preparation. The first sample hasn't overlaid, the second one is overlaid on top, and the third one is overlaid on the bottom. For the specimen with NO failed in shear, specimen OT similarly failed in shear but with higher load and crack couldn't penetrate to the UHPC layer but horizontally moved to separate both concrete layers, and for OB the top concrete crushed before the specimen fail in tension. However, the bottom overlay is not practical and is just an illogical exercise.

Bae et al. (2019) evaluated the failure mode of deck slabs with reinforced joints and without joints using 120 MPa of HPC. For specimens without a joint, with increasing load the tensile crack will increase at the

bottom and the top concrete begin to crush. For specimens with joints, no crack can be observed on the deck surface rather and joint areas will become the failure point that is why the researcher serves to advise strengthening the joint places. Elnono et al. (2009) depended on the conventional materials cement, sand, gravel, water, and superplasticizer for producing concrete and sifcon using different lengths of fiber. This mix obtained the property of 40 MPa compressive strength and 3100 MPa modulus of elasticity which was used to evaluate the connection joints because joints are considered a failure point due to opening and closing by bending moment, the best result obtained with increased volume of fiber to 8%. All studies observed that the use of fiber has a great influence on the results, which can reduce the width of cracks largely.

Sritharan and Aaleti (2017)'s education investigated bond strength by slant shear test for 60 samples to evaluate the effect of the following variables: substrate compressive strength 35 MPa, 48 MPa, and 69 MPa, five types of texture, and two types of curing (heat treatment and wet curing). The result showed that if the shear failure in the substrate material did not occur, the UHPC could resist the higher load. Also, the strength, quantity, length, and orientation of steel fiber and the curing condition of UHPC have a great influence on tensile strength. In addition, this study indicated that bond strength is greatly influenced by interface roughness, and delamination was observed with a substrate texture of 1.25 mm because the volume changes due to the shrinkage of UHPC and old concrete in the substrate material led to internal stress being greater than bond strength. Furthermore, the shear crack in the normal concrete did not penetrate through the UHPC overlay, instead, the crack propagated horizontally along the interface, causing delamination. In the other two specimens, due to a higher interface capacity resulting from a deeper interface texture, the delamination due to shear cracking in the normal

concrete did not occur until there was a greater amount of deformation compared to the broom finish specimen.

Stefaniuk (2020) designed the transformation of live and environmental loading between the deck and girders, and transfer the traffic loading down to the support girders. As shown in Figure 2.13, 6-stud and 3-stud compared in the same slab dimensions. In the result have understood that 6-stud can transfer load greatly than 3-stud because the length of shear stud is reduced. Many other shapes and arrangements of studs were designed in this study which indicated that circular shear pockets with fewer studs had the superior load resistance behavior.

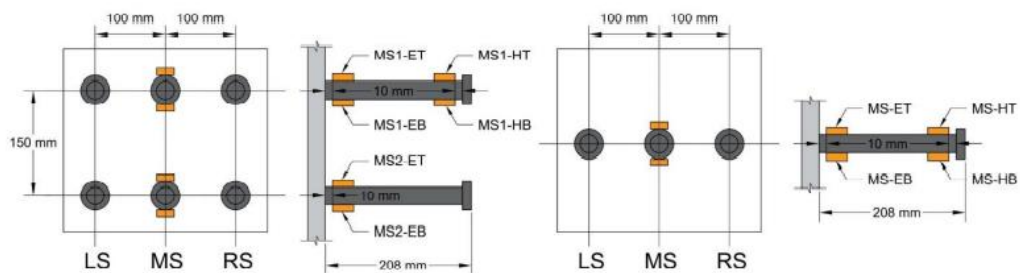


Figure 2.13: Shear stud layout, Right-hand 3-stud, and left hand 6-stud

Zhang et al. (2020a), Mohsen A. Issa et al. (2007), Perez et al. (2009) studies concluded that a rough surface can prove the best bond strength among others, and Stefaniuk (2020)'s study explained the benefit of using a stud in load transformation. Therefore, it is suggested that the combination of these two parameters in one sample may have a pretty big effect on the results, especially for old structures.

Choi (2016) investigated the structural response and failure mode of beam strengthened with UHPC and compared with theoretical analysis. A rough texture of about 3-4 mm was used by the sand blast and the specimens were cured at a controlled temperature for 3 days. This study observed that the UHPC strain is 10% higher than the strain of NSC. The RC beam is strengthened in bending by base restriction in movement,

strengthened in shear by side restriction, and strengthened in both flexural and shear in terms of U-shaped jacketing as presented in Table 2-8. Many variables are investigated in this study, but all are focused on strengthening the existing structures under unloading conditions. But to represent the actual circumstance, the existing structure has to be strengthened under sustained loading.

Sometimes to obtain a drivable surface, after overlay application Eight centimeters of the asphalt layer and bituminous pavement are finally placed on the top surface (Brühwiler and Denarié, 2018).

Table 2-8: Summary of strengthening Bridge Deck slabs with an overlay

<b>Paper</b>	<b>Substrate</b>	<b>Strengthening</b>	<b>Preparation</b>	<b>Result</b>
(Graybeal and Haber, 2018)	Bridge deck of NSC	Overlay with LMC -3.8 MPa tensile strength	Substrate surface prepared by Scarification	The failure occurred at the interface
		Overlay with UHPC -5.7 MPa tensile strength	Substrate surface prepared by Scarification	The failure occurred at the interface
		Overlay with LMC -3.8 MPa tensile strength	Substrate surface prepared by Hydrodemolition	The failure occurred at the interface
		Overlay with UHPC -5.7 MPa tensile strength	Substrate surface prepared by Hydrodemolition	The failure occurred at the substrate
	Bridge deck of UHPC	Overlay with LMC -3.8 MPa tensile strength	Substrate surface prepared by Scarification	The failure occurred at the overlay
		Overlay with UHPC -5.7 MPa tensile strength	Substrate surface prepared by Scarification	The failure occurred at the interface
		Overlay with LMC -3.8 MPa tensile strength	Substrate surface prepared by Hydrodemolition	The failure occurred at the overlay
		Overlay with UHPC -5.7	Substrate surface prepared by Hydrodemolition	The failure occurred at the interface

<b>Paper</b>	<b>Substrate</b>	<b>Strengthening</b>	<b>Preparation</b>	<b>Result</b>
		MPa tensile strength		
(Aaleti et al., 2013)	One-way bridge deck slabs of NSC/ 32 MPa compressive strength	Overlay with UHPC -107 MPa compressive strength	Substrate surface prepared with texture depth from (2-6) mm	The failure occurred at shear (interface)
(Wibowo and Sritharan, 2018)	Two-way slabs	No overlay	-	Failed at shear
		Overlay with 3.8 cm of UHPC on top	Substrate surface prepared with 6 mm rough texture depth	Failed at shear
		Overlay with 3.8 cm of UHPC on bottom	Substrate surface prepared with 6 mm rough texture depth	top concrete crushed before the specimen failed in tension
(Bae et al., 2019)	Deck slabs with reinforced joint	Overlay with 120 MPa HPC	Epoxy coating	Joint areas have become a failure point
	Deck slabs without reinforced joint	Overlay with 120 MPa HPC	Epoxy coating	tensile crack at bottom and concrete crush at the top
(Sritharan and Aaleti, 2017)	2.4 m long by 0.6 m width one-way slabs/ 27 MPa	Overlay with 3 cm UHPC Ductal mix production	Substrate surface prepared with 1.26 mm texture depth + a thin layer of cement paste	Delamination happened across the part width of slab
			Substrate surface prepared with hand broom finish texture + a thin layer of cement paste	Delamination happened across the part width of slab
			Substrate surface prepared with 3 mm texture depth + a thin layer of cement paste	Delamination with a great amount of deformation
			Substrate surface prepared with	Delamination with a great

Paper	Substrate	Strengthening	Preparation	Result
			5mm texture depth + a thin layer of cement paste	amount of deformation
(Stefaniuk, 2020)	Natural strength concrete slab/ 45 MPa	UHPC overlay	Two rows and three columns of shear stud	Debonding between the steel and UHPC shear pocket
			One row and three columns of shear stud	Debonding between the UHPC shear pocket and its RC slab
(Choi, 2016)	Natural strength concrete beam	Base strengthened with UHPC/ thickness 20, 30, and 40 mm evaluated	Substrate surface prepared by rough texture (2-4) mm	Strengthened in bending- Increasing of thickness is proportion with increasing thickness but 40mm is a limit because more than this limit the dead load will increase
		Side strengthened with UHPC/ thickness 20, 30 and 40 mm evaluated		Strengthened in shear- Increasing of thickness is proportion with increasing thickness but 40mm is a limit because more than this limit the dead load will increase
		UHPC overlay with changing the ratio of steel fiber (0.5, 1.5, and 2) %		The highest strengthening ratio obtained with 2% of steel fiber volume
		U shaped Jacketing with UHPC		U-Shaped jacketing, (strengthened

Paper	Substrate	Strengthening	Preparation	Result
		(thickness of base and thickness of side- 20 by 20, 40 by 20, 40 by 40) mm		in both flexural and shear) increases strength, stiffness, and ductility more than others
		U shaped Jacketing with additional wire mesh		Wire mesh addition hasn't significant effect, didn't help to improve any performance
		U shaped Jacketing with additional rebar		The addition of a steel bar provides a good combination with UHPC
		Overlay with U shaped Aramid FRP sheet		Has a little increase in strength

## 2.7 Summarization

Almost all studies discussed the benefits of using UHPC for overlay application, but the lack of knowledge on the parameters that have an influence on this process sometimes makes it difficult to use UHPC for overlaying. Based on previous studies, it has been found that the structural performance of bridge deck slabs overlaying UHPC requires further investigation due to the lack of established design guidelines. There exist many studies that focused on using different pattern shapes at the interface to obtain good bond strength, but it still needs investigation. The following section discusses the influence of using a mechanical connector at the interface, the thickness of the overlay, and the compressive strength of the substrate and overlay.



## **3 CHAPTER THREE**

### **3.1 Experimental Program**

To characterize the strength and behavior of reinforced concrete bridge deck slabs overlay with UHPC a total of seventeen 1500 mm length by 500 mm width one-way slabs were cast and tested up to failure with variable thickness. Three types of concrete were experimented in this study, substrate material made of NSC and overlay materials made of HPC and UHPC with depending on some variables. The main objective of the testing was to investigate the structural behavior of the bridge deck slab when overlaid with UHPC.

### **3.2 Concrete Compositions and Materials**

#### **3.2.1 Concrete Types**

In the practical point of view trial mixes were performed for three types of concrete depending on the compressive strength as presented below:

##### **3.2.1.1 Normal Strength Concrete (NSC)**

This concrete type is designed to be used as a substrate material which includes conventional materials; cement, sand, aggregate, and water. A maximum aggregate size of 12.5 mm was used in this mix and cured at 28 days of normal 20 °C water curing, that the idea temperature for curing is between 10-32 °C (Kim and Rens, 2008). Also, NSC experimented to obtain three different types of compressive strengths that include of (20, 30 and 40) MPa.

### **3.2.1.2 High Performance Concrete (HPC)**

This concrete mix was designed to be used for an overlay which was produced by using the same materials that were used for NSC, but with a different mix proportion and with the addition of high range water reducer (HRWR) and Silica fume. Generally, HPC has higher compressive strength compared with NSC, this increment in strength is obtained with higher cement content, lower w/c ratio, and using HRWR superplasticizer to increase workability. According to ASTM C39/C39M (2017), HPC must have a compressive strength between 70 and 140 MPa at 28 to 91 days, along with a number of additional qualities like high flexural strength, low permeability, low shrinkage, and many others. However, not all of these properties can be attained together.

### **3.2.1.3 Ultra-High Performance Concrete (UHPC)**

UHPC is the essential type of concrete that is used for overlay application in this study. Over fifteen trial mixes have been completed to produce this type of concrete using the following materials: cement, fine sand, silica fume, steel fiber, HRWR, and water. Silica fume is used to increase compressive strength, and steel fiber is used to increase tension and bond strength. A low quantity of water in the w/c ratio was used to reduce porosity, but this low quantity of water reduced workability, which is why HRWR is used to increase workability. Also, high-temperature water curing was used for the first four days to accelerate hydration.

### 3.2.2 Materials:

#### 3.2.2.1 Cement

The essential binder material used for all types of concrete is Ordinary Portland Cement (CIMKO-TS EN 197-1 CEM-I 42.5 R). The chemical properties are shown in Table 3-1 and physical properties of the cement are shown in Table 3-2.

Table 3-1: Chemical Analysis of Cement

<b>Cement contents %</b>	<b>Results*</b>	<b>(ASTM C150/C150M, 2017)</b>
<b>Typical oxide composition percent %</b>		
CaO	63	
SiO <sub>2</sub>	20	
Al <sub>2</sub> O <sub>3</sub>	6	
Fe <sub>2</sub> O <sub>3</sub>	3	
MgO	1.5	6.00 max.
SO <sub>3</sub>	2	3.00 max.
K <sub>2</sub> O	1	
Na <sub>2</sub> O	1	
Others	1	
Loss on ignition	2	3.00 max.
Insoluble residue	0.5	0.75 max.
<b>Compound composition %</b>		
C <sub>3</sub> A	10.8	
C <sub>3</sub> S	54.1	
C <sub>2</sub> S	16.6	
C <sub>4</sub> AF	9.1	
Minor compounds	-	

\*Tested by Directory of Lafarge Laboratory-Hawler.

Table 3-2: Physical properties of the cement

<b>Physical tests</b>	<b>Results*</b>	<b>(ASTM C150/C150M, 2017)</b>
Initial setting time	120 minutes	$\geq 45$ minutes
Final setting time	160 minutes	$\leq 375$ minutes
Specific Surface	240 $m^2/kg$	160 $m^2/kg$ , lower limit
3 days Compressive Strength	18.7 MPa	$\geq 12$ MPa
7 days Compressive Strength	27.3 MPa	$\geq 19$ MPa

\*Tested by Directory of Erbil Polytechnique University Laboratory

### 3.2.2.2 Silica Fume

Silica Fume is a binder material that can be added directly to concrete or combined with cement, it is used to enhance concrete properties (Aldred et al., 2006). The silica fume used in the present study is type (ECA MICRO SILICA-D), a dry densified silica fume powder that is designed to increase compressive and flexural strengths, reduce permeability, and increase durability; the properties are presented in APPENDIX A. The physical and chemical properties are shown in Table 3-3 and Table 3-4.

Table 3-3: Physical properties of the Silica fume

<b>Physical properties</b>	<b>Results*</b>	<b>(ASTM C1240, 2017)</b>
Appearance	Ultra-fine amorphous light to dark grey, colored powder	Light to dark gray
Specific Gravity	2.25 $\pm$ 15 % at 20°C	Approximately 2.2
Bulk Density	$\geq 650$ kg/m <sup>3</sup>	(130-430) $kg/m^3$
Freezing Point	N.A	
Air Entrainment	Nil.	

N.A-Not Available

\*Provided by manufacturer: [www.alfaihaengineering.com](http://www.alfaihaengineering.com)

Table 3-4: Chemical Analysis of Silica fume

Cement contents %	Results*	(ASTM C1240, 2017)
SiO <sub>2</sub>	90 % min	85 min.
Sulphate Content	<1.0% as S03	

\*Provided by manufacturer: [www.alfaihaengineering.com](http://www.alfaihaengineering.com)

### 3.2.2.3 Normal Sand

The normal sand used in this study was obtained from the aski-kalak quarry. Which was washed and then dried in the oven for one day according to the (ASTM C33/C33M, 2016). The grading of sand with upper and lower limits of ASTM C33 are shown in Table 3-5 and Figure 3.1.

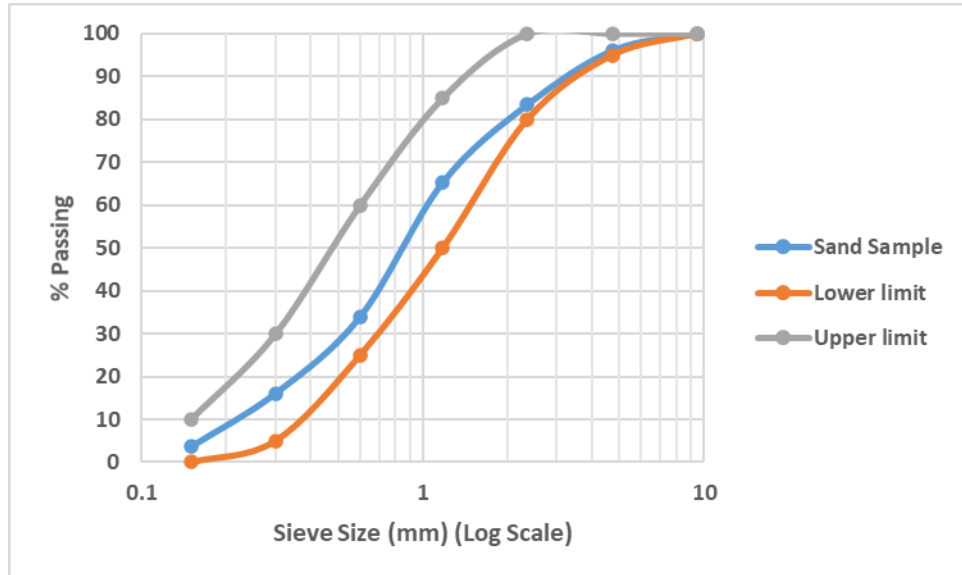


Figure 3.1: Grading of Normal Sand with ASTM C33 limits

Table 3-5: Grading of Aggregates with ASTM C33 Limits

<b>Aggregates</b>	<b>Sieve Size</b>	12.5	9.50	4.75	2.36	1.18	0.60	0.30	0.15
<b>Gravel</b>	Upper limit	100	90	40	0	0			
	% Passing	100	95.11	59.8	8.54	0.008			
	Lower limit	100	100	70	15	5			
<b>Normal sand</b>	Upper limit		100	95	80	50	25	5	0
	% Passing		100	96	83.4	65.3	34	16.13	3.7
	Lower limit		100	100	100	85	60	30	10
<b>Fine sand</b>	% Passing				100	78	62	37.4	0

#### 3.2.2.4 Fine Sand

The fine sand that was used in this study was obtained from the askikalak quarry, then washed, oven-dried, and sieved with a sieve number (2.36) mm as shown in Table 3-5. This type of good grading of sand is used to produce UHPC particularly.

#### 3.2.2.5 Coarse Aggregate

The type of aggregate used in this study was obtained from the askikalak quarry with a maximum size of 12.5 mm, which was washed and oven dried before sieve analysis to satisfy (ASTM C33/C33M, 2016). The grading of aggregate with upper and lower limits of ASTM C33 are shown in Table 3-5 and Figure 3.2.

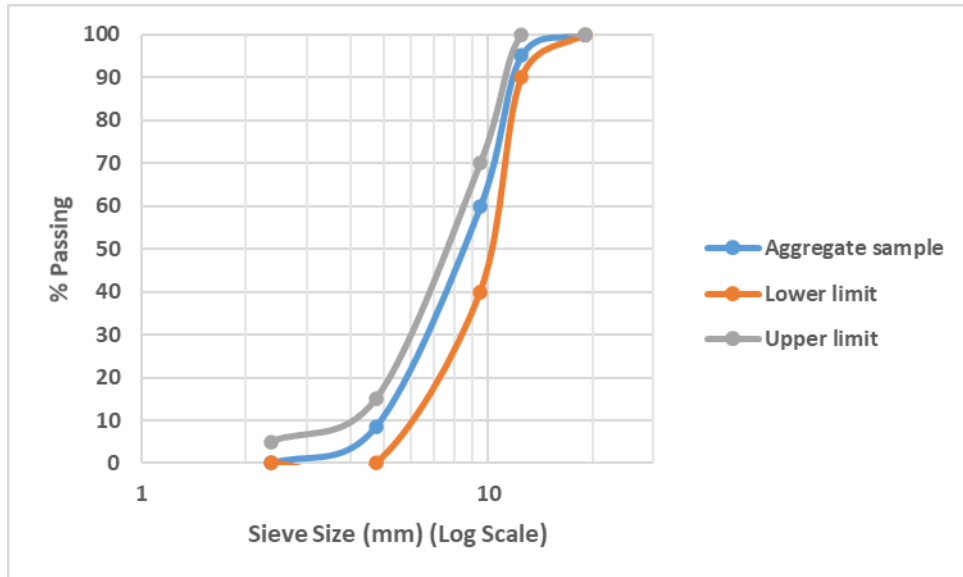


Figure 3.2: Grading of Gravels with ASTM C33 limits

### 3.2.2.6 Superplasticizer

Due to the low w/c ratio of UHPC superplasticizer admixture is used to increase workability. In this study two types of admixture were experimented with, type one was hyperplast PC800M, and type two was sika viscocrete whose properties and instructions for use are presented in APPENDIX A.

### 3.2.2.7 Water

For washing materials, mixing, and curing all types of concrete clean water was used which was free from injurious amounts of oil, organic materials, and other deleterious substances.

### 3.2.2.8 Steel Fiber

Steel fiber is used in the production of UHPC to obtain excellent tensile, bending, and shearing strength and to create resistance against cracking. The type of steel fiber that used in this study is china's steel fiber in the

production of H7 which was achieved by sika company in baghdad governorate, the properties of steel fiber obtained from its datasheet as presented in APPENDIX A and clarified below:

- Type: Micro steel fiber
- Material: Low carbon steel wire, copper coated
- Diameter: 0.2 mm- 0.25mm
- Length: 12 mm-14mm
- Tensile strength: > 2850 MPa

### 3.2.2.9 Steel Reinforcing Bar

All slabs are reinforced with one layer of deformed Ø10 mm bars size in the transverse direction at tension zone with 25 mm clear cover. The properties of the Ø10 mm bar size obtained from the tension test as presented in Table 3-6:

Table 3-6: Properties of the Reinforcing Steel Bar

<b>Properties</b>	<b>Yield</b>	<b>Ultimate</b>	<b>Ultimate (ASTM 615/A 615M, 2004)</b>
Stress (MPa)	453	602	593
Strain (mm/mm)	0.0021	0.0049	0.0039
Modulus of Elasticity (GPa)	215.7		

## 3.3 Mix Details

### 3.3.1 Mix Proportions

The constituent material proportions were determined based on the regular particle packing density to minimize the weakening points. From



the practical point of view, a total of twenty-three trial mixes have been performed for all concrete types. For each trial, six 10X10X10 cm cubes were cast to test their compressive strength at ages 7, 28, and 56 days. In the beginning, ACI 318R-19 (2019) design method was used to obtain the required strength for substrate concretes. The conventional materials used to produce NSC consist of cement, normal sand, gravel, and water. These mixtures are cured at room temperature, with water curing at 20 degrees Celsius. The constituents for each trial are shown in the Table 3-8.

Two trials have been carried out to obtain the required strength for the HPC overlay. For this purpose, the quantity of cement was increased, the w/c ratio decreased, and a low quantity of superplasticizer admixture was added to the mixes to obtain the required workability. Also, in one of the mixes, the addition of a low quantity of silica fume with cement binder was experimentally evaluated. The constituents of each mix can be shown in the Table 3-9.

To produce UHPC as an overlay material, a total of fifteen trial mixes have been performed as presented in Table 3-7 which were divided into four groups. Also the materials that used are presented in Figure 3.3. UHPC1 through UHPC7 represent the first group, which includes the same proportion of cement, fine sand, and silica fume but eliminates coarse aggregate. In this group, the addition of steel fiber, HRWR, and w/c ratio with variable proportions were investigated experimentally. Two quantities of steel fiber were evaluated at 0.1 and 0.2; the HRWR/c ratio was examined from 0.03 to 0.05, and the w/b ratio was studied from 0.15 to 0.24. All of the increases in the proportions occurred gradually to optimize the optimum one.

The UHPC8–UHPC10 groups represent trial mixes for the second group, in which the binder ratio increased and the amount of fine sand

decreased compared to the first group. In the second group, the values of the w/b ratio and fiber/c ratio remained constant at 0.2 for both, but the value of the HRWR/c ratio increased from 0.04 to 0.08 gradually.

In the first and second groups, participants understood that 0.2 percent of steel fiber can reach the optimum mix, but different proportions of type 1 water reducer couldn't reach the optimum amount because the initial setting time was delayed by more than three days.

In the UHPC11 and UHPC12 trial mixes, gravel was added to the concrete to evaluate its effect on UHPC strength, and the second type of water reducer was evaluated. At this stage, it was understood that with the second type of water reducer, adequate workability was obtained with a lower quantity, but even the initial setting time increased to more than two days. Also, the addition of gravel produced pores inside the concrete and reduced its compressive strength.

In UHPC13 to UHPC15 trial mixes optimum mix was obtained for UHPC depending on the last three groups' experience. The problem of the delayed setting time was solved with the addition of grouting material which increased compressive strength and initial setting time to the first ten hours. The constituents for all trials can be shown in the Table 3-7.

In addition, UHPC and HPC trial mixes were cured at hot temperature water curing at 80 °C for the first three days to accelerate chemical reactions and obtained higher strength at an earlier age, then put into the normal temperature water curing until the day of the test. In the curing process for the first three groups of UHPC, it was noticed that due to power outages, concrete cubes experienced a cooling shock and decreased compressive strength significantly. Then this problem is solved and the required strength is obtained.

Table 3-7: Trial mixes for UHPC overlay

Trial no.	Curing Regime	Binders			Aggregate		Steel fiber	Water	Superplasticizer	
		Cement Kg/m <sup>3</sup>	Silica fume Kg/m <sup>3</sup>	Grout Kg/m <sup>3</sup>	Sand Kg/m <sup>3</sup>	Gravel Kg/m <sup>3</sup>	Fiber/c	w/b	Type1 HRWR/c	Type2 HRWR/c
UHPC1	Curing1	795.92	107.78	-	1282.32	-	0.2	0.158	0.05	
UHPC 2		795.92	107.78	-	1282.32	-	0.2	0.176	0.05	
UHPC 3		795.92	107.78	-	1282.32	-	0.2	0.211	0.05	
UHPC 4		795.92	107.78	-	1282.32	-	0.2	0.246	0.05	
UHPC 5		795.92	107.78	-	1282.32	-	0.1	0.211	0.05	
UHPC 6		795.92	107.78	-	1282.32	-	0.2	0.246	0.03	
UHPC 7		795.92	107.78	-	1282.32	-	0.2	0.211	0.04	
UHPC 8		951.65	128.86	-	1057.39	-	0.2	0.2	0.04	
UHPC 9		951.65	128.86	-	1057.39	-	0.2	0.2	0.06	
UHPC 10		951.65	128.86	-	1057.39	-	0.2	0.2	0.08	
UHPC 11	Curing1	433	35	-	909	1039	0.1	0.28		0.01
UHPC 12		457	55	-	960	1096	0.1	0.25		0.01
UHPC 13	Curing2	795.92	159	-	1192.5	-	-	0.219		0.01
UHPC 14		795.92	159	79.5	1192.5	-	-	0.23		0.017
UHPC 15*		795.92	159	79.5	1192.5	-	0.2	0.23		0.017

\* Mix proportions selected for casting slab specimens; based on cube (10x10x10) cm compressive strength

HRWR: High Range Water Reducer, w: water, c: cement, b: binder

Curing1: Hot temperature water curing at 80 °C for the first three days, that faced to the loss of electricity several times.

Curing2: Control hot temperature water curing at 80 °C for the first three days.

Type1 HRWR: Hyperplast PC800M

Type2 HRWR: Sika ViscoCrete

Table 3-8: Trial mixes for the substrate material

Trial no.	Curing regime	Binder	Aggregates		Water
		Cement Kg/m <sup>3</sup>	Sand Kg/m <sup>3</sup>	Gravel Kg/m <sup>3</sup>	w/c ratio
NSC1	Normal 28 days water curing	500	893.4	795	0.43
NSC2		430	952.1	795	0.5
NSC3		565.8	837.4	795	0.38
NSC4*		364.8	810.67	1368	0.5
NSC5*		300	750	900	0.45
NSC6*		273.6	912	1368	0.75

\*Mix proportions selected for casting slab specimens; based on cube (10x10x10) cm compressive strength

w: water, c: cement

Table 3-9: Trial mixes for HPC overlay

Trial no.	Curing regime	Binder		Aggregates		Water	Superplasticizer
		Cement Kg/m <sup>3</sup>	Silica Fume Kg/m <sup>3</sup>	Sand Kg/m <sup>3</sup>	Gravel Kg/m <sup>3</sup>	w/c ratio	Type2 HRWR/c
HPC1	Hot water curing at 80 °C for two days	521.14	-	810.67	1172.5	0.28	0.01
HPC2*		541.78	9.78	722.37	1219	0.32	0.005

\* Mix proportions selected for casting slab specimens; based on cube (10x10x10) cm compressive strength

w: water, c: cement, HRWR: High Range Water Reducer

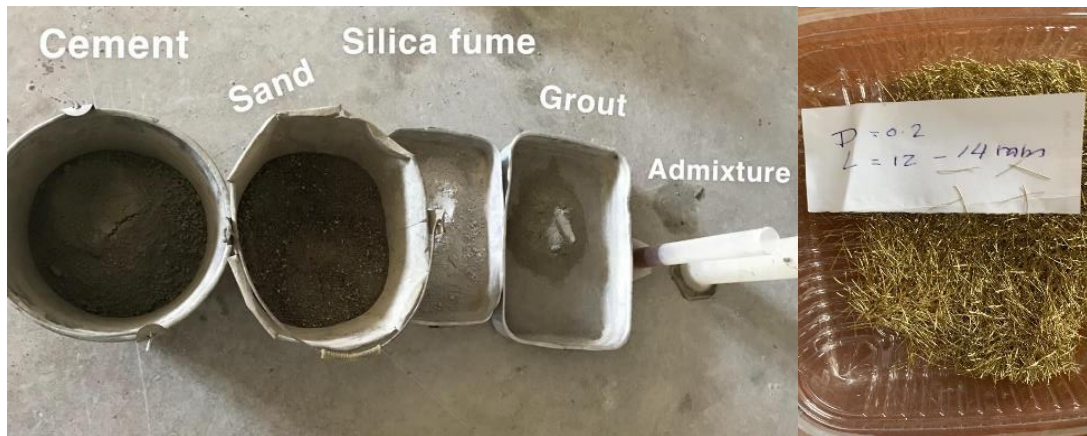


Figure 3.3: Materials used: Cement, Sand, Silica fume, Grout, Superplasticizer admixture and Steel fiber

### 3.3.2 Mixing Procedure

Concrete is one of the most demanding materials for construction. To obtain the concrete mix as pre-designed, the ingredients have to be mixed properly with each other otherwise very poor-quality concrete may be obtained that isn't qualified to be called concrete. Concrete mixer is the machine that helps in mixing the ingredients of concrete, mixing is the heart of concrete and it helps to produce workable concrete. In addition, mixing time and mixing tool speed have a great influence on the properties of concrete, for example, optimal flowability can be obtained with 240 s at

a mixing speed of 1.3 m/s, and overmixing led to loss of flowability. In another hand, concrete compositions affect mixing time, for example increasing the mixing speed of UHPC to 2.9 m/s reduces the time to 90s. If compared with conventional concrete, increasing the mixing speed of UHPC will reduce mixing time with a lower value due to dense ingredients (Schießl et al., 2007). There exist different types of concrete mixer, in this study Tilting mixer is used which consists of a bowl-shaped drum with vanes inside. The mixer has the capacity of 125 lt. and (600X1100X1250) mm dimensions. The fiber used in this study is easily dispersed because it has an aspect ratio of 57 which according to Daniel et al. (2002)'s study balling of steel fiber can be avoided with an aspect ratio less than 50.

The mixing procedure for conventional concrete was started with mixing dry materials in a tilting mixer for two minutes then water was added gradually until a homogeneous mix has been obtained after 20 minutes. Also, for HPC the same procedure has been repeated except that water is added into the mix in two steps, in the first step 75% of water is added gradually and the remained amount of water is mixed with HRWR superplasticizer in a glass container for two minutes then added into the concrete gradually in the second step. From the experimental point of view considered that mixing procedure for UHPC required significant knowledge which is explained below:

- Dry materials cement, fine sand, and silica fume are mixed in the tilting mixer for two minutes.
- Through the continuous mixing 75% of water separated onto the dry materials gradually for four minutes.
- The remained amount of water mixed with HRWR superplasticizer admixture in a glass container until soluble well then added into the

mix gradually for 2 minutes because if HRWR is added directly to the concrete ingredients the agglomeration of silica fume may occur.

- The steel fiber is added to the concrete after step two continuously.
- UHPC mixing has to be continued for 20 minutes but the nature of this concrete type requires a 1.5-minute break before the last 3 minutes of mixing to complete its special chemical reaction. Finally, homogeneous UHPC is produced in the form of honey.

### **3.4 Selection of Bridge Deck Slab Specimen**

The specimen could be regarded as the one-second scale of a prototype structure which consists of a one-half bridge deck slab with the dimensions of 3000 mm wide, 8200 mm in length, and 220 mm thickness as shown in Figure 3.4 and Figure 3.5. One meter has been taken along the entire length of the slab for representing the prototype structure.

The thickness of the slab selected according to ACI 318R-19 (2019) for a solid no prestressed one-way slabs with simple support along two opposite edges. The dimensions and reinforcement details of the typical test specimen are shown in Figure 3.5 that designed according to section 13.2 design of One-Way slab Darwin et al. (2016), the sample specimen with 1500 mm length, 500 mm width, and 110 mm thickness have planned for experiment and reinforced with ( $\phi$  10 mm of bar size at 150 mm c/c) in transverse direction except for extra reinforcement at support conditions ( $\phi$  10 mm at 62.5 mm c/c).

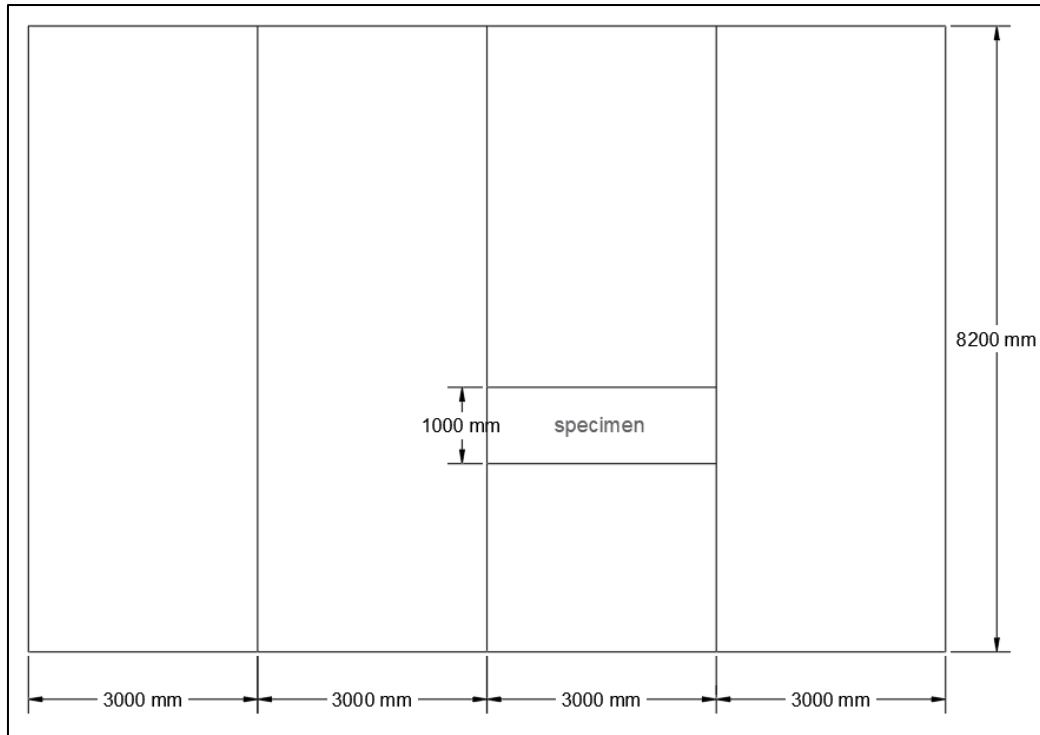


Figure 3.4: Prototype of Bridge Deck Slab System and Selected Specimen

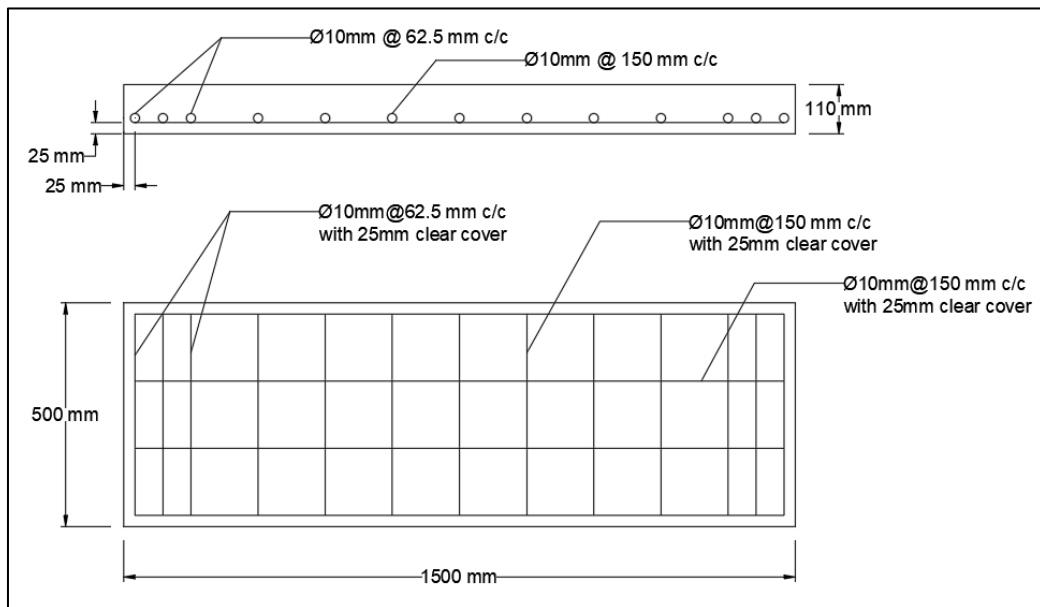


Figure 3.5: Dimensions and Reinforcement of Typical Specimen

### 3.5 Variables and Details

The experimental work of this investigation was based on casting and testing seventeen concrete slabs divided into six groups G1, G2, G3, G4, G5, and G6, as illustrated in Table 3-10, to investigate the effects of the following variables depending on the control specimen :

1. Overlay thickness varied from 20 to 50 mm.
2. In addition, a layer of steel in the transverse direction with an overlay to obtain protection and resistance, 5 mm of rebar diameter at 50, 100, and 150 mm spaces are used for this purpose. This layer of steel embedded into the substrate concrete layer with the using of cross head bolt and washer as presented in
3. Figure 3.6.
4. Four types of substrate surface layouts were investigated which consist of rough, horizontal grooves, vertical grooves, cross hatch, and diagonal grooves at 45° inclined as presented in
5. Figure 3.7, the texture depth was between 3-4 mm.
6. Substrate material compressive strength varied from 21 to 40 MPa.
7. Overlay material compressive strength varied from 30 to 130 MPa.
8. To investigate the bonding strength screw anchor have used with rough surface preparation, that consist of three-rows of anchors at 228 mm and two-rows of the anchor at 228 mm as presented in Figure 3.8. Three days before overlay application, holes created at substrate with diameter 6 mm and depth 65 mm. Then the screw anchors with the dimensions 5 mm diameter and 80 mm length used for this purpose, that 60 mm in its length embedded into the holes with using epoxy and 20 mm remained at top to be locate into the overlay.



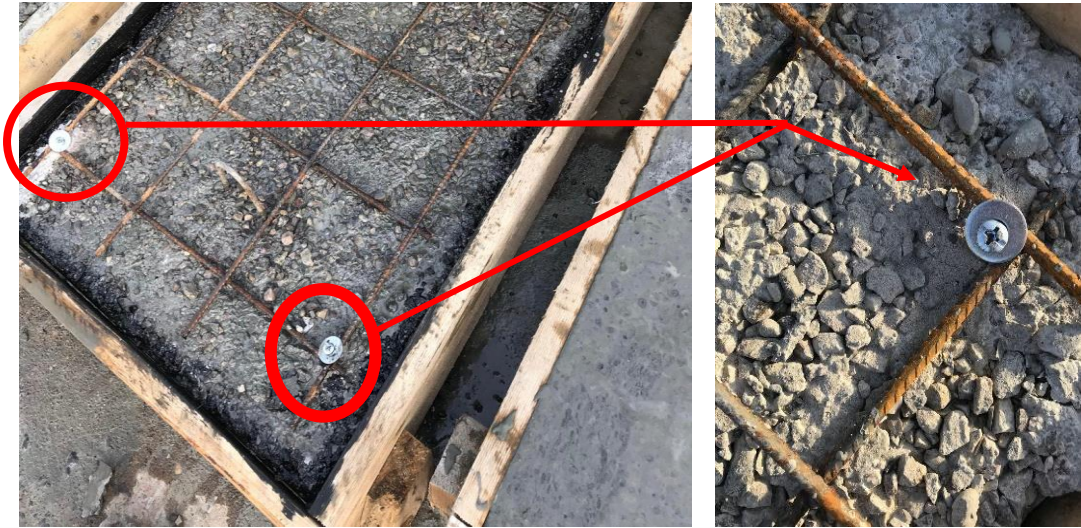


Figure 3.6: Steel layer embedded into the substrate concrete through the steel bolt and washer

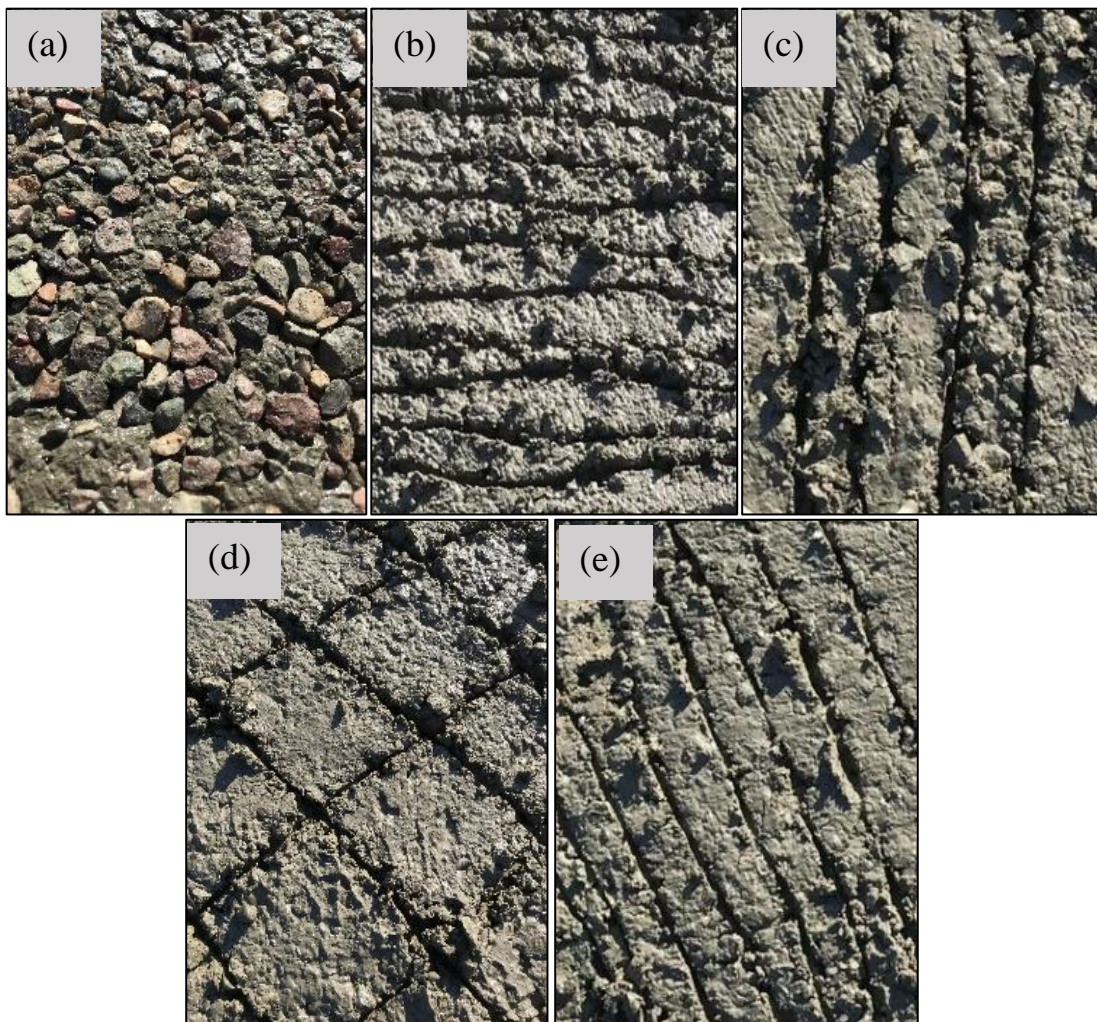


Figure 3.7: Substrate surface textures: (a) Rough, (b) Horizontal, (c) Vertical, (d) Cross Hatch and (e) Diagonal Groove

Table 3-10: The Characteristics of the Tested Slabs

Group no.	Variables						
	Specimen	UHPC overlay for Protective- thickness (mm)	R-UHPC overlay with steel rebar for Protective and Resistance	Substrate Surface layout	Substrate material- attempt NSC Compressive Strength MPa	Attempt UHPC Compressive Strength MPa	Screw Anchor with Diam. (5) mm and Length (80) mm
<b>Ctr.</b>	1	30	NR	Rough	30	140	NA
<b>G1</b>	2	20	NR	Rough	30	140	NA
	3	40	NR	Rough	30	140	NA
	4	50	NR	Rough	30	140	NA
<b>G2</b>	5	30	5mm @ 50 mm	Rough	30	140	NA
	6	30	5mm @ 100 mm	Rough	30	140	NA
	7	30	5mm @ 150 mm	Rough	30	140	NA
<b>G3</b>	8	30	NR	Horizontal Groove	30	140	NA
	9	30	NR	Vertical Groove	30	140	NA
	10	30	NR	Cross Hatch	30	140	NA
	11	30	NR	Diagonal Groove @ 45° inclined	30	140	NA
<b>G4</b>	12	30	NR	Rough	21	140	NA
	13	30	NR	Rough	40	140	NA
<b>G5</b>	14	30	NR	Rough	30	30	NA
	15	30	NR	Rough	30	80	NA
<b>G6</b>	16	30	NR	Rough	30	140	Three rows of anchor at 228 mm
	17	30	NR	Rough	30	140	Two rows of anchor at 228 mm

NR: No Reinforcement, NA: No Anchor



Figure 3.8: Anchor bolt embedded into the substrate concrete, (Left: three rows at 228 mm) and (Right: two rows at 228 mm)

### 3.6 Slab Specimen Molds

Molds used for casting slab specimens were made from smooth 25 mm thickness white oak wood with the clear dimensions of the molds 1500X500X110 mm for casting substrate concrete. Details of the molds are shown in Figure 3.9. Four sides of the molds could move to cast the overlay concrete. Plywood was used for rectangular mold with clear dimensions of 75X75X300 mm to take specimens for a flexural test. Plastic molds with square and cylinder shapes were used to take specimens for compressive, tensile, shear, and permeability strength with the dimensions of; 100X100X100 mm for cube specimens and 150X300 mm for cylinder specimens.



Figure 3.9: Slab mold used in this study

### 3.7 Casting of Specimens

Casting of specimens include of two stages, first stage was casting substrate concrete; when the concrete mix became ready, the batch was cast in the slab molds with taken control specimen for each batch. The second stage was casting overlay concrete which started after 28 days of substrate casting, also three days before overlay casting the substrate surfaces prepared for the purpose of investigation and the molds are prepared for overlay application. After placing concrete in the mold vibrating stage started immediately with 180 seconds to remove internal air voids aside and prevent fibers orientation or sedimentation on another side, vibrating rod was used for substrate material and overlay material. Figure 3.10 and Figure 3.11 shows substrate and overlay casting. Five minutes before overlay casting the bonding slurry separated over the substrate concrete in order to improve bonding strength with the amounts of 1:0.08 cement and silica fume, 0.005 HRWR/c high range water reducer per cement ratio, and 0.8 w/c water per cement ratio.



Figure 3.10: Casting substrate concrete



Figure 3.11: Casting overlay concrete

### 3.8 Curing Processes

The substrate concrete and its control specimens were cured with clean water for seven days then covered with nylon until 28 days because nylon prevents contact outside moisture with slabs and retain moisture in the slabs, therefore the concrete continued to gain strength. After overlay application with UHPC and HPC on the NSC, the slabs with overlay control specimens were cured in the hot water tank with an average

temperature of 80°C for 3 days as shown in Figure 3.12. After heat treatment the slabs were left in the water tank for a day until they were cooled to avoid the problem of cooling shock because the cooling shock affects the concrete properties too much, then the slabs were taken out from the tank and covered with wet burlap until the date of testing.



Figure 3.12: Water tank for slab specimens

### **3.9 Test Measurements and Instruments**

#### **3.9.1 Load Measurements**

The slab specimens were tested in a self-supporting steel frame through a hydraulic jack of 250 kN capacity. The control specimens were tested by amsler testing machine of 2000 kN capacity. The entire testing machines

are available in the structural laboratory at the department of civil engineering in university of Salahuddin, as shown in

Figure 3.13.



Figure 3.13: Details of the testing machine (Salahuddin university laboratory)

### 3.9.2 Deflection Measurements

A dial gauge of 0.01 mm sensitivity with 30 mm maximum travel was used to measure the central deflection of the slab specimens, as shown in Figure 3.14.

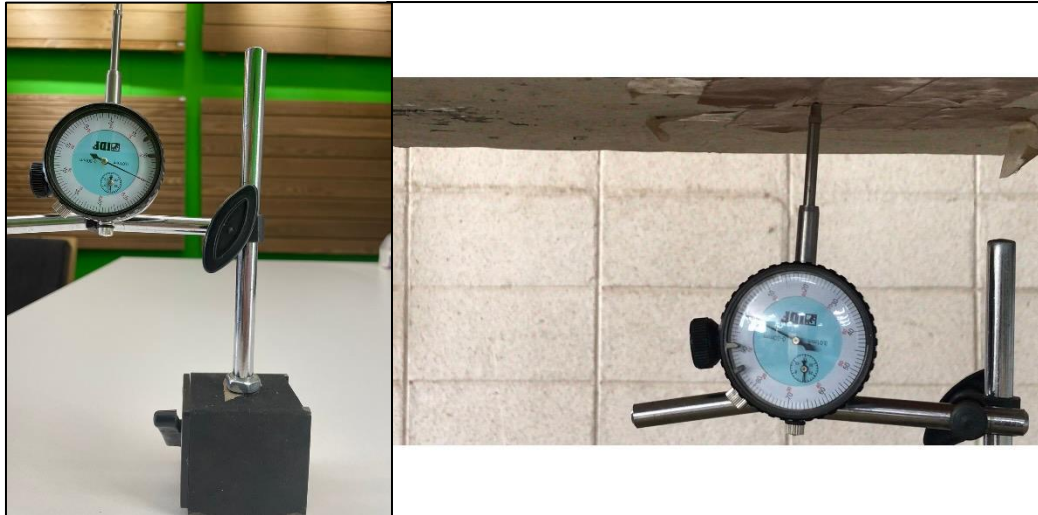


Figure 3.14: Dial gauge

### 3.9.3 Concrete Strain Measurements

Electronic strain gauges of type BE120-80AA-X-3.5 cm manufactured by HT sensor technology company with length eight centimeter has been used for measuring the tensile strains and compression strain of concrete to obtain more accurate results. Two strain gauges are used in tension zone and one strain gauge at compression zone. However, as they were proportionally more difficult to procure, a lower number was employed. The strain gauge shape is shown in Figure 3.16 and the locations of electronic strain gauges in slab specimens are shown in Figure 3.15. Also, the more details of electronic concrete strain gauges are given in APPENDIX A.

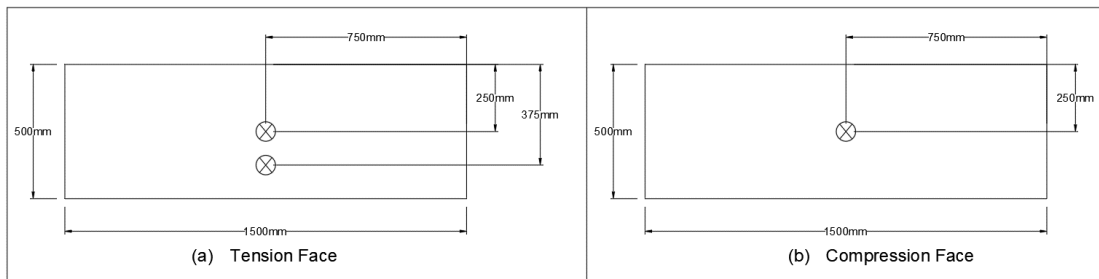


Figure 3.15: Locations of concrete strain gauges in slab specimens



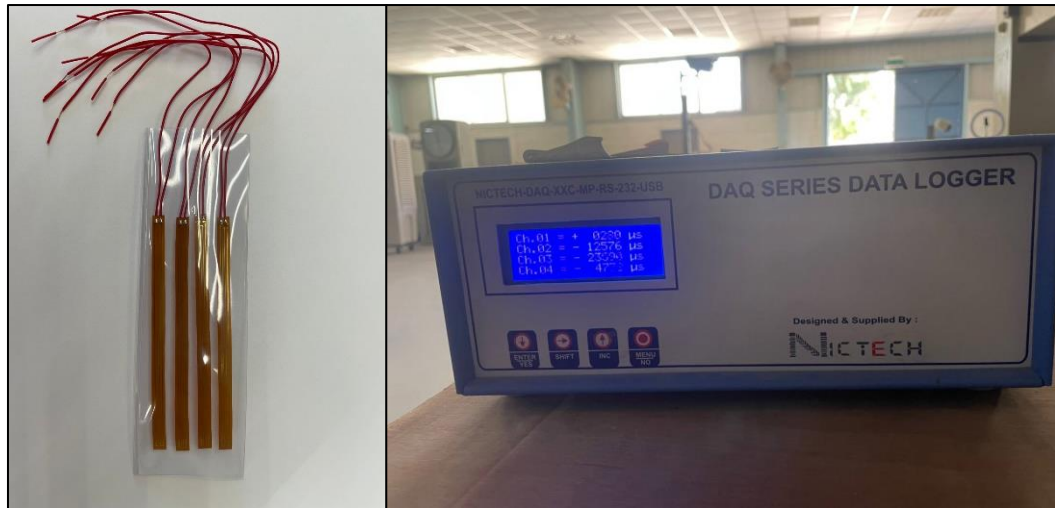


Figure 3.16: Strain gauge and data logger

### 3.10 Age of Concrete Specimens at Testing

The 28-day test age for concrete specimens has generally produced favorable results for concrete within lower strength levels that don't call for early strengths or early evaluation. At older ages, HPC becomes significantly stronger. As a result, it is commonly evaluated at intervals like 56 or 90 days. In selecting mix proportions, the type of curing anticipated should be considered along with the test age, since concrete gain strength as a function of maturity, which is usually defined as a function of time and curing temperature (ACI 363R-92, 1997). UHPC is somewhat different in this manner from conventional concrete mixes because in this type of concrete the stabilization is complete at an early age. UHPC gain approximately 90 % of its 28 days compressive strength and other mechanical properties, with no further expansion or shrinkage as the heat treatment finished (Graybeal, 2006). Initially, the plan was to perform the testing of one way slab specimens at 56 days age, but after casting of specimens was completed and 56 days passed, it was found that; due to some problems the testing machine of Erbil polytechnic university laboratory can't be used; that is why the decision of testing the slab

specimens in Salahuddin university laboratory was cause to delay the testing till the specimen's age reaches 90 days. Fortunately, at these ages, there are no considerable changes in concrete properties because we had extra control specimens that tested in 90 days, we observed about a 4 MPa increase in compressive strength, and hot temperature water curing at early ages leads to concrete obtaining 90% of its strength.

### **3.11 Testing Procedure for Slab Specimens**

Two days before testing, the tension faces of slabs were cleaned and painted white in order to help in locating cracks and taking photographs. The slabs were tested in an inverted position. Before testing, the supports, applied load and dial gauge position were adjusted as shown Figure 3.17, also the position of the strain gauges were attached and checked. The vertical load was applied and divided into two-line loads on one-way slab specimens along the short direction in increments. The load was increased by an equal constant increment of 10 kN. At each load stage the deflection and strains were recorded, also a search was made for the appearance of any cracks. The positions and extents of the first visible and other consequent cracks were marked. As the failure was reached, the failure load was recorded, and the load was removed to allow taking photographs of the final crack patterns. The time spent in testing one specimen slab was about 30 to 60 minutes.

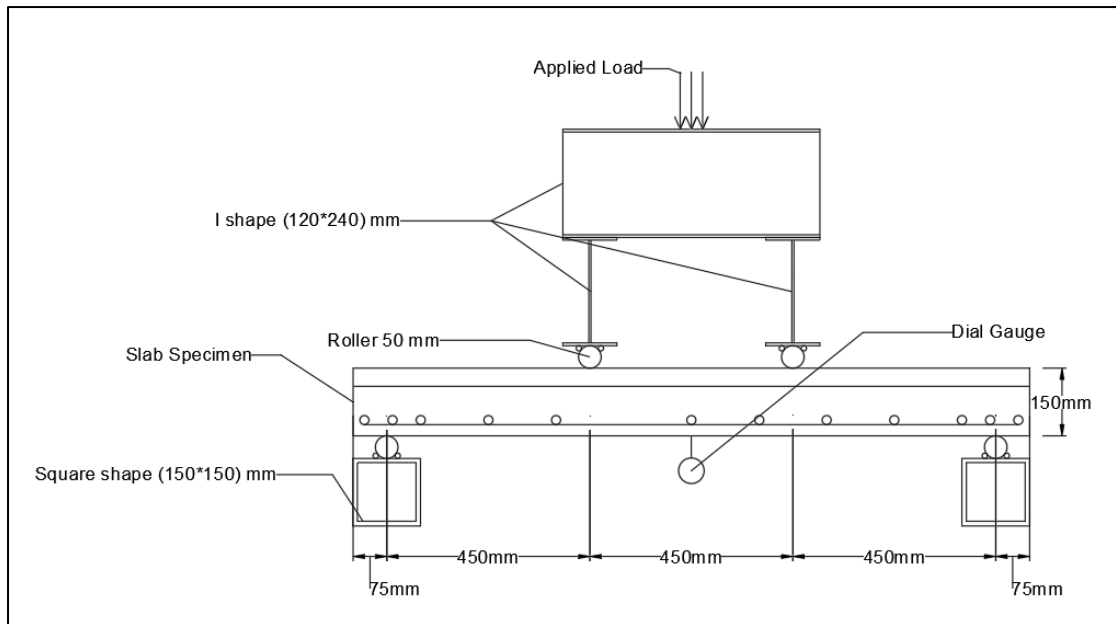


Figure 3.17: Loading arrangement of the tested slabs

### 3.12 Properties of Specimen's Concrete Mixes

#### 3.12.1 Compressive Strength

For determination of compressive strength, a testing machine was used with a maximum capacity of 2000 kN. For testing NSC compressive strength cylinder specimen  $\text{Ø}150/300$  mm according to ASTM C39/C39M (2017) was used to obtain accurate results because the cylinder is the standard specimen geometry for concrete compression test (Graybeal, 2006). For testing UHPC compressive strength, a cube specimen  $100 \times 100 \times 100$  mm according to ASTM C109/C109M (2016) was used for 200 MPa by dividing the maximum capacity by the area of the specimen. Because the cube compression test result is higher than the cylinder compression test result, the strength reduction factor must be used for cube specimens. This component is influenced by numerous concrete properties (Graybeal, 2006). De Larrard et al. (1994) defined that strength reduction

value is approximately equal to 0.82 for normal-weight concrete and approaches one with increasing compressive strengths for HPC and UHPC (De Larrard et al., 1994, Weiße and Holschemacher, 2003, Graybeal, 2006).

### **3.12.2 Splitting Tensile Strength**

Tests were carried out on Ø100/200 mm cylindrical specimens according to ASTM C496 (1996) for NSC, HPC, and UHPC by placing wooden thin strips and supplement bars along the contact lines, then applying a compressive load along the entire length until failure occurs. Finally, the average splitting tensile strength was recorded for three-cylinder specimens.

### **3.12.3 Flexural Strength**

Flexural Strength was performed for three concrete types NSC, HPC, and UHPC according to ASTM C 1018 (1997). The mold size dimension of 75X75X300 mm was used for this test and the load was applied at the long middle third point and increased until failure occurs. Finally, the average flexural strength was recorded for three specimens.

### **3.12.4 Bond Strength**

For testing bond strength between two concrete types Slant Shear Test (SST) was conducted according to ASTM C882/C882M (2013), basically in this test procedure epoxy is used to obtain a good bond but in this study epoxy bonding agent isn't used rather than different substrate surface preparations were used to characterize the bond between the substrate and overlay material as shown in

Figure 3.19, the following substrate surface preparation evaluated; rough, horizontal groove, vertical groove, diagonal groove and cross hatch, with the texture depth between 3-5 mm. For this purpose, Ø100/200 mm cylinder was used and the half base of the mold was filled with NSC at a 60-degree angle from vertical as shown in Figure 3.18. After 24 hours removed from the mold and curried until 28 days age then turned back into the mold and the remained part of the mold was filled with UHPC, after the application of hot water treatment for UHPC, the specimens were left in the lab room until the day of the test. The compression testing machine was used for this test, in which the specimens were subject to both compression and shear to evaluate the optimum bond strength.

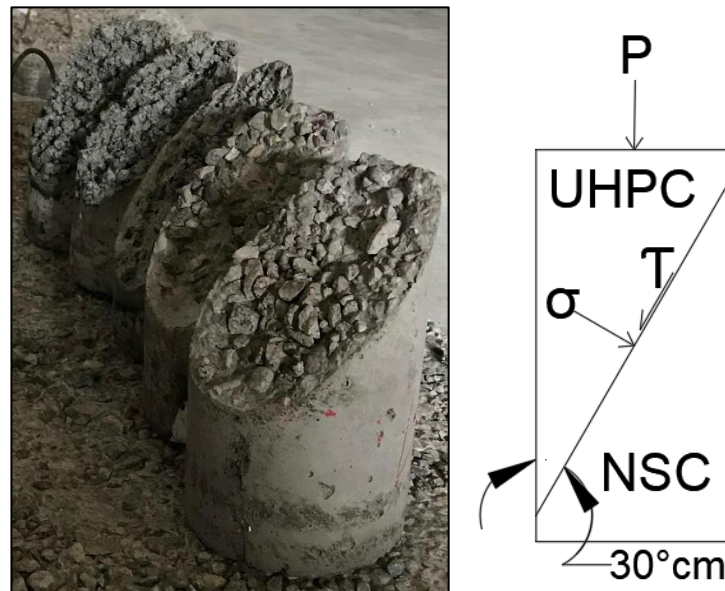


Figure 3.18: Half of cylinder filled with NSC at a 60-degree angle

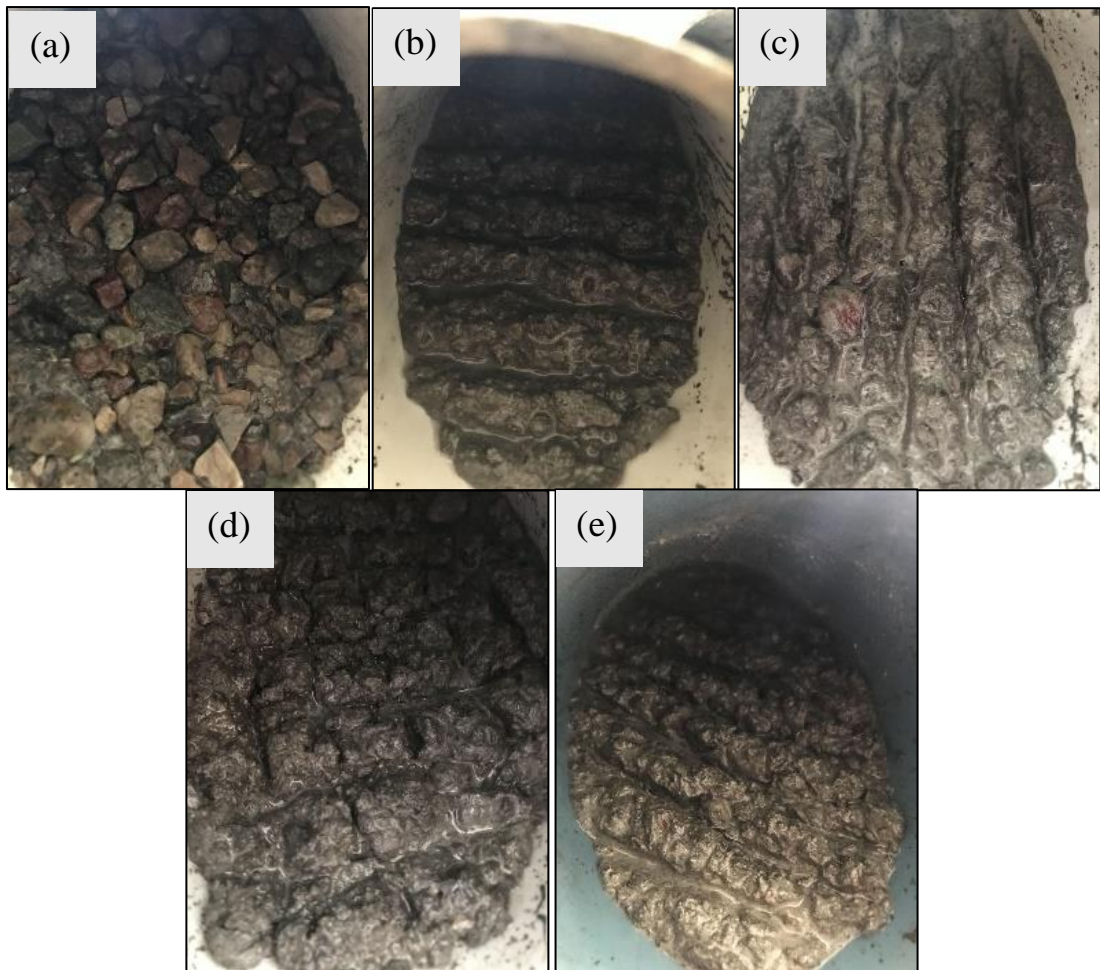


Figure 3.19: Types of substrate texture: (a) Rough, (b) Horizontal groove, (c) Vertical groove, (d) Cross hatch and (e) Diagonal groove

### 3.12.5 Permeability Strength

This test was performed for NSC, HPC, and UHPC in the 77 company's lab according to IS 516 (2018), for each type three cube specimens 150X150X150 mm were cast. For this test, water is used and performed at 28 days of age oven-dried for one day then left in the permeability machine for three days, pressure gauge is established on 550 kPa for 72 hours to calculate the coefficient of permeability.

## **4 CHAPTER FOUR**

### **4.1 Results and Discussion**

In order to choose the best mix, 26 trial mixes were tested for various properties on UHPC and compared to normal concrete mixes. The results are presented in this chapter.

Results of seventeen simply supported reinforced concrete one-way slab specimens subjected to vertical load through two central line load were discussed. Load versus deflection at the center of the loaded area, concrete strains in compression and tension faces of the slab were recorded for each slab specimen.

### **4.2 UHPC Properties and Comparisons**

UHPC properties were show an order of amount difference compared with conventional concrete mixes, and the main tested properties can be explained as the following:

#### **4.2.1 Compressive Strength**

##### **4.2.1.1 Trial Mixes**

The results of trial mixes for UHPC overlay are presented in Table 4-1 and trial mixes for the substrate material NSC are presented in Table 4-2 and trial mixes for HPC overlay are presented in Table 4-3, which show that: UHPC gave compressive strength 2 times higher than HPC and 4 times higher than NSC, and these ratios are higher in early ages. The rates of strength regularly increasing in all groups, except for UHPC, it should be observed that there was a proportionally less interesting increase in

strength with age. The three days compressive strength for UHPC isn't obtained for trials UHPC1 till UHPC12 because of delayed the initial setting time to more than three days and trial UHPC1 is failed because the quantity of water wasn't adequate to produce concrete mix as presented in Table 4-1.

In the first and second group of Table 3-7 understood that with 0.2 percent of steel fiber can reach the optimum mix but unfortunately with different proportions of type one water reducer couldn't reach the optimum amount because delayed the initial setting time to more than three days. Then, in third stage understood that with the second type of water reducer adequate workability obtained with a lower quantity but even initial setting time increased to more than two days. Also, the addition of gravel produced pore inside the concrete and reduced in compressive strength. Finally, In UHPC13 to UHPC15 trial mixes optimum mix obtained for UHPC with depending on the last three groups experience. The problem of delayed setting time solved with addition of fine grouting material which increased in compressive strength and initial setting time to the first ten hours. In addition, HPC and UHPC trial mixes curried at hot temperature water curing at 80 °C for the first three days to accelerate chemical reactions and obtained higher strength at earlier age, then putted into the normal temperature water curing until the day of test. In the curing process for the first three groups of UHPC noticed that the cutting off electricity let to freeze-thaw cycle will occur and decreased in compressive strength significantly. Then this problem is solved and the required strength is obtained.



Table 4-1: Trial mixes for UHPC overlay

Trial No.	$f_{cu}$ (MPa)			
	3	7	28	56
UHPC1	F.	-	-	-
UHPC2	-	53.2	77.8	78.8
UHPC3	-	69.11	100	102.3
UHPC4	-	46.28	77.0	80.4
UHPC5	-	56.38	87.14	90.5
UHPC6	-	87.91	93.86	95.7
UHPC7	-	87.59	88.87	91.3
UHPC8	-	50.45	90.83	91.2
UHPC9	-	39.53	94.17	96.5
UHPC10	-	36.99	75.1	77.3
UHPC11	-	84.26	84.99	87.1
UHPC12	-	84.34	90.7	92.32
UHPC13	22.7	102.8	113.7	114.21
UHPC14	30.9	112.0	119.2	121.1
UHPC15*	31.3	108.4	129.78	130.7

(\*) Selected mixes for casting slab specimens (Control Mixes)

(F) This trial is failed

(-) The result couldn't be obtained

Table 4-2: Trial mixes for the substrate material (NSC)

Trial No.	$f_{cu}$ (MPa)		
	1	7	28
NSC1	13.8	25.3	49.0
NSC2	15.9	28.9	38.23
NSC3	17.2	39.5	50.88
NSC4*	15.47	38.67	45.6
NSC5*	24.8	42.9	57.23
NSC6*	8.7	19.9	24.8

(\*) Selected mixes for casting slab specimens (Control Mixes)

Table 4-3: Trial mixes for HPC overlay

Trial No.	$f_{cu}$ (MPa)		
	1	7	28
HPC1	37.8	61.15	64.3
HPC2*	42.5	80.58	81.2

(\*) Selected mixes for casting slab specimens (Control Mixes)

#### 4.2.1.2 Control Mixes Used for Slabs

The optimum mix proportion obtained depending on the concrete compressive strength with cube mold ten centimeter due to its small size. Compressive strength is the basic concrete specification especially for this study because it is used to repair the compression zone in order to strengthen all structural member. Then the cylinder compressive strength is tested which is generally used for design purposes, for this reason cylinders was capped and tested in compression for NSC, HPC and UHPC. Table 4-4, are showing the results, and it can be noted that NSC and HPC generally have a higher unit weight with higher porosity ratio than UHPC because UHPC not contain gravel particles. No considerable change in compressive strength after the effect of heat treatment for NSC and UHPC, but for NSC the changes in compressive strength is exist with ages (Zingaila et al., 2016).

Table 4-4: Control Mixes specifications

Mix	Slump mm	Weight $kN/m^3$		Porosity %	$f_{cu,100}$ (days) (MPa)				$f_{cyl,100 \times 200}$ (days) (MPa)	$\frac{f'_c}{f_{cu}}$
		Fresh	Oven Dry		7	28	56	90		
NSC1	50	26.3	24.1	6.4	38.67	45.6	49.3	52.4	42.33	0.808
NSC2	120	26.7	23.8	5.3	42.9	57.23	61.25	65.17	52.65	0.808
NSC3	130	26.7	23.9	6.7	19.9	24.8	28.3	29.0	23.43	0.806
HPC	60	26.1	25.4	4.1	80.58	81.2	82.3	83.0	75.53	0.91
UHPC	185	25.2	23.4	3.5	108.4	129.7	130.7	132.5	131.9	0.995

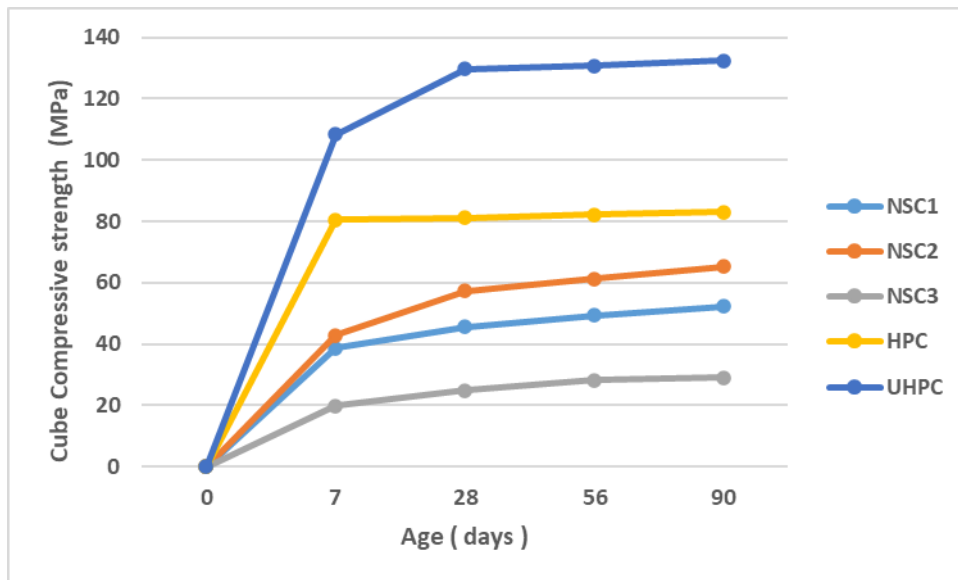


Figure 4.1: Compressive Strength of Control Mixes vs. Age

#### 4.2.2 Splitting Tensile Strength

One of the perfectly enhanced characteristics of UHPC was splitting tensile strength. The results of tests performed on splitting tensile strength are shown in Table 4-5, and there can be noted that UHPC have a splitting

tensile strength twice that of HPC and 3 to 5 times as for NSC, and the table show that generally, splitting tensile strength is about 7-9 % of its compressive strength, and it is clear that Ø100 mm cylinders give the results about 3.6 % higher than Ø150 mm cylinders for UHPC, while for NSC the value is about 9 %. It is widely acknowledged that concrete's real strength is provided by Ø150 mm cylinders.

Table 4-5: Splitting Tensile Strength of Control Mixes (90 days)

Mix type	$f'_c$ (MPa)	$f_{ct}$ (MPa)		$\frac{f_{ct}}{f'_c}$ (%)		Ø (150/100) mm/mm
		Ø 150mm	Ø 100mm	Ø 150mm	Ø 100mm	
NSC1	42.33	3.46	3.76	8.10	8.80	0.92
NSC2	52.65	3.87	4.12	7.30	7.80	0.93
NSC3	23.43	2.12	2.43	9.04	10.37	0.87
HPC	75.53	-	5.30	-	7.07	-
UHPC	131.9	11.82	12.25	8.96	9.28	0.96

### 4.2.3 Flexural Strength

The results of 75X75X300 mm prisms tested in third point loading are shown in Table 4-6, for control mixes, and there can be noted that flexural strength of UHPC is three times higher than UPC and about five times higher than NSC. Flexural strength of UHPC is about 10% of its compressive strength, while the values for HPC and NSC are of lesser magnitude.

Table 4-6: Flexural Strength of Control Mixes (90 days)

Mix type	$P_{max}$ kN	$f_r$	$f'_c$	$\frac{f_r}{f'_c}$ (%)
		(MPa)		
NSC1	7.2	3.84	42.33	9.07
NSC2	7.9	4.21	52.65	7.90
NSC3	-	-	23.43	-
HPC	12.14	6.47	75.53	8.50
UHPC	24.55	13.10	131.9	9.93

#### 4.2.4 Bond Strength

The results of tests which were carried out for investigating the bond strength between the control concrete mixes at 90 days age are presented in Table 4-7, and the regions of failure are presented in Figure 4.2. In the result observed that the weakest result obtained with cross-hatch crack pattern. Almost all modes of failure happened through the substrate NSC, however the mode of failure tried to pass through the UHPC overlay but couldn't for all pattern shapes.

Table 4-7: Average maximum failure load, shear stresses and normal stresses from slant-shear test

Texture type	$P_{max}$ kN	Shear Stress	Normal Stress	Region of failure
		MPa	MPa	
Rough	217.47	11.98	6.90	NSC
Horizontal Groove	265.46	14.60	8.45	NSC
Vertical Groove	263.26	14.50	8.37	NSC
Diagonal Groove	206.90	11.40	6.58	NSC
Cross-Hatch	188.10	10.37	5.98	NSC

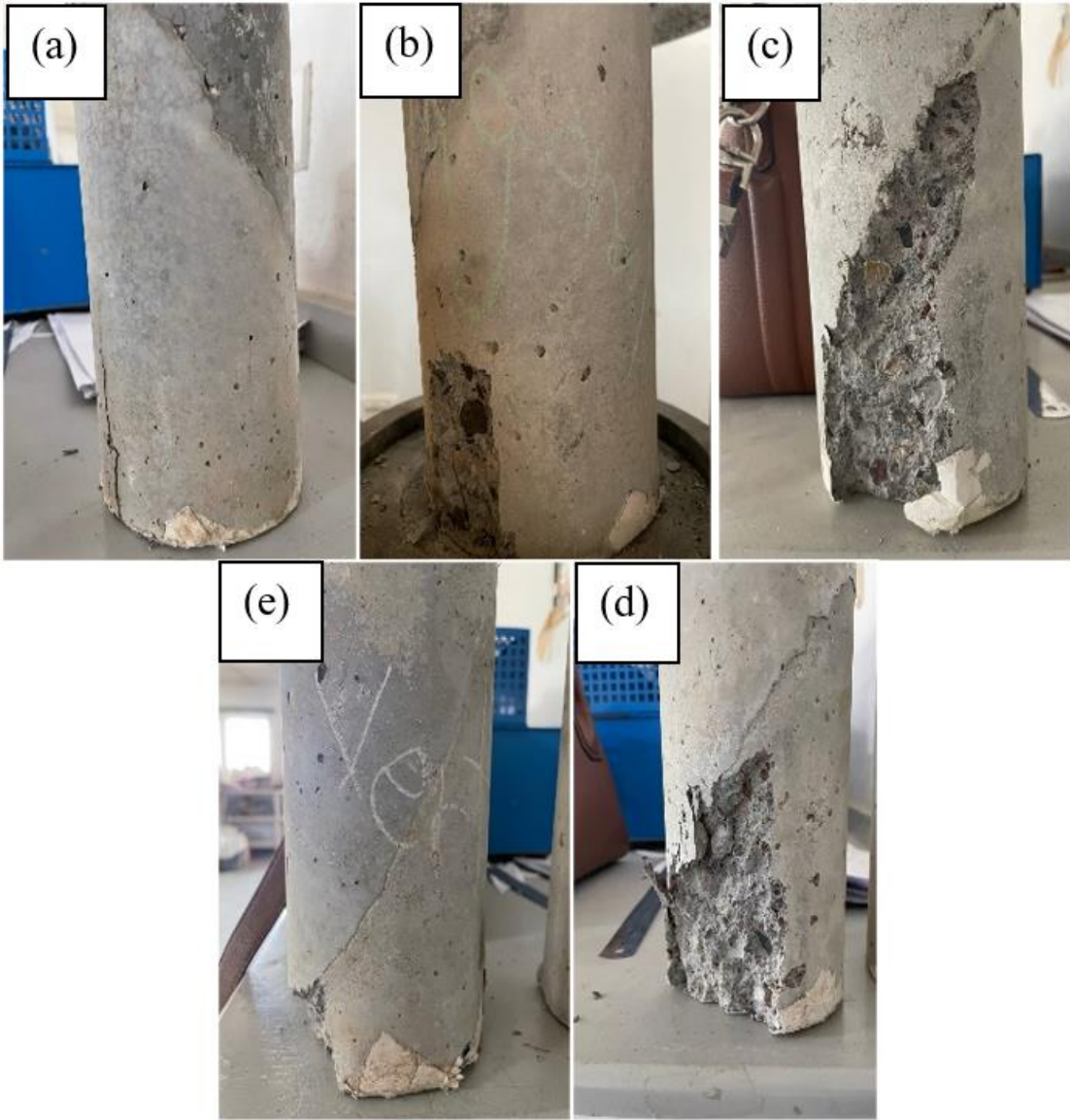


Figure 4.2: Failure region for (a) Rough, (b) Diagonal, (c) Cross-Hatch, (d) Horizontal, and (e) Vertical

#### 4.2.5 Permeability

Water permeability was determined for all NSC, HPC and UHPC. Results from this test showed in Figure 4.3 that the average 5.5 cm and 4 cm maximum permeability depth observed for NSC and HPC, while zero permeability observed for UHPC. The zero permeability can be attributed to the high density of UHPC that may have limited saturation when specimens under pressurized with water and discontinuity in the UHPC passageway pores. Additionally, in NSC and HPC adding gravel particles tends to produce voids which lead to significant change from passing through specimens. The results of water permeability testing are important especially in this study, in order to evaluate the ability of UHPC for overlay among others, and to improve durability against deicing salts that can cause corrosion of reinforcements.

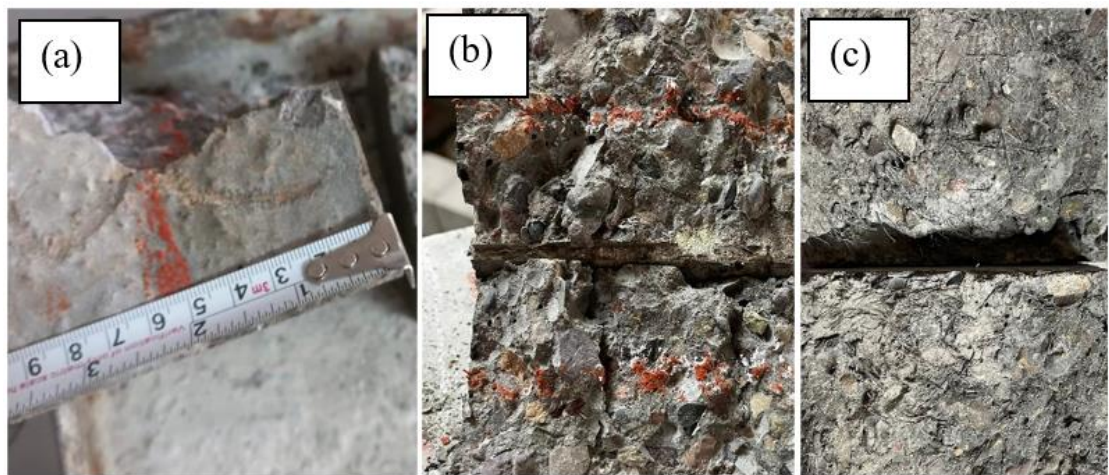


Figure 4.3: The result of water permeability testing; (a) NSC, (b) HPC and (c) UHPC

### **4.3 Control Specimens**

The control specimens were of the same proportions of control mixes, they cast in the same concrete batch used for casting of slabs, tested immediately after slabs, and their properties are shown in Table 4-8.

### **4.4 Reinforced Concrete Flat Plate Specimens**

The purpose of the following sections is to explain the effect of different parameters on the behavior of reinforced concrete bridge deck slab specimens overlaid with UHPC, and the observed failure load of the tested slabs are listed in Table 4-9 and Figure 4.4. The results are of the same slab properties but with disregarding of the little difference of UHPCs compressive strength because they aren't taken from the same batch of concrete mix.



Table 4-8: Mechanical Properties of Control Specimens

Sr.	Specimen Symbol	Concrete Types	$f'_c$ (MPa)	$f_{ct}$ (MPa)	$f_r$ (MPa)
1	CS	Substrate: NSC	33.7	3.2	3.7
		Overlay: UHPC	120.8	11.3	13.97
2	TH20	Substrate: NSC	33.7	3.2	3.7
		Overlay: UHPC	124	11.7	14.4
3	TH40	Substrate: NSC	33.7	3.2	3.7
		Overlay: UHPC	124	11.7	14.4
4	TH50	Substrate: NSC	33.7	3.2	3.7
		Overlay: UHPC	102	9.54	11.9
5	R-UHPC5	Substrate: NSC	33.7	3.2	3.7
		Overlay: UHPC	125	11.8	14
6	R-UHPC10	Substrate: NSC	33.7	3.2	3.7
		Overlay: UHPC	124	11.7	14.4
7	R-UHPC15	Substrate: NSC	33.7	3.2	3.7
		Overlay: UHPC	129	12.89	15.2
8	HG	Substrate: NSC	33.7	3.2	3.7
		Overlay: UHPC	125.7	11.7	14.96
9	VG	Substrate: NSC	33.7	3.2	3.7
		Overlay: UHPC	102	9.54	11.9
10	CH	Substrate: NSC	33.7	3.2	3.7
		Overlay: UHPC	125.3	11.72	15.3
11	DG	Substrate: NSC	33.7	3.2	3.7
		Overlay: UHPC	125.3	11.72	15.3
12	S21	Substrate: NSC	20	2.5	2.7
		Overlay: UHPC	130	13.5	16.5
13	S40	Substrate: NSC	42.6	3.8	4.1
		Overlay: UHPC	130	13.5	16.5
14	O30	Substrate: NSC	33.7	3.2	3.7
		Overlay: NSC	21	2.3	2.9
15	O80	Substrate: NSC	33.7	3.2	3.7
		Overlay: HPC	80.2	5.1	6.8
16	2RA	Substrate: NSC	33.7	3.2	3.7
		Overlay: UHPC	102	9.54	11.9
17	3RA	Substrate: NSC	33.7	3.2	3.7
		Overlay: UHPC	113.2	10.59	13.1

Table 4-9: Test results of the slab specimens

Group no.	Specimen No.	Specimen Symbol	UHPC overlay for Protective- thickness (mm)	R-UHPC overlay with steel rebar for Protective and Resistance	Top face of substrate Surface layout	Substrate material- NSC Compressive Strength MPa	UHPC Compressive Strength MPa	Screw Anchor Diam. (5) mm Length (80) mm	Experimental Failure Load kN
Control	1	CS	30	NR	Rough	33.7	120.8	NA	72
	2	TH20	20	NR	Rough	33.7	124	NA	71.7
G1	3	TH40	40	NR	Rough	33.7	124	NA	87
	4	TH50	50	NR	Rough	33.7	115	NA	90
G2	5	R-UHPC5	30	5mm @ 50 mm	Rough	33.7	125	NA	67
	6	R-UHPC10	30	5mm @ 100 mm	Rough	33.7	124	NA	100
	7	R-UHPC15	30	5mm @ 150 mm	Rough	33.7	129	NA	91.9
G3	8	HG	30	NR	Horizontal Grooves	33.7	125.7	NA	80
	9	VG	30	NR	Vertical Groove	33.7	115	NA	70
	10	CH	30	NR	Cross Hatch	33.7	125.3	NA	66
	11	DG	30	NR	Diagonal Grooves @ 45° inclined	33.7	125.3	NA	101
G4	12	S21	30	NR	Rough	20	130	NA	76.8
	13	S40	30	NR	Rough	42.6	130	NA	82.9
G5	14	O20	30	NR	Rough	33.7	21	NA	65
	15	O80	30	NR	Rough	33.7	80.2	NA	72
G6	16	2RA	30	NR	Rough	33.7	115	Two rows of anchor at 228 mm	73
	17	3RA	30	NR	Rough	33.7	113.2	Three rows of Anchor at 228 mm	108

NR: No Reinforcement, NA: No Anchor

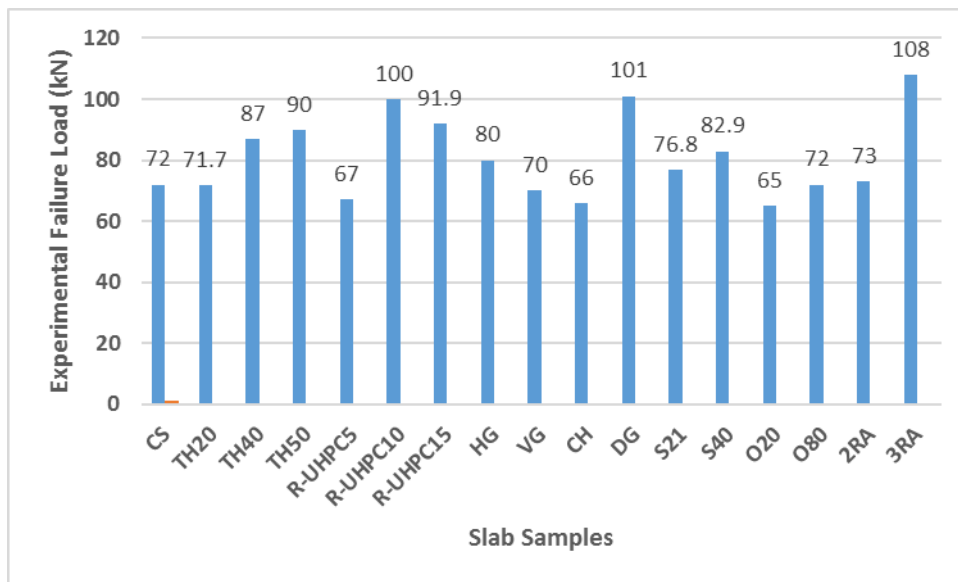


Figure 4.4: the observed failure load of the tested slabs

#### 4.4.1 UHPC Thickness

This discussion is related to the increase in ultimate strength versus UHPC thickness as presented in Figure 4.5. UHPC thickness is a crucial parameter that requires significant discussion before the final decision. In the result no significant increase observed in the ultimate failure load when overlay thickness increased from 20 mm to 30 mm, but significant increase observed when the thickness of the UHPC layer thickness increased from 30 mm to 40 mm that ultimate failure load increased by 17.24%, then the ultimate failure load increased by 3.33% when the overlay thickness increased from 40 mm to 50 mm.

Based on the existing experimental studies in Table B-1 APPENDIX B and section 2.5.2, the most preferred thickness for the UHPC layer is 50 mm. Buitelaar et al. (2004) obtained that 10-12 cm stress reduction factor exists with a 50 mm overlay. However, ultimate strength has to be increased directly with increased overlay thickness because tension stress reduces with increased overlay thickness (Shann, 2012), and increased

overlay thickness provides an ideal wearing surface that increases the life of the existing structure and reduces maintenance costs (Denmark). But irregularity increases in ultimate strength in this study belong the reason that the experimental application of this variable is very sensitive to control. Additionally, all thicknesses can produce an appropriate wearing surface, but a 50 mm overlay thickness can provide the best results.

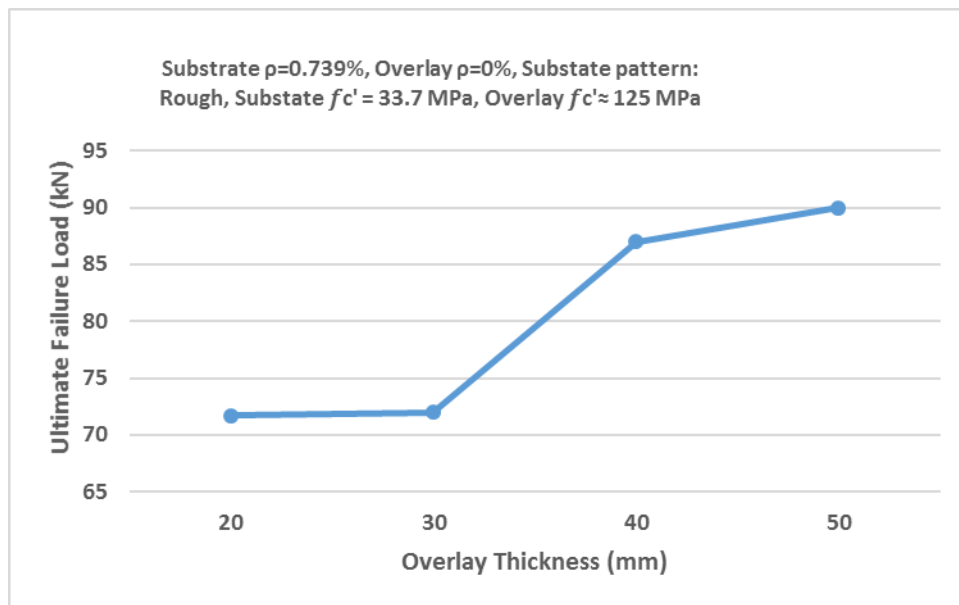


Figure 4.5: Ultimate failure load versus UHPC thickness, Group (1)

#### 4.4.2 Reinforcement Ratio in UHPC Layer

The following discussion is related to the increase in ultimate strength versus steel reinforcement ratio inside the UHPC layer. This crucial parameter can directly affect the strengthening characteristics and give the strengthening composite structure the ability to be protected and resistant. The reinforcement ratio in the overlay layer is calculated by using equation 4-1. With reinforcement in the UHPC layer, the ultimate failure load increased by 21.65% and 28%, respectively, with reinforcement ratios of

0.523% and 0.654%. But when 1.31% of reinforcement ratio increased to UHPC layer the ultimate failure load decreased by 7% unexceptionally as presented in Figure 4.6.

According to equation 4-2, the maximum reinforcement ratio for this study's composite structure is 6.8% derived in APPENDIX A which asserted that it is under reinforced structure but using reinforcement at compression zone and complement UHPC to R-UHPC suggested by main investigators especially for old structures as explained in detail in section 2.5.3. Conferring to the previous studies that are summarized in Table B-1 APPENDIX B, the reinforcement ratio in the UHPC overlay ranges from 0% to 4%. Also, with an increased reinforcement ratio in the UHPC layer, the ultimate load increased directly. However, this statement isn't true for all cases because many other parameters exist that can change the mode of failure. When compared to maximum reinforcement ratios and earlier studies, it can be shown that the reinforcement ratios employed in this research are on the safe side; nonetheless, the unexpected failure of the slab with a 1.31% reinforcement ratio was brought on by a malfunction with the test machine.

$$\rho = \frac{A_{st}}{bd} \quad \text{Equation 4-1}$$

Where:

$A_{st}$ : longitudinal steel reinforcement

$b$ : cross-section width of UHPC layer

$d$ : effective depth of interface steel layer

$$\rho_{max} = 0.85 \left( \frac{f'_{cH}}{f_y} \right) \left( \frac{h_H}{d} \right) + 0.85 \left( \frac{f'_{cN}}{f_y} \right) \left[ \beta_1 \left( \frac{\epsilon_{cuH}}{\epsilon_{cuH} + \epsilon_y} \right) - \frac{h_H}{d} \right] \quad \text{Equation 4-2}$$

Where:

$\rho_{max}$ : Maximum reinforcement ratio

$\beta_1$ : Concrete stress block parameter

$\epsilon_{cuH}$ : Ultimate Strain of UHPC

$\epsilon_{cuN}$ : Ultimate Strain of NSC

$f'_{cN}$ : Ultimate Strength of NSC (MPa)

$f'_{cH}$ : Ultimate Strength of UHPC (MPa)

$f_y$ : Yield strength of overlay rebar (MPa)

$h_H$ : UHPC height (mm)

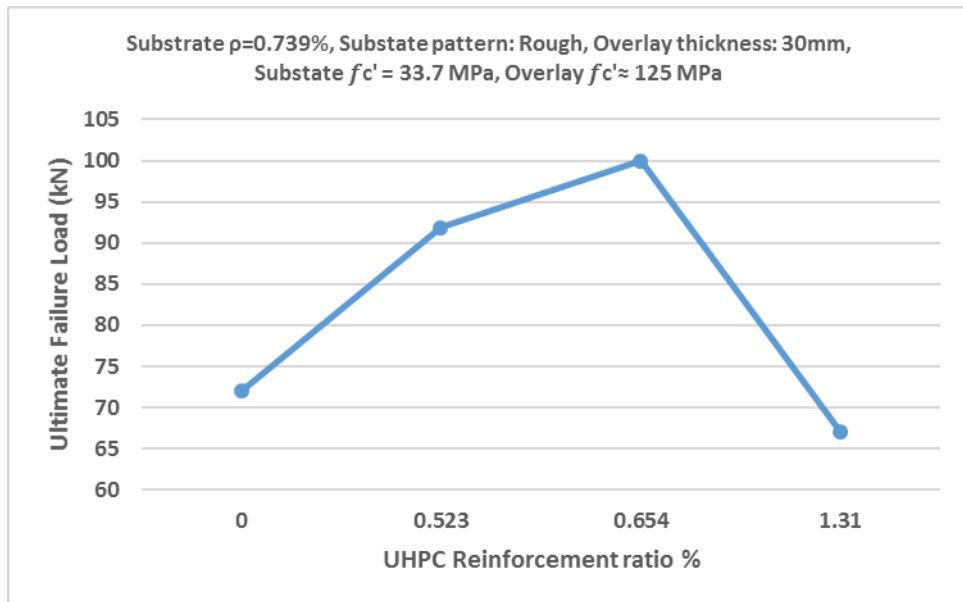


Figure 4.6: Ultimate failure load versus UHPC reinforcement ratio, Group (2)

### 4.4.3 Substrate Surface Patterns

The various methods of substrate surface preparation are evaluated in this study, and in this section, the final failure load is used to choose the best method. In general interface preparation is divided into five basic types according to ultimate failure load from smallest to largest value as presented in Figure 4.7; cross hatch, vertical groove, rough, horizontal groove and diagonal groove. Although the diagonal groove surface pattern failed under the highest ultimate load and the cross-hatch surface pattern failed under the lowest, none of the specimens showed delamination, which would have required a higher load capacity at failure.

Almost all present and previous studies insisted that the best bond strength can obtain by using rough surface preparation Perez et al. (2009), Zhang et al. (2020a), Zhang et al. (2020b), Zhang et al. (2019), Al-Madani et al. (2022) but there exist many techniques to obtain a rough surface that has a great influence on the results. The basic idea behind creating a rough surface that is widely utilized is to remove the top layer of the old structure using a sand blast, jackhammer, or water-jet technique, then keep the surface free of all foreign substances like oil, grease, dirt, and dust. Finally, the surface is covered with cement paste prior to applying an overlay. But in this experiment, none of those methods were utilized to create it; instead, a rough surface was created by covering the substrate with 12 mm of gravel after casting directly. Regardless of the fact that this technology helped us make a rough surface, it realized that the substrate wasn't entirely connected. Additionally, it is crucial to ensure that the HG, VG, DG, and CH pattern shapes entirely interlock in accordance with the principle learned with direct casting while grooving the substrate surface.

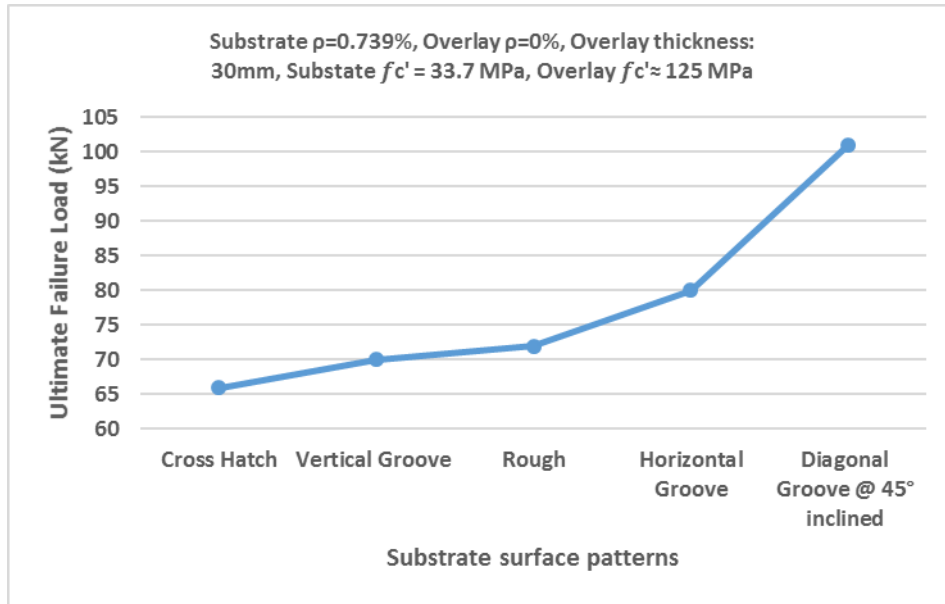


Figure 4.7: Ultimate failure load versus Substrate surface patterns, Group (3)

#### 4.4.4 Substrate NSC Compressive Strength

Figure 4.8, presented the effect of substrate natural strength concrete versus ultimate failure load that evaluated 20, 30 and 40 MPa of NSC compressive strength, in the result observed that ultimate load increased by 13% when the substrate compressive strength increased from 30 MPa to 40 MPa. However, failure load of composite structures increases directly with increased NSC compressive strength due to adhesion and cohesion properties between two types of material as clarified by Ahmed and Aziz (2015), Aaleti et al. (2013) but ultimate failure load decreased by 6.25% when substrate NSC compressive strength increased from 20 MPa to 30 MPa. In addition, flexural crack didn't penetrate through the UHPC layer, substrate with overlay behaved like the same layer of concrete except with 20 MPa substrate NSC compressive strength delamination was observed across the part width of the specimen as presented in Figure 4.9.

This parameter significantly affects failure mode, but it isn't working alone. The effect of NSC compressive strength is comparable with overlay



material compressive strength and interface preparation. This decrease in compressive strength in S30 is also due to the fact that in S30, 120 MPa of UHPC compressive strength is used for the overlay, while in S21 and S40, 130 MPa is used as shown in Table 4-8 because they aren't taken from the same batch of concrete.

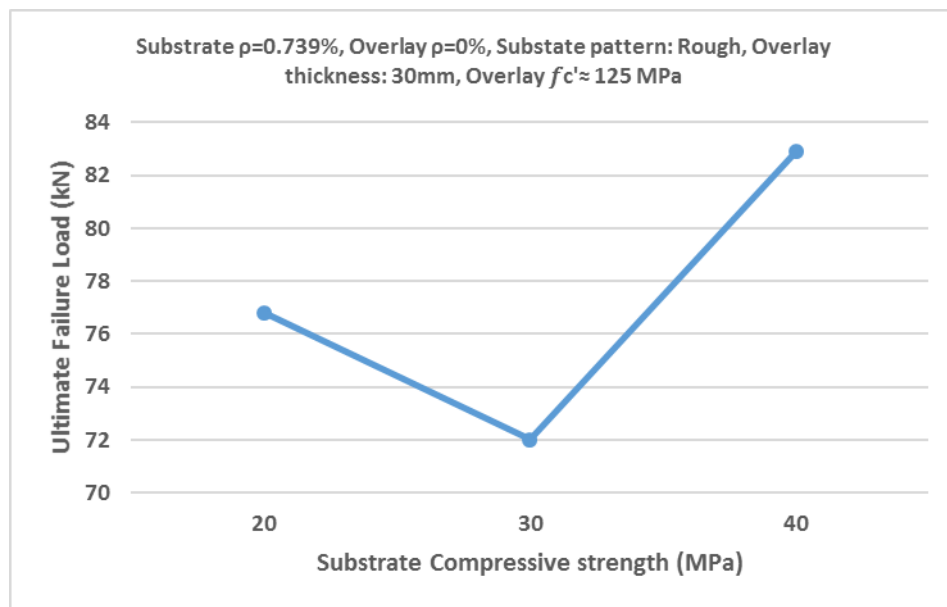


Figure 4.8: Ultimate failure load versus substrate NSC Compressive strength, Group (4)



Figure 4.9: Delamination in a part width of S20 slab

#### 4.4.5 Overlay Compressive Strength

This section deals with the relationship between the overlay compressive strength parameter and the increase in ultimate load since it has a significant impact on the strengthening process that is why discussed in detail about the use of NSC  $f'_c$  21 MPa, HPC  $f'_c$  80 MPa and UHPC  $f'_c$  125 MPa for overlay application. As presented in Figure 4.10, the ultimate failure load increased with 10% when overlay material compressive strength increased from 20 MPa to 80 MPa. In composite structure with overlay  $f'_c$  21 MPa, flexural crack in substrate concrete penetrated through the overlay material, mid-span slip observed and top concrete crushed, also for overlay  $f'_c$  80 MPa similar failure mode was found but with a closer width and higher load as presented in Figure 4.11.

However, the ultimate failure load has to increase directly with increased overlay material compressive strength, as Bao et al. (2017) stated that the increases in bond and ultimate strength are proportional to the increase in overlay material compressive strength, but when overlay material compressive strength increased from 80 MPa to 125 MPa, the ultimate load remained constant because the failure was not in the compression zone, it was in the tension zone, which was identical for the overlay 125 MPa specimen alone. Furthermore, for the overlay material at 125 MPa compressive strength, flexural cracks didn't penetrate through the UHPC layer rather than horizontally propagate through the interface, but they couldn't cause delamination as presented in Figure 4.11 because the existing steel fiber in the overlay material enhances the bond strength greatly as our results are agree with Aziz and Ahmed (2012), Sharma et al. (2022).

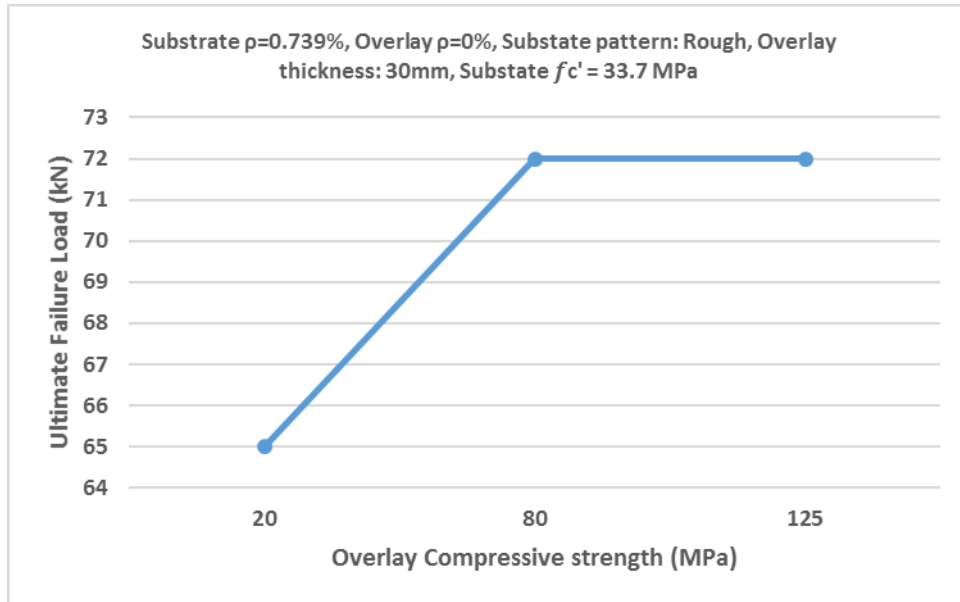


Figure 4.10: Ultimate failure load versus overlay compressive strength, Group (5)



Figure 4.11: Failure mode of composite specimens: (a) Overlay  $f'_c$  20MPa, (b) Overlay  $f'_c$  80MPa and (c) Overlay  $f'_c$  125MPa

#### 4.4.6 Mechanical Connectors

The following discussion is related to the increase in ultimate strength versus mechanical connector at interface, this parameter is essential and can directly influence the strengthening characterization as recommended by some researchers because sometimes debonding will happen in composite structures (Lapi et al., 2018). The results are presented in Figure 4.12, which detected that ultimate failure load increased by 1.3% when two rows of anchor increased with rough surface pattern. Then 33.3% increase

in ultimate failure mode observed when three rows of anchor added that considered as a greatest increase in ultimate failure load compared with all other molds. This great difference in increasing ultimate load is due to difference in overlay compressive strength because they aren't taken from the same concrete batch as shown in Table 4-8. In Table 2-8, Stefaniuk (2020) explained that more anchors result in a significant increase in load transmission because the length of the shear stud. In addition, Zhang et al. (2019) detected that rough surface plus post installed stud (P.I.S.) have better bond strength compared with P.I.S alone, but limited data is reported about the number of screw anchor with rough surface.

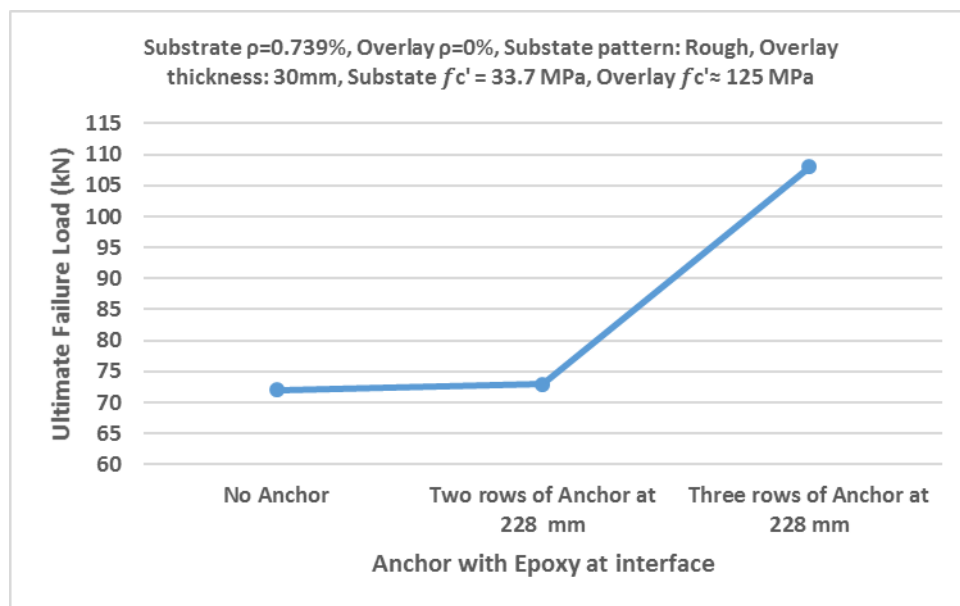


Figure 4.12: Ultimate failure load versus mechanical connector, Group (6)

#### 4.5 Load-Central Deflection Relationship

The load-central deflection curves for the tested slabs are shown in Figure 4.13 to Figure 4.19. The first group curves shown in Figure 4.13, that deal with UHPC thickness, the center deflection of the slab change in a large amount when thickness changed, decreasing the slab thickness from

50 mm to 40, 30, and 20 mm increased the central deflection by 7.4, 30, and 46%. Stronger slabs with UHPC overlays have more ductility and crack patterns distributed more densely in the tension zone as a result of the coupled effects of the height increase of the compression zone caused by the thickness of the overlay and the upward shift of the neutral axis.

The second group curves shown in Figure 4.14, represent adding reinforcement bar in UHPC layer with different ratios, It should be noted that increasing the reinforcement ratio to 0.523% with the UHPC layer increased the slab's deflection by 55% inappropriately, and the failure did not follow the yield line theory. However, when the ratio was increased to 0.654%, the failure deflection decreased by 11% and tension zone cracks were more evenly dispersed, and when the reinforcement ratio was increased to 1.31% due to a problem with the testing machine, sudden brittle failure was observed. The use of reinforcement in UHPC overlay was almost universally recommended because it directly increases ultimate load when the reinforcement ratio in the UHPC layer is increased. However, there is little accurate information available about this ratio, so this study optimized the reinforcement ratio at overlay by 0.654% in order to increase ultimate failure load and decrease maximum central deflection in comparison to control specimen.

The Measured force-displacement response for all composite test specimens of group three are shown in Figure 4.15. as a result, it was discovered that the stronger slabs that failed at higher ultimate loads had a smaller maximum central deflection, which was divided between higher and lower values in the HG, control, VG, and CH samples. Because of the improved interface bond strength, the tension zone experienced wider and denser shear cracks that spread horizontally along the interface but did not break through the overlay because of the superior surface preparation.

The fourth group curves shown in Figure 4.16, represent a wide range of changes in substrate compressive strength. Once the substrate compressive strength increased from 33.7 MPa to 42.6 MPa, the maximum central deflection increased by 18%; however, a similar failure mode was found, but S40 underwent larger central deformations. In the S21 specimen, the substrate compressive strength decreased to 20 MPa, and the maximum midspan deflection increased by 30% compared with the control specimen.

Although the substrate's compressive strength increased from 20 MPa to 40 MPa, the ultimate load increased by 7.3%, the mid-span deflection decreased by 20%, and the tension face crack patterns were more subdivided, the S20 and S40 perform better than the S30 because the compressive strength of the covering layer was disregarded. Additionally, in S40, the flexural crack in the normal concrete did not spread through the UHPC overlay. In contrast, in the S21 slab specimen, the substrate flexural crack could not spread through the overlay and instead resulted in delamination. In the control specimen, a minor slide of the substrate concrete crack into the overlay was seen at maximum failure load and deflection as presented in Figure 4.17.

In Figure 4.18 the effect of different overlay compressive evaluated, which seen that maximum central deflection of UHPC overlay is twice than NSC overlay, then the use of HPC for overlay evaluated which shown that failed in flexure with more brittle manner, central deflection 7% lower that NSC overlay and 55% lower than UHPC overlay, this is why it was stated clearly that the results aren't much affected by increasing compressive strength without adding steel fibers. As optimized in Sritharan and Aaleti (2017); wider shear cracks, larger shear deformations, greater

reinforcement yielding, and higher displacement capacity at failure are all effects of stronger slabs failing under higher failure loads.

The effect of mechanical connector on the behavior of central deflection is shown in Figure 4.19, no significant change in central deflection was observed when the number of rows increased to two rows of anchors for interface bonding, but when the number of anchors increased to three rows, the deflection capacity increased twice. According to Darwin et al. (2016), chapter 6, a one-way simple support slab's maximum central deflection is 7.5 cm; fortunately, all slab deformation is much below this value, with the exception of 3RA and R-UHPC15, which are just minimally close to the maximum.

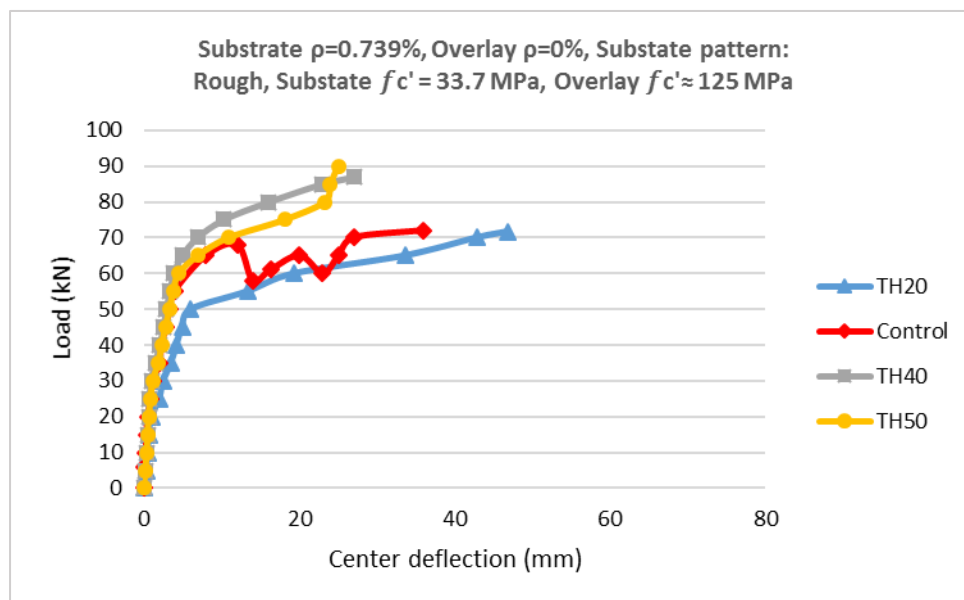


Figure 4.13: Load-Central Deflection Relationship of Group (1), effect of overlay thickness

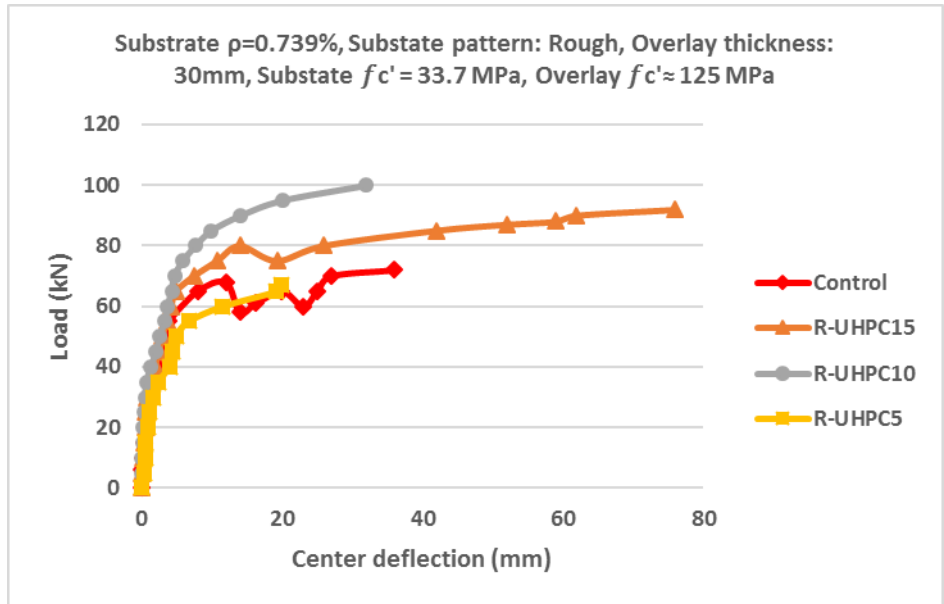


Figure 4.14: Load-Central Deflection Relationship of Group (2), the effect of UHPC reinforcement ratio

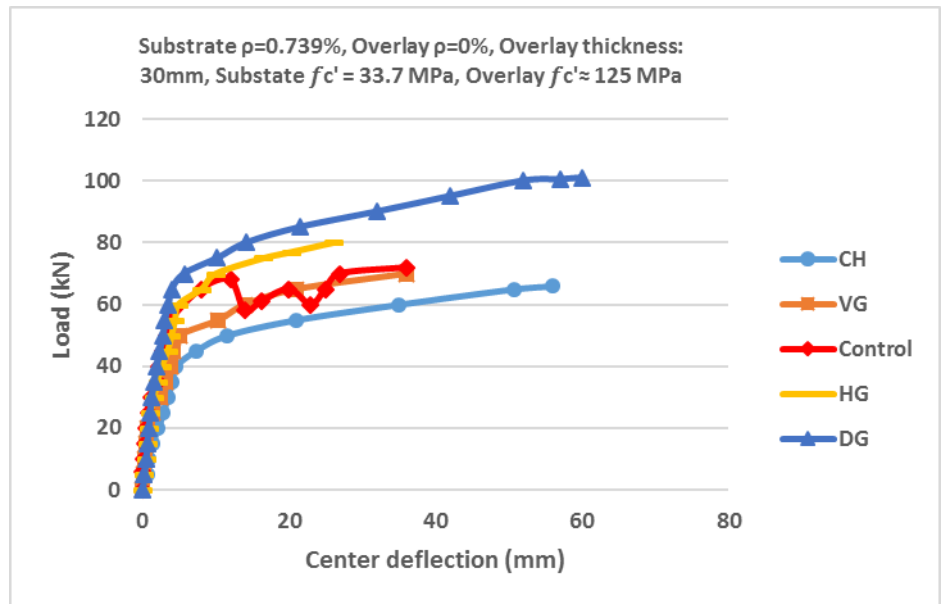


Figure 4.15: Load-Central Deflection Relationship of Group (3), the effect of different interface patterns



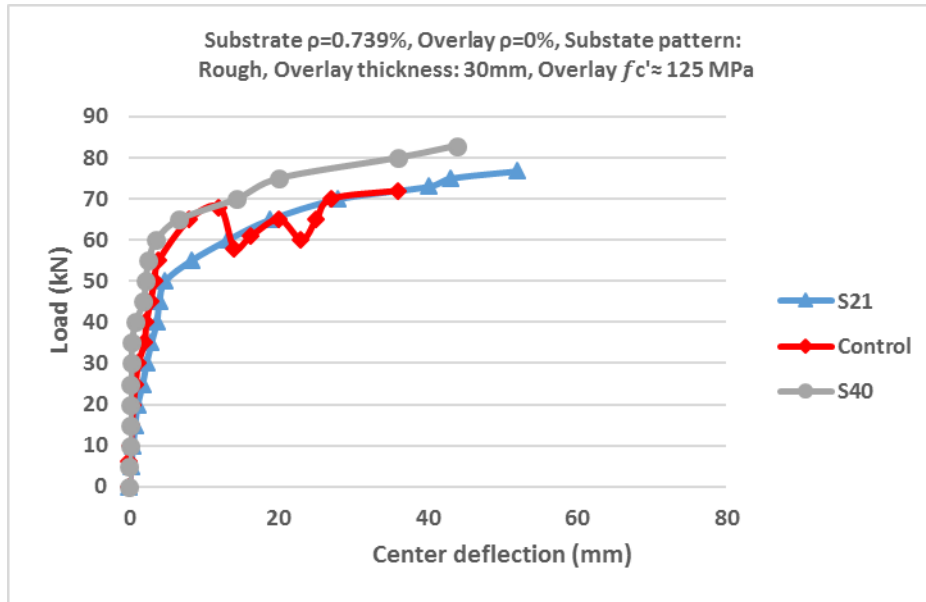


Figure 4.16: Load-Central Deflection Relationship of Group (4), the effect of different substrate compressive strength

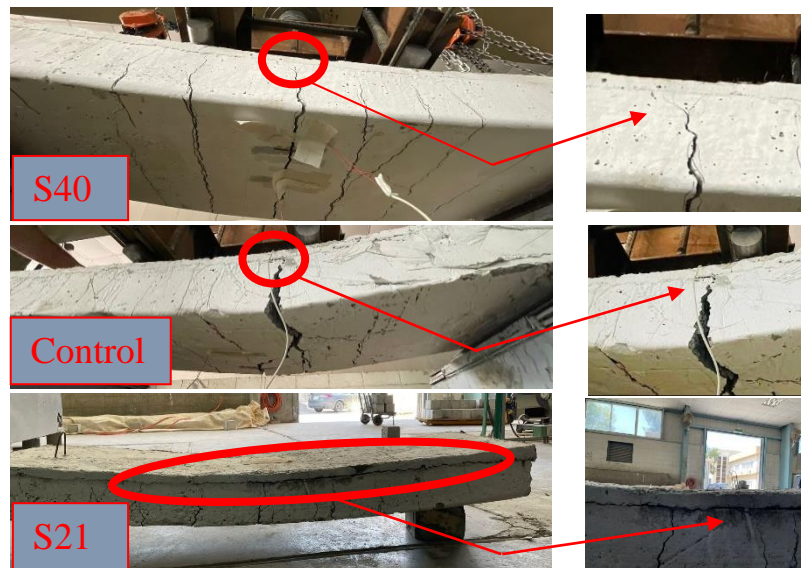


Figure 4.17: Cracking in the composite specimens at the ultimate failure load and deflection

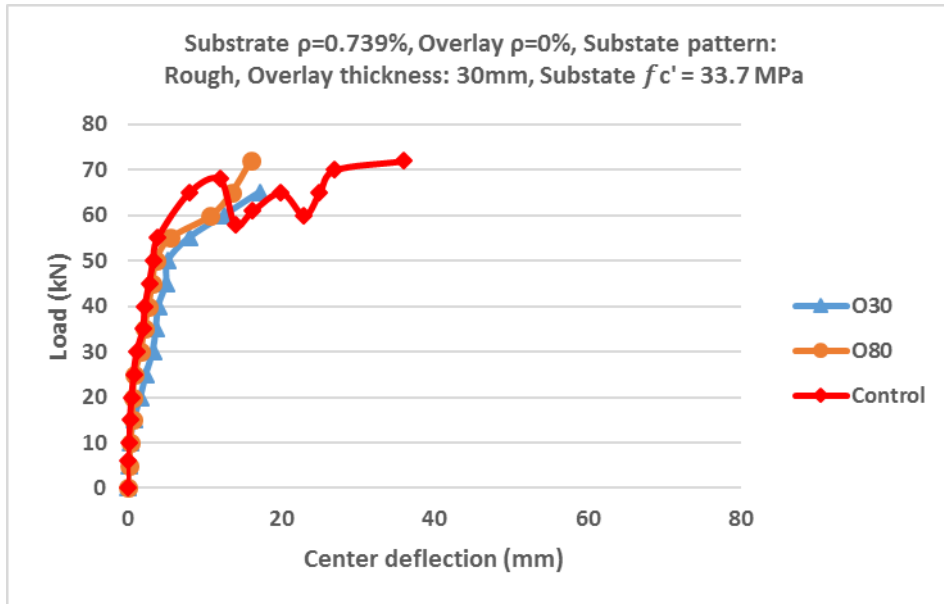


Figure 4.18: Load-Central Deflection Relationship of Group (5), the effect overlay compressive strength

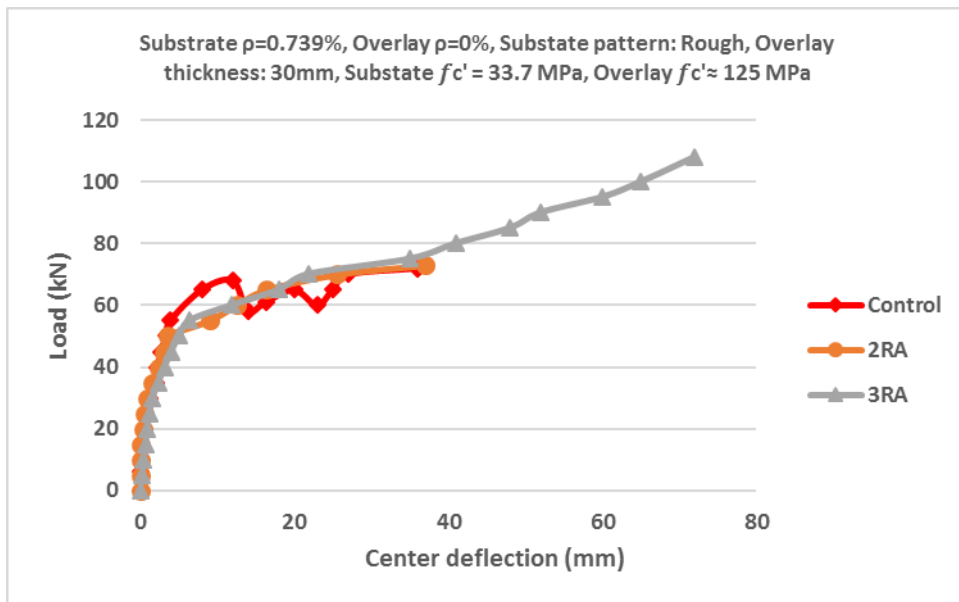


Figure 4.19: Load-Central Deflection Relationship of Group (6), the effect of mechanical connector

#### 4.6 Load-Concrete Strains Relationships

Relationship between the vertical applied load and the strains of concrete was determined using 80 mm strain gauges for both compression

and tension faces. The inaccuracy which must be expected and the non-obtainability of some data in this section is belong to; the cracks may not pass through the line of strain gauges; on the other side the strain gauges that attached to the concrete surfaces were one-way strain readers, so the transverse strains were not obtained.

#### **4.6.1 Concrete Compressive Strains**

This section discusses about the relationship between the load and the strain at the middle of compression face of slab samples. The minimum compressive strain recorded for HPC overlay which reached about 50% of ultimate strain of concrete that specified by Section 10.3 of (ACI 318R-19), the maximum compressive strain of NSC is lower than HPC by 13.3% because increase in compressive strength without addition of steel fiber reduce the compressive strain of concrete. The maximum strain for UHPC slabs was produced in slab R-UHPC15 which was 0.002 and it is just 13% of ultimate UHPC strain that specified by (Azmeem and Shafiq, 2018). With increasing overlay thickness, the compression strains are increased regularly except TH50 slab, because lowest deflection rate recorded in this slab. The sudden change in some points of compressive strain curve of DG, O30 and O80 slabs are believed, that consider as the flexural cracking load condition. In addition, the parallel relationship was observed between ultimate strain and maximum central deflection, this note especially observed for S21 and S40 slabs; which increase in central deflection in S21 slab by 15% increased the compressive strain extremely compared with S40 slab.

#### **4.6.2 Concrete Tensile Strains**

The relationship between vertical applied load and the strains at the bottom surface of slabs in longitudinal, at early loading stages, the low strain values observed at the slabs' tension face were exceedingly. The highest recorded tensile strain value 0.0025 was found in the R-UHPC10 specimen, which reached 15% of the ultimate strain, as defined by Section 10.3 of (ACI 318R-19). The regular relation between ultimate strain and maximum central deflection observed in all samples especially in S21 and S40 slabs, which detected that with increasing central deflection by 15% in S21 slab the ultimate strain increased by 50%.

#### **4.7 Crack Patterns and Modes of Failure**

The crack patterns for the tested slab specimens are the final patterns after the slabs fail; the use of white and black colors aids in identifying a very small crack. Comparing crack patterns shown in Figure 4.20 till Figure 4.36, the following points can be concluded:

1. TH20, TH40 TH50 slabs are failed under the assumed flexural crack patterns, which the cracks highly concentrated in the middle zone and lowly propagated toward the sides but fortunately are far away from the supports. When the thickness of slabs increased from 20 mm to 40 mm and 50 mm, the crack patterns are distributed more intensively along the short direction toward the edges, as shown in Figure 4.20 till Figure 4.23.
2. Slabs R-UHPC15 and control did not meet the assumed concept. When the tests were performed, the concrete matrix experienced the first failure but was only partially damaged, retaining 80% of its initial strength. The slabs then resisted 20% of their remaining strength as the

load increased, which is why each of them exhibit about the same cracked patterns, which include a huge crack width of around five centimeters and a few additional little cracks in the middle of the slabs along the short direction. Also, R-UHPC10 slab has a very low crack width but extensively subdivided in all its area. It is crucial to observe that the lowest rate of cracks is shown in R-UHPC5 slab comparing with all others. All results are presented in Figure 4.24 till Figure 4.26.

3. In HG, VG, CH slabs the same mode of failure and crack patterns are repeated which consist of five basic crack lines along the short span of slabs. One of them immediately at the middle of slabs and the others are located under the line load directly, seven centimeters away from the left and seven centimeters away from the right on each side, as shown in Figure 4.27, Figure 4.28 and Figure 4.29. However, the crack patterns were more widely spaced out in the slab sample that failed at a higher load rate like DG specimen that the width of cracks isn't very wide, but they are very dense and have subdivided paths which much of them located in the flexural zone and only a few of them propagated toward the shear zone in the left side as shown in Figure 4.30. For all slabs, crack patterns in UHPC roughly followed the yield line theory in flexural failure.
4. Figure 4.31 Figure 4.32 and Figure 4.20 show S21, S40, and control slab crack patterns in which the same mode of failure was observed for all slabs approximately, but the difference is that in the S21 specimen, failure tried to pass through the overlay but couldn't, which is why it horizontally propagated through the interface and caused delamination along the width part of the slab as presented in Figure 4.9. But in S40 and control slabs, cracks couldn't cause delamination because the bond strength between two layers of concrete is increased by an increase in the substrate material's compressive strength.

5. In O30 and O80 as publicized in Figure 4.33 and Figure 4.34, the same five basic crack paths are observed, but the difference is that the cracks didn't subdivide, even immediately splitting the slab in the middle. Also, in the O80 slab, in addition to the five basic crack paths, the paths were subdivided lowly, and the top concrete was crushed as a result of the absence of steel fiber. These findings proved that UHPC is the optimum type of material for overlay because it couldn't penetrate into the top, causing crushing overlay and failure at a greater rate of load as shown in Figure 4.11.
6. The 3RA pattern shape is very densely distributed because this slab fails at the maximum load stage and experiences maximum deflection, as shown in Figure 4.36, whereas the 2RA slab crack patterns did not subdivide rather than fail under the assumed mode of failure, as shown in Figure 4.35, because this slab has a lower overlay material compressive strength compared 3RA slab, which influences the results.



Figure 4.20: Control mold Crack pattern

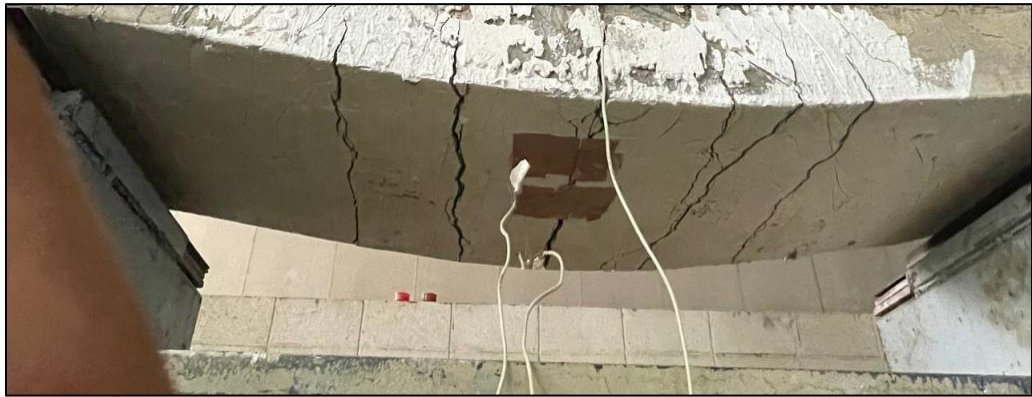
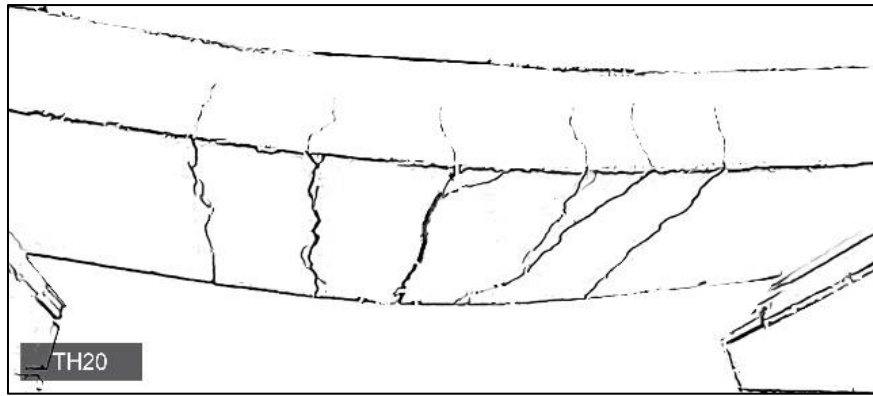


Figure 4.21: TH20 mold Crack pattern

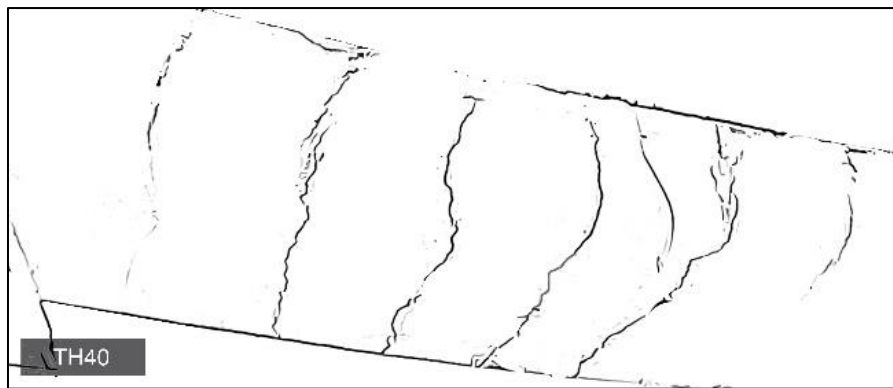


Figure 4.22: TH40 mold Crack pattern

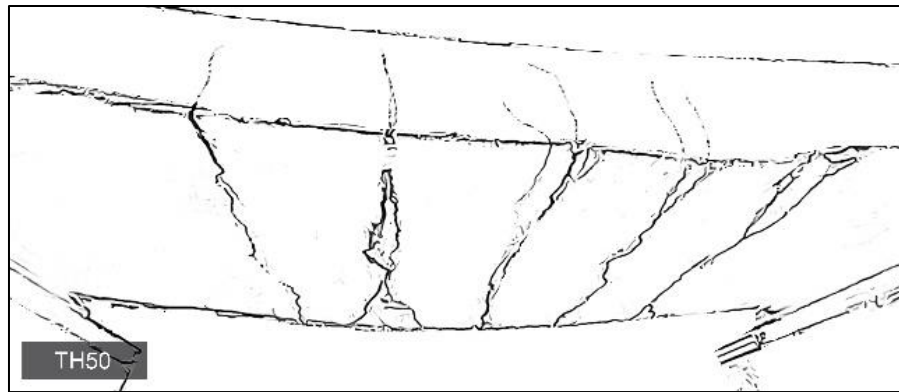


Figure 4.23: TH50 mold Crack pattern

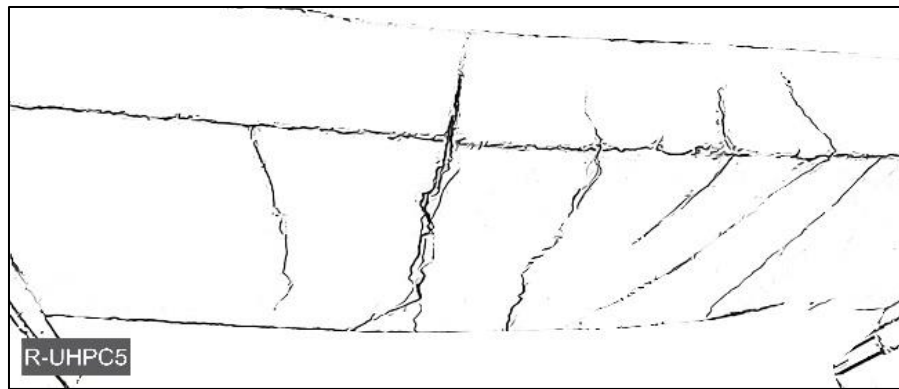


Figure 4.24: R-UHPC5 mold Crack pattern



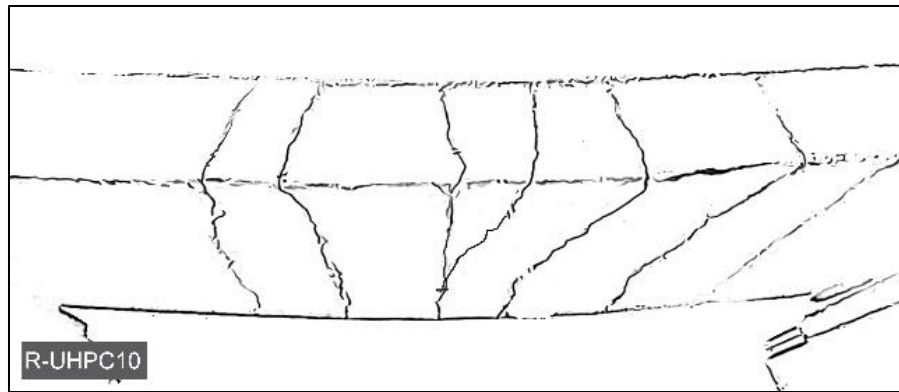


Figure 4.25: R-UHPC10 mold Crack pattern

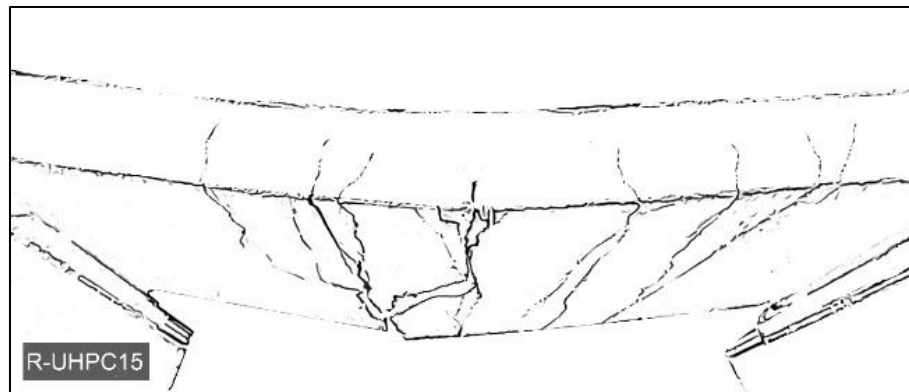


Figure 4.26: R-UHPC15 mold Crack pattern

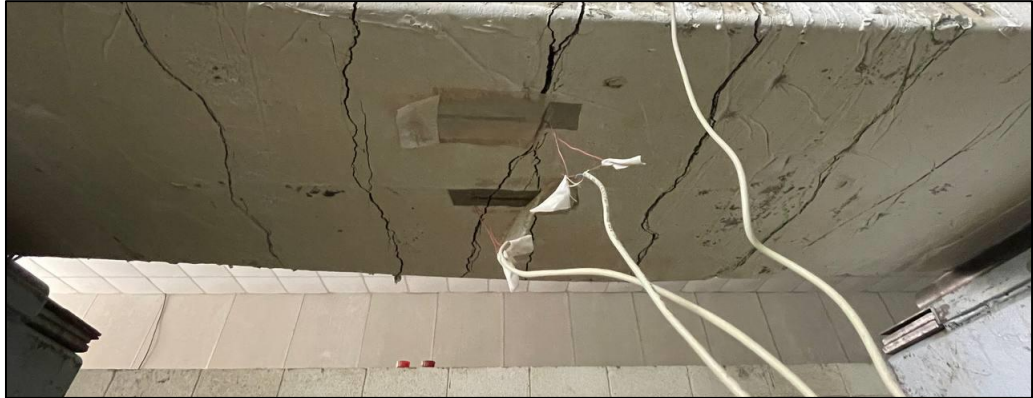
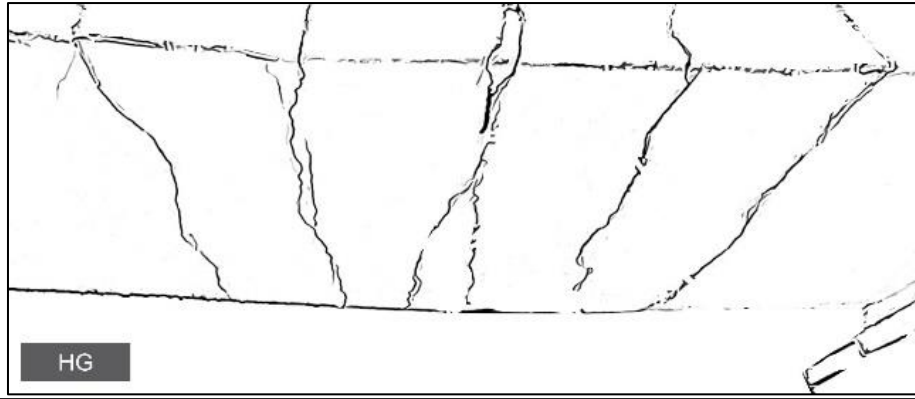


Figure 4.27: HG mold Crack pattern

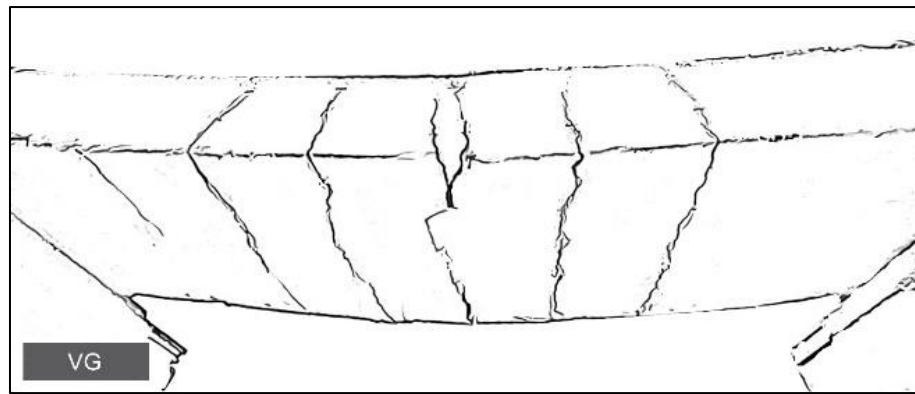


Figure 4.28: VG mold Crack pattern

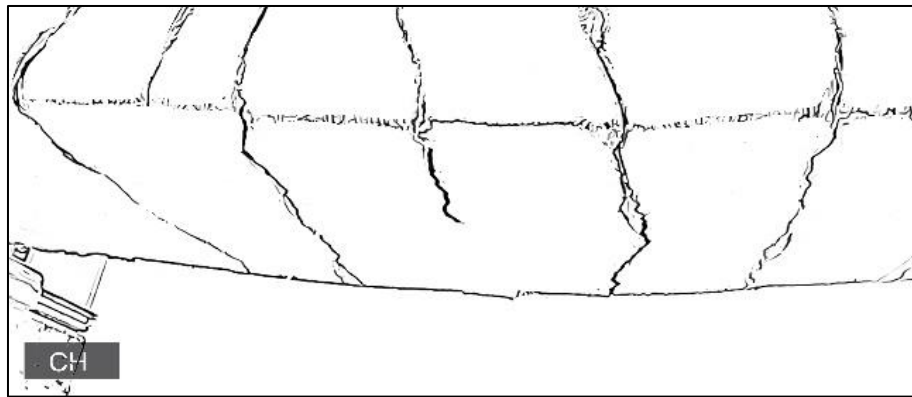


Figure 4.29: CH mold Crack pattern

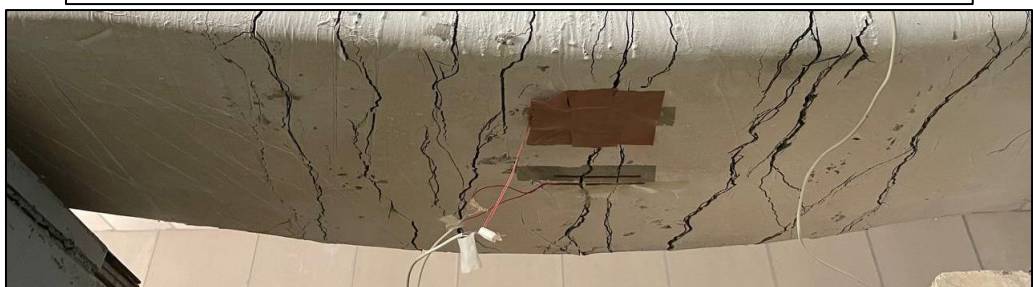
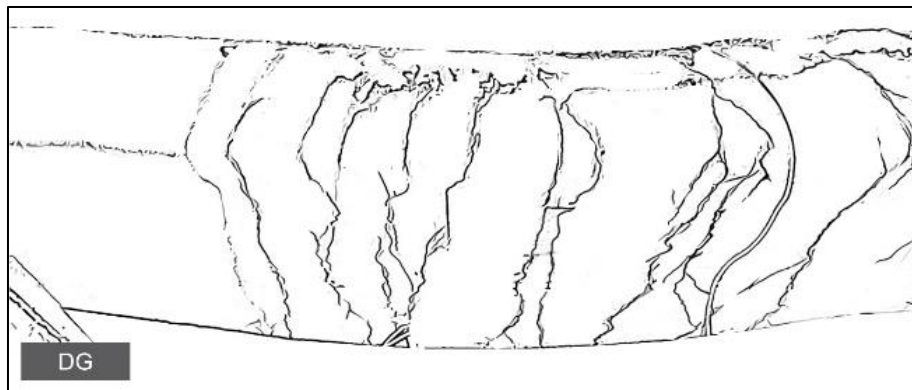


Figure 4.30: DG mold Crack pattern

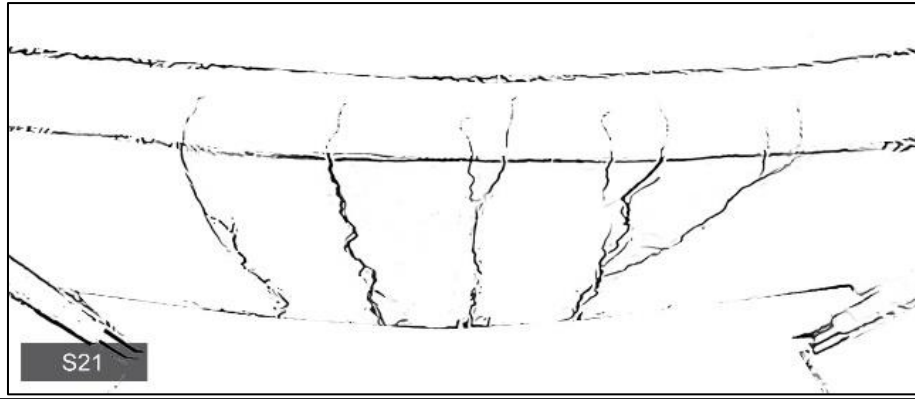


Figure 4.31: S21 mold Crack pattern

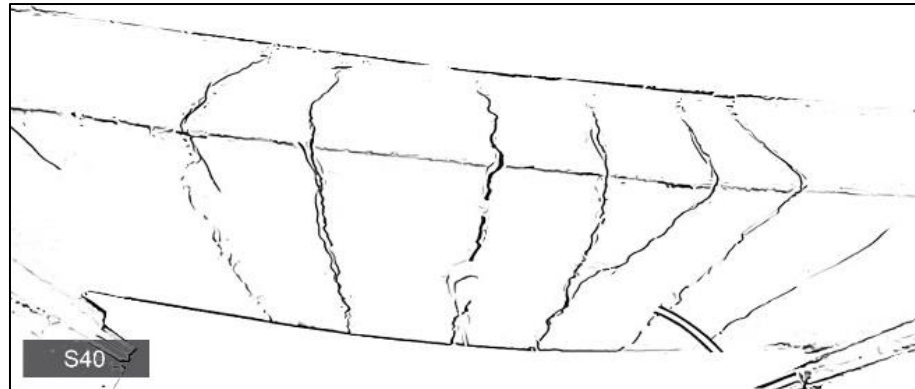


Figure 4.32: S40 mold Crack pattern

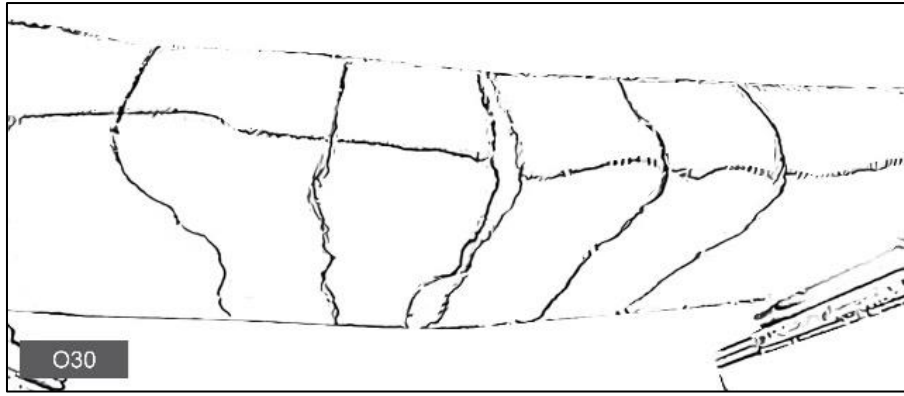


Figure 4.33: O30 mold Crack pattern

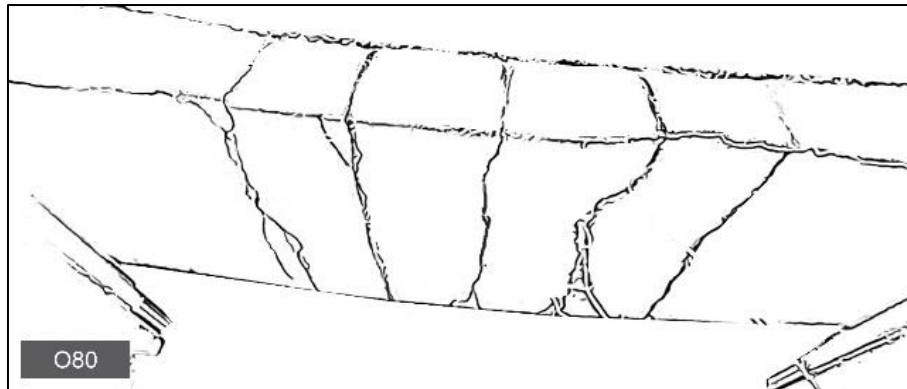


Figure 4.34: O80 mold Crack pattern

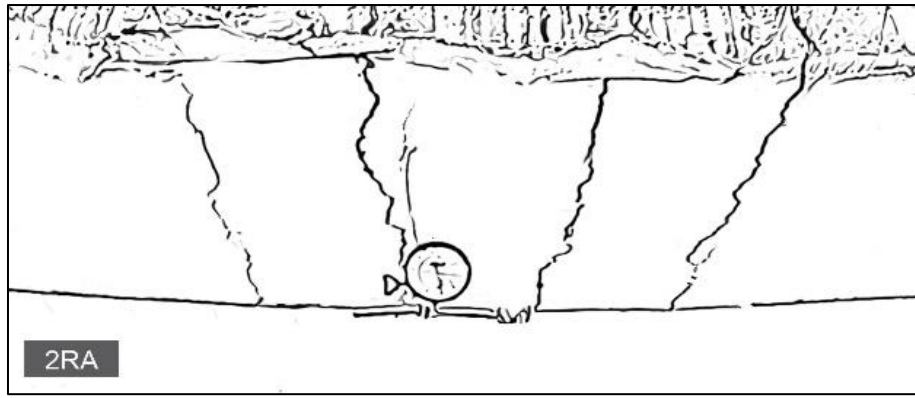


Figure 4.35: 2RA mold Crack pattern

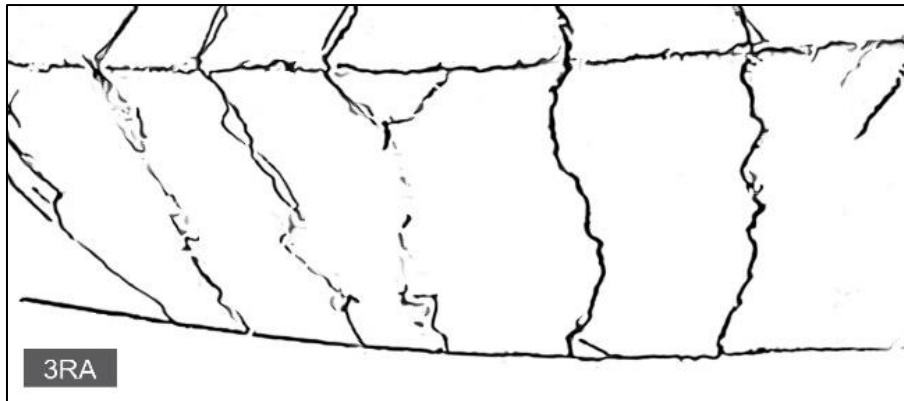


Figure 4.36: 3RA mold Crack pattern

## **5 CHAPTER FIVE**

### **5.1 Statistical Analysis**

In this chapter a statistical regression analysis was applied to the data obtained from the experimental work of this investigation. The first comparison has been made between the theoretical and experimental results based on the ultimate failure moment. The second comparison has been made between the experimental results and the proposed empirical equation. This equation is proposed to predict the ultimate load based on the 105 slabs in 25 references that experimentally evaluated bridges or slabs overlaying UHPC, as summarized in Table B-1 in APPENDIX B.

### **5.2 Theoretical Analysis Design Equation**

#### **5.2.1 Design of Concrete Structures**

Prediction of the deformational behavior of bridge deck slab overlaid with UHPC based on ultimate failure moment presented and the comparison bar chart between the theoretical and experimental results are shown in this section, the nominal strength of a composite structure calculated based on the current knowledge of member and material behavior then compared with the required strength. Bridge deck slab overlay with UHPC will act as like as T Beams, overlay layer forms the beam flange that stressed laterally due to slab action in that direction, while the substrate concrete projecting below the overlay layer forms web (Darwin et al., 2016). However, strength analysis method of T Beam is based on the assumption that web and flange are reinforced monolithically with each other but it can be used to predict the nominal moment of slabs and with disregarding the monolithically, according to equation 5-4. Then,

the ultimate failure moment of the section determined with equation 5-6 and the details are shown in Figure 5.1. After that the bar chart comparison between ultimate and nominal moment for all slabs presented Figure 5.2, The equations are as following:

A design of cross sections subjected to ultimate moment shall be based on:

$$M_u < \phi M_n \quad \text{Equation 5-1}$$

$$M_{n1} = A_{sf} f_{yf} \left( d - \frac{h_f}{2} \right) \quad \text{Equation 5-2}$$

$$M_{n2} = (A_s - A_{sf}) f_{yw} \left( d - \frac{a}{2} \right) \quad \text{Equation 5-3}$$

$$M_n = A_{sf} f_{yf} \left( d - \frac{h_f}{2} \right) + (A_s - A_{sf}) f_{yw} \left( d - \frac{a}{2} \right) \quad \text{Equation 5-4}$$

$$a = \frac{(A_s - A_{sf}) f_y}{0.85 f'_c b_w} \quad \text{Equation 5-5}$$

$$M_u = \frac{2PL}{12} \quad \text{Equation 5-6}$$

Where:

$M_{n1}$ : Flange (overlay) nominal moment

$M_{n2}$ : Web (substrate) nominal moment

$M_n$ : The total nominal resisting moment

$A_{sf}$ : Flange (overlay) steel area

$A_s$ : Web (substrate) steel area

$f_{yf}$ : Yield strength of flange (overlay) steel

$f_{yw}$ : Yield strength of web (substrate) steel

$f'_c$ : Overlay compressive strength

$d$ : Effective depth

$h_f$ : Hight of flange (overlay layer depth)



$M_u$ : Ultimate failure moment

$P$ : Ultimate failure moment

$L$ : Effective length of slab

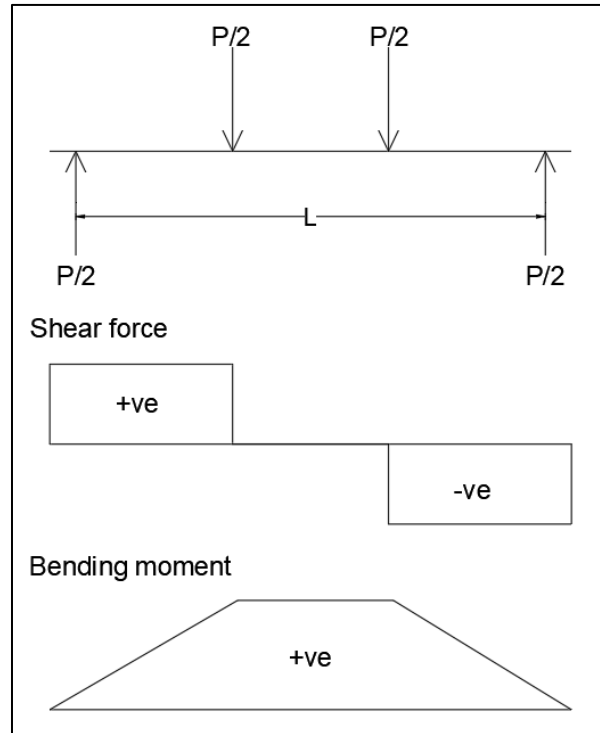


Figure 5.1: Ultimate failure moment data system

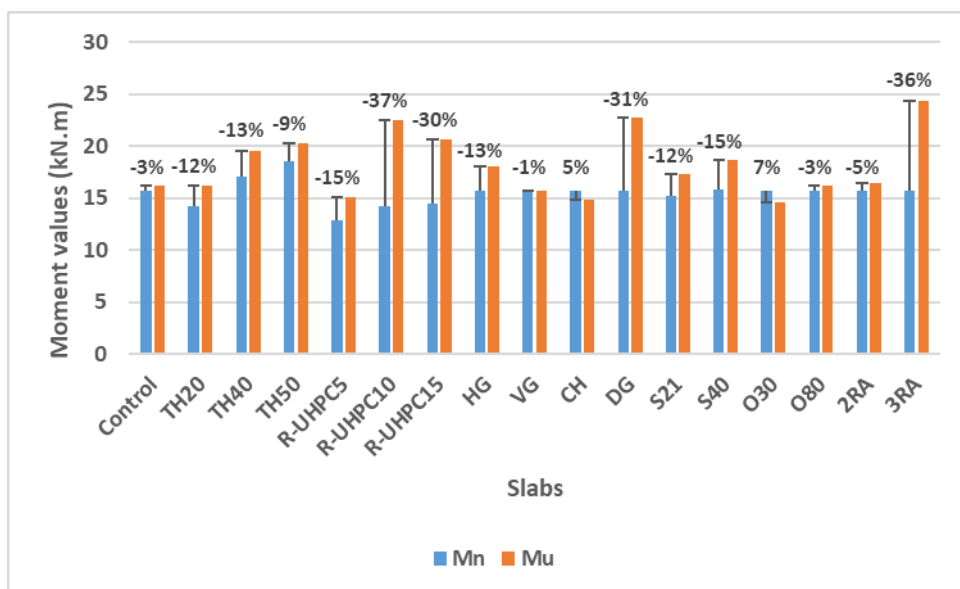


Figure 5.2: Comparison of ultimate and nominal moment of slabs

### 5.3 Analysis of Proposed Empirical Equation

The empirical equation is proposed to predict the ultimate failure load of the composite structure NSC-UHPC under flexure for the purpose of regression analysis based on 105" specimen data points collected from current and previous experimental works, as shown in Table B-1 APPENDIX B. For this purpose, the non-linear interpolation polynomial method is used for a set of data to pass through them fitly, and represent the experimental data. In order to create an equation, the "IBM SPSS Statistics 26" program is used with dependent and independent variables. This equation is summarized in different kinds of literature [(Luo, 2002, Habel, 2004, Buitelaar et al., 2004, Mohsen A. Issa et al., 2007, Perez et al., 2009, Shann, 2012, Tayeh et al., 2012, Muñoz and Ángel, 2012, Hussein et al., 2016, Bao et al., 2017, Sritharan and Aaleti, 2017, Wibowo and Sritharan, 2018, Sritharan et al., 2018, Newtonson and Weldon, 2018, Lapi et al., 2018, Graybeal and Haber, 2018, Sadek et al., 2019, Zhang et al., 2019, López-Carreño et al., 2020, Zhang et al., 2020b, Savino et al., 2020, Zhu et al., 2020, Freeseaman et al., 2020, Zhang et al., 2020a, Teng et al., 2021)] on studies which have been performed. Equation 5-7 assists to understand better the flexural performance and predicting the ultimate failure load of the existing NSC structure which is planned to be strengthened with a UHPC overlay. This equation is used to predict the results for the limited data values as shown in Table 5-1, which discovered that substrate and overlay compressive strengths have a significant effect on the ultimate failure load, and when compared to the structure's length and width, the effect is halved. Increasing the overlay layer thickness increases the failure load, but only to a certain extent; otherwise, the dead load increases and the effect is reversed. Also, the effect of the overlay

reinforcement ratio in composite structure reinforcement is much higher than the substrate reinforcement ratio.

The experimentation results of this study and some chosen slabs from Table B-1 in APPENDIX B, for which complete information is available for investigation, are compared with prediction equation results as shown in Figure 5.3 and Figure 5.4. The substrate parameters consist of; the effect of dimension, material compressive strength and reinforcement ratio. Also, for overlay application, the following parameters are taken into consideration; material type, compressive strength, thickness, and reinforcement ratio. Although many different interface pattern shapes have been evaluated in the literature, this equation is predicted based on the rough pattern shape since practically most findings were based on the rough pattern shape, and all studies emphasized that the best bond could be achieved with this shape.

$$P = 36000 + (2.92 \times 10^{-6} S_{R_r} S_{f_y} W S_{th}) + \left( \frac{O_{f_y} W O_{th}}{727500} (25 O_{R_r})^3 \right) + 10 F_{ac}$$

..... Equation 5-7

$$F_{ac} = \left[ \{0.1(S_{f'_c} + O_{f'_c})\} \times \{0.1(S_{th} + O_{th})\} \times \{0.02(L + W)\} \right]$$

Where:

P: Ultimate Failure Load (N)

L: Length of one-way slab (mm)

W: Width of one-way slab (mm)

$S_{th}$ : Substrate thickness (mm)

$S_{f'_c}$ : Substrate NSC Compressive strength (MPa)

$S_{R_r}$ : Substrate Reinforcement Ratio

$S_{f_y}$ : Substrate NSC steel yield strength (MPa)

$O_{f'_c}$ : Overlay UHPC compressive strength (MPa)

$O_{th}$ : Overlay UHPC thickness (mm)

$O_{Rr}$ : Overlay Reinforcement Ratio

$O_{fy}$ : Overlay UHPC steel yield strength (MPa)

Table 5-1: Proposed empirical equation data limits summary

	Length (mm)	Width (mm)	Substrate thickness (mm)	Substrate concrete compressive strength (MPa)	Substrate reinforcement ratio (%)	Overlay thickness (mm)	Overlay concrete compressive strength (MPa)	Overlay reinforcement ratio (%)	Substrate steel yield strength (MPa)
<b>Minimum</b>	100	75	38	31	0	25	106	0	0
<b>Maximum</b>	3200	2000	310	60	1.102	50	170	4.16	517
<b>Average</b>	1650	1037.5	174	45.5	0.551	37.5	138	2.08	258.5

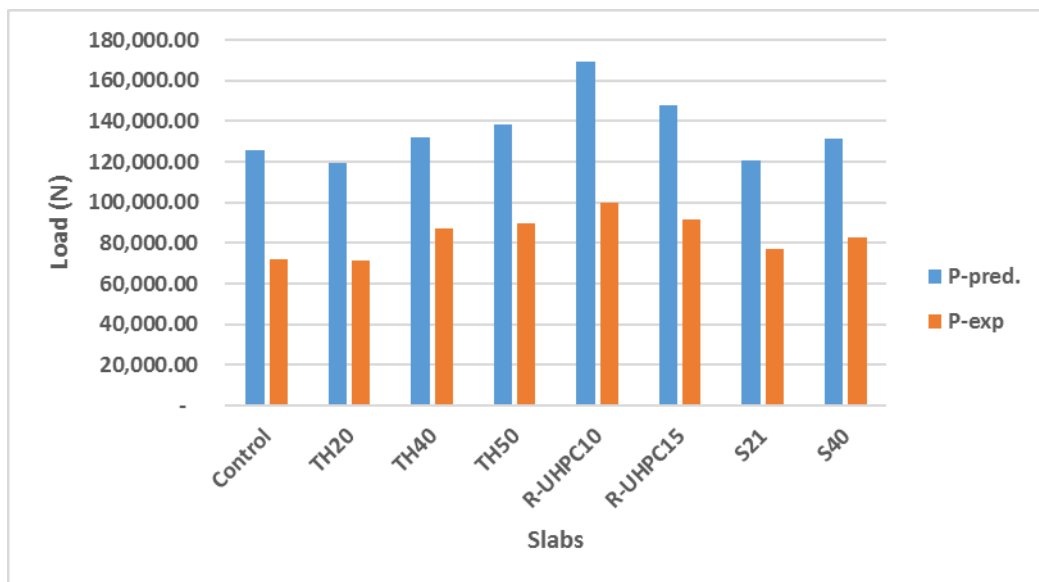


Figure 5.3: The comparison between this study's experimentation result and the proposed empirical equation

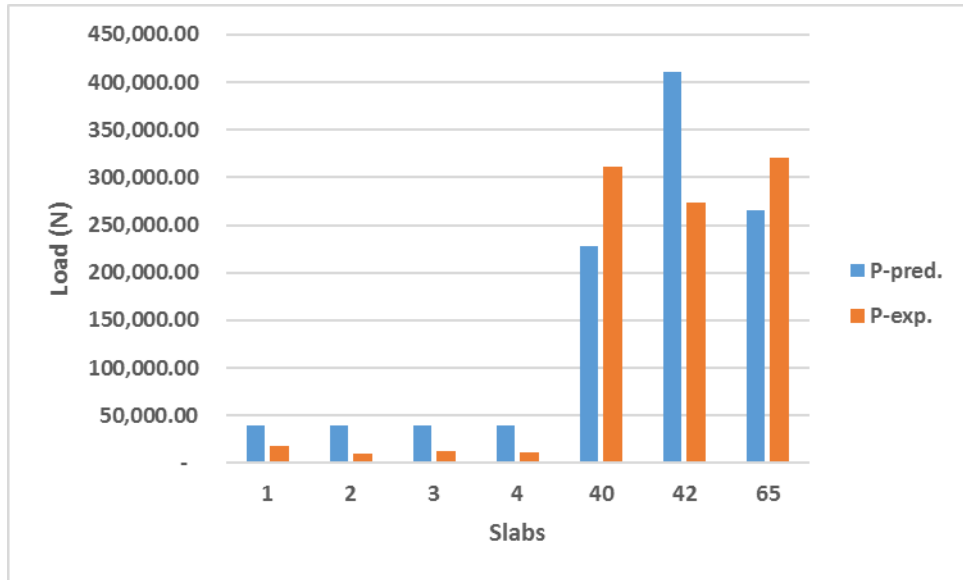


Figure 5.4: The comparison between the experimental results of some chosen slabs from Appendix B and the proposed empirical equation

#### 5.4 Regression Analysis

Many parameters influence the ultimate strength of concrete slabs, so the development of a theoretical explanation for their behavior appears to be rather difficult and can't relate in a linear model. Regression analysis is an important statistical method; the objective of regression is to evaluate the coefficients of an equation relating the criterion variable to one or more other variables, which are called predictor variables independent variables. After the regression equation is calibrated, it is very important to examine the rationality of the regression coefficients. In addition to the checking for rationality, the goodness-of-fit static, correlation factor ( $r$ ), standard deviation (SD), coefficient of variation (COV) and mean ( $\mu$ ) must be computed to assess the accuracy of predictions. In a large amount of data, the accuracy is strongly affected by  $r^2$  and COV.

### 5.4.1 Comparison of Practical Results with Theoretical Analysis Design Equation and Prediction Equation Analysis

Table 5-2 shows the statistical calculation for evaluating the experimental results and relative designed equations. In theoretical analysis  $M_u/M_n$  ultimate experimental failure moment per nominal composite structure moment are calculated, while in proposed equation analysis  $P_{exp}/P_{pred}$  ultimate experimental failure load per prediction equation's ultimate load results are calculated. In statistical analysis the higher  $r$  value and the lower COV are evidence for the excellent results. It is evident from the statistical results that prediction equation gave the better results compared with theoretical equation due to its lower value percent of coefficient of variance and higher value of correlation factor. The higher coefficient of variance of literature results compared with this study's results is related to the dispersion of data points in a data series around the mean because the information is obtained from several different sources and there are significant differences in the dimensions and working conditions. In addition, prediction analysis couldn't take the results for R-UHPC5, 3RA, 2RA, and Interface pattern shapes subs because of the lack of data in this area, and the theoretical analysis disregarded the interface patterns between the composite structure.

Table 5-2: Comparison between practice results and designed equation

Equation	<i>Mean</i>	<i>SD</i>	<i>COV (%)</i>	<i>r</i>
Theoretical analysis	1.18	0.202	17	0.1918
Proposed empirical equation analysis of this study results	0.62	0.029	4.8	0.9208
Proposed empirical equation analysis of literature results	0.65	0.454	69.6	0.893

## 6 CHAPTER SIX

### 6.1 Conclusion

From the tests performed on properties of UHPC, tests on reinforced concrete flat slab specimens and statistical analysis, the following conclusions can be drawn:

- UHPC has an extra ordinary mechanical property, compared with HPC and NSC, in which increase in: compressive strength by 43% and 68%, splitting tensile strength by 57% and 70%, flexural strength by 50% and 70%. Using a superplasticizer admixture leads to adequate workability of fresh mix and behaves in a moldable manner; UHPC slump is around 33% higher than NSC and 66% higher than HPC.
- The interface patterns are dependable parameters to obtain adequate bonds between NSC and UHPC. The substrate failure region for all interface patterns is evidence that desirable bond strengths can be obtained with all surface patterns without the use of a bonding agent.
- The dense unique matrix of UHPC let to zero permeability happen compared with NSC and HPC, this property makes the UHPC become the pretty desirable material for the purpose of overlay application because it behaves as like as the wearing surface that enhance the resistance to corrosion of steel and prolong the life of composite structure.
- A 10-millimeter increase in overlay thickness for slab specimens leads to an increase in ultimate failure load of around 20, and a decrease in maximum central deflection of around 40%. However, increase overlay thickness improve the capacity of composite structure but this increasing has to be limited, otherwise it increases dead load on the

structure. The laboratory test concluded that 20-50 mm UHPC overlay thickness can develop the strength of bridge deck slab overlay with UHPC positively.

- Strengthening the interface layer with addition a layer of embedded 5mm rebar at 15 and 10 cm; leads to increase the ultimate failure load by 28% and 39%. It is clear that addition a layer of rebar with UHPC overlay has a real affect to increase the resistance and durability of structure.
- Increase substrate concrete compressive strength from 30 MPa to 40 MPa leads to increase the ultimate failure load by 15 % and maximum central deflection by 22%, but if the substrate compressive strength decreased to 20 MPa the delamination may observe in the part length of composite structure under the point load. The substrate compressive strength has a great influence on the mode of failure, lower substrate material compressive strength UHPC overlay reduces adhesion and cohesion properties because of cracks and failure of the substrate.
- High value of tensile strength and zero permeability of overlay material are two essential concrete properties that can increase the mechanical and durability properties of bridge deck slabs overlay because bridge deck slabs exhibit to tension stress and penetration of water into the base continuously due to high traffic volume and moisture.
- The manner of fracture will go through the overlay and cause top concrete crush in the case of NSC and HPC overlay with suitable surface preparation. Due to the removal of coarse aggregate, the addition of 0.2% steel fiber, and the reduction of the water to cement ratio to 0.23% in UHPC overlay, cracks cannot penetrate the overlay and cannot result in delamination. The qualities of the composite construction are not significantly improved by increasing the compressive strength of the overlay material without adding steel fiber.



- The use of mechanical connectors with rough surface preparation is proposed for bridge deck slab overlay with UHPC. To transfer load more effectively and considerably improve composite structure's structural behavior, more anchors are suggested at the interface. This study recommended a maximum spacing of 150 mm between anchors, which results in a 50% increase in the ultimate failure load.
- Crack patterns in UHPC also followed yield line theory in flexural failure for all slabs approximately, the pattern of cracks will distribute more densely with stronger composite slabs. The control slab and the slab with rebar at the interface with 15 cm spaces did not follow the yield line hypothesis. When the tests were run, the first failure involved the concrete matrix, which was partially damaged but maintained 80% of its previous strength. This phenomenon might be regarded as excellent safety for design engineers since when the load increased, the slabs continued to resist with 20% of their remaining strength.
- In statistical analysis it is appeared that, theoretical analysis design equation can predict the results but with disregarding the interface patterns. And prediction equation analysis will provide more closer result with reality because it takes the interface preparation into consideration, but this equation couldn't include of all parameters that have effect on the strengthening process due to limited data that available in this area of study.

## 6.2 Recommendations

To better understand the behavior of bridge deck slab overlay with UHPC, the following works are recommended for the future:

- The effect of steel reinforcement in UHPC overlay on failure mode requires further investigation. Also, the effect of embedded bar diameters and spaces in the overlay should be investigated extensively. The effect of UHPC curing methods on the behavior of substrate NSC should be investigated. Furthermore, the impact of UHPC thickness and steel fiber volume in the UHPC matrix should be further validated.
- Almost all studies were experimentally tested based on the static loading only. An additional study is required to investigate the effect of cyclic loadings like seismic.
- Nearly all previous studies focused on strengthening the existing structures at unloading conditions. But to represent the actual circumstance, the existing structure has to be strengthened under sustained loading.
- Most of the experimental studies focused on strengthening the undamaged structures which aren't suitable with reality. Further study is required to investigate the effect of strengthening application on the damaged structures.
- The roughness patterns were investigated extensively. Further research is needed to focus on the degree of roughness quantitatively to obtain the required bond strength.

## REFERENCES

- AALETI, S., SRITHARAN, S. & ABU-HAWASH, A. 2013. Innovative UHPC-Normal Concrete Composite Bridge Deck. *RILEM-fib-AFGC Int. Symposium on Ultra-High Performance Fibre-Reinforced Concret*, 217-224.
- AASHTO 2017. AASHTO Bridge Design Specification, 8th Ed. Washington, DC: American Association of State Highway Transportation Officials.
- ACI 318R-19 2019. Building Code Requirements for Structural Concrete and Commentary. Farmington Hills, MI: American Concrete Institute.
- ACI 363R-92 1997. State-of-the-Art Report on High-Strength Concrete Reported by ACI Committee 363. American Concrete Institute.
- AHMED, G. H. 2009. *Punching Shear Strength and Behavior of Ultra High Performance Reinforced Concrete Flat Plate Slabs*. Master of Science, University of Salahaddin-Hawler.
- AHMED, G. H., AHMED, H., ALI, B. & ALYOUSEF, R. 2021. Assessment of High Performance Self-Consolidating Concrete through an Experimental and Analytical Multi-Parameter Approach. *Materials (Basel)*, 14.
- AHMED, G. H. & AZIZ, O. Q. Punching Shear Strength and Behavior of UHPC Flat Plate Slabs Thirteenth International Conference on Recent Advances in Concrete Technology and Sustainability, 2015 Ottawa, Canada. 1-10.
- AİTCIN, P. C. 2016. Ultra high strength concrete. *Science and Technology of Concrete Admixtures*.
- AL-BASHA, A. J., TOLEDO, W. K., NEWTON, C. M. & WELDON, B. D. 2019. Ultra-High Performance Concrete Overlays for Concrete Bridge Decks. *IOP Conference Series: Materials Science and Engineering*, 471.
- AL-MADANI, M. K., AL-OSTA, M. A., AHMAD, S., KHALID, H. R., AL-HURI, M. J. C. & MATERIALS, B. 2022. Interfacial bond behavior between ultra high performance concrete and normal concrete substrates. 320, 126229.
- ALDRED, J. M., HOLLAND, T. C., MORGAN, D. R., ROY, D. M., BURY, M. A., HOOTON, R. D., OLEK, J., SCALI, M. J., DETWILER, R. J. & JABER, T. M. J. A. A. C. I. C. F. H., MI, USA 2006. Guide for the use of silica fume in concrete. 234.
- ASTM 615/A 615M 2004. Standard Specification for Deformed and Plain Carbon Steel Bars for Concrete Reinforcement<sup>1</sup>. American Association State Highway and Transportation Officials Standard.
- ASTM C33/C33M 2016. Standard Specification for Concrete Aggregates. American Society for Testing and Material.
- ASTM C39/C39M 2017. Standard Test Method for Compressive Strength of Cylindrical Concrete Specimens. American Society for Testing and Material.
- ASTM C109/C109M 2016. Standard Test Method for Compressive Strength of Hydraulic Cement Mortars (Using 2-in. or [50-mm] Cube Specimens). American Society for Testing and Material.
- ASTM C150/C150M 2017. Standard Specification for Portland Cement. American Society for Testing and Material.
- ASTM C496 1996. Standard Test Method for Splitting Tensile Strength of Cylindrical Concrete Specimens. American Society for Testing and Material.
- ASTM C882/C882M 2013. Standard Test Method for Bond Strength of Epoxy-Resin Systems Used With Concrete By Slant Shear. American Society for Testing and Material.
- ASTM C1240 2017. Standard Specification for Use of Silica Fume for Use as a Mineral Admixture in Hydraulic-Cement Concrete, Mortar, and Grout. American Society for Testing and Material.

- ASTM C 1018 1997. Standard Test Method for Flexural Toughness and First-Crack Strength of Fiber-Reinforced Concrete (Using Beam With Third-Point Loading). American Society for Testing and Material.
- AZIZ, O. Q. & AHMED, G. H. Mechanical properties of ultra high performance concrete (UHPC). Proceedings of the 12th International Conference on Recent Advances in Concrete Technology and Sustainability Issues, Prague, Czech Republic, 2012.
- AZMEE, N. M. & SHAFIQ, N. J. C. S. I. C. M. 2018. Ultra-high performance concrete: From fundamental to applications. 9, e00197.
- BAE, J. H., HWANG, H. H. & PARK, S. Y. 2019. Structural Safety Evaluation of Precast, Prestressed Concrete Deck Slabs Cast Using 120-MPa High-Performance Concrete with a Reinforced Joint. *Materials (Basel)*, 12.
- BAJABER, M. A. & HAKEEM, I. Y. 2021. UHPC evolution, development, and utilization in construction: a review. *Journal of Materials Research and Technology*, 10, 1058-1074.
- BAO, Y., VALIPOUR, M., MENG, W., KHAYAT, K. H. & CHEN, G. 2017. Distributed fiber optic sensor-enhanced detection and prediction of shrinkage-induced delamination of ultra-high-performance concrete overlay. *Smart Materials and Structures*, 26.
- BONNEAU, O., POULIN, C., DUGAT, M. & TCIN, P.-C. A. J. C. I. 1996. Reactive powder concretes: from theory to practice. 18, 47-49.
- BRÜHWILER, E. & BASTIEN-MASSE, M. 2015. Strengthening the Chillon viaducts deck slabs with reinforced UHPFRC. *IABSE Conference*.
- BRÜHWILER, E. & DENARIÉ, E. 2018. Rehabilitation and Strengthening of Concrete Structures Using Ultra-High Performance Fibre Reinforced Concrete. *Structural Engineering International*, 23, 450-457.
- BRÜHWILER, E. & SHEN, X. Strengthening of existing structures using R-UHPFRC: principles and conceptual design. The 2nd ACF Symposium 2017–Innovations for Sustainable Concrete Infrastructures, 2017.
- BUITELAAR, P. 2004. Heavy Reinforced Ultra High Performance Concrete. *ResearchGate*, 33.
- BUITELAAR, P., BRAAM, R. & KAPTIJN, N. Reinforced high performance concrete overlay system for rehabilitation and strengthening of orthotropic steel bridge decks. Orthotropic Bridge Conference, Sacramento, USA, 2004. 384-401.
- CHILWESA, M., MINELLI, F., REGGIA, A. & PLIZZARI, G. 2017. Evaluating the shear bond strength between old and new concrete through a new test method. *Magazine of Concrete Research*, 69, 425-435.
- CHOI, J.-T. 2016. *Strengthening of RC beams with Ultra High Performance Concrete*.
- DANIEL, J. I., GOPALARATNAM, V. S. & GALINAT, M. A. 2002. Report on Fiber Reinforced Concrete. *ACI 544.1R-96*, section 2.2.2.
- DARWIN, D., DOLAN, C. W. & NILSON, A. H. 2016. *Design of concrete structures*, McGraw-Hill Education New York, NY, USA:.
- DE LARRARD, F., BELLOC, A., RENWEZ, S., BOULAY, C. J. M. & STRUCTURES 1994. Is the cube test suitable for high performance concrete? 27, 580-583.
- DENMARK, P. B. C. A. Ultra Thin Heavy Reinforced High Performance Concrete Overlays.
- DU, J., MENG, W., KHAYAT, K. H., BAO, Y., GUO, P., LYU, Z., ABU-OBEIDAH, A., NASSIF, H. & WANG, H. 2021. New development of ultra-high-performance concrete (UHPC). *Composites Part B: Engineering*, 224.
- ELNONO, M. A., SALEM, H. M., FARAHAT, A. M. & ELZANATY, A. H. 2009. Use of Slurry Infiltrated Fiber Concrete in Reinforced Concrete Corner Connections Subjected to Opening Moments. *Journal of Advanced Concrete Technology*, 7, 51-59.
- ESMAEILI & KASAEI 2016. Effect of Different Curing Regimes on Strength and Transport Properties of UHPC Containing Recycled Steel Tire Wires as Micro Steel Fibers. *First International Interactive Symposium on UHPC*, 1-7.

- FENG, S., XIAO, H., MA, M., ZHANG, S. J. C. & MATERIALS, B. 2021. Experimental study on bonding behaviour of interface between UHPC and concrete substrate. 311, 125360.
- FRESEMAN, K., WANG, K. & TAN, Y. 2020. Bond strength and chloride resistance of epoxy and concrete overlays on bridge decks. *International Journal of Pavement Engineering*, 1-6.
- GRAYBEAL, B. 2007. Compressive behaviour of ultra-high-performance fibre-reinforced concrete. *ACI Materials Journal*. 104, 146–152.
- GRAYBEAL, B., BRÜHWILER, E., KIM, B.-S., TOUTLEMONDE, F., VOO, Y. L. & ZAGHI, A. J. J. O. B. E. 2020. International perspective on UHPC in bridge engineering. 25, 04020094.
- GRAYBEAL, B. & HABER, Z. 2018. Ultra-High Performance Concrete for Bridge Deck Overlays. *U.S. Department of transportation FHWA*, 40, 4-16.
- GRAYBEAL, B. A. 2006. Material Property Characterization of Ultra-High Performance Concrete. Federal Highway Administration
- GUNAVATHY, J. & INDUMATHI, G. J. B. M. E. 2011. Leadership and Organization Citizenship Behavior-A Study among Employees of a Civil Engineering Company. 4.
- HABEL, K. 2004. *Structural behaviour of elements combining ultra-high performance fibre reinforced concretes (UHPRFC) and reinforced concrete*. EPFL.
- HABER, Z. B., MUNOZ, J. F. & GRAYBEAL, B. A. 2017. Field testing of an ultra-high performance concrete overlay. United States. Federal Highway Administration. Office of Infrastructure.
- HEINZ, D. & LUDWIG, H.-M. Heat treatment and the risk of DEF delayed ettringite formation in UHPC. Proceedings of the international symposium on UHPC, Kassel, Germany, 2004. 717-730.
- HUSSEIN, H. H., WALSH, K. K., SARGAND, S. M. & STEINBERG, E. P. 2016. Interfacial Properties of Ultrahigh-Performance Concrete and High-Strength Concrete Bridge Connections. *Journal of Materials in Civil Engineering*, 28.
- IS 516 2018. Properties of Hardened Concrete other than Strength. *Density of Hardened Concrete and Depth of Water Penetration Under Pressure*. BUREAU OF INDIAN STANDARDS.
- KAZEMI, S. & LUBELL, A. S. J. A. M. J. 2012. Influence of specimen size and fiber content on mechanical properties of ultra-high-performance fiber-reinforced concrete. 109, 675.
- KIM, S.-K., KIM, W. & HAN, S.-M. 2019. Behavior Evaluation of Ultrahigh-Performance Concrete Beam Containing Para-Aramid Fibers. *Advances in Civil Engineering*, 2019, 1-17.
- KIM, T. & RENS, K. L. J. J. O. M. I. C. E. 2008. Concrete maturity method using variable temperature curing for normal-strength concrete mixes. II: theoretical study. 20, 735-741.
- KRAUSS, P. D., LAWLER, J. S. & STEINER, K. A. 2009. Guidelines for Selection of Bridge Deck Overlays, Sealers and Treatments. National Cooperative Highway Research Program (NCHRP)
- LAFARGE NORTH AMERICA 2009. Product Data Sheet: Ductal® JS1000.
- LAPI, M., FERNANDES, H., ORLANDO, M., RAMOS, A. & LÚCIO, V. J. M. O. C. R. 2018. Performance assessment of flat slabs strengthened with a bonded reinforced-concrete overlay. 70, 433-451.
- LARRARD, F. D. 1989. Ultrafine Particles for The Making of Very High Strength Concretes. *Pergamon*, 19.
- LARRARD, F. D. & SEDRAN, T. 1993. Optimiztion of Ultra-High-Performance Concrete by The Use of a Packing Model *Pergamon*, 24, 997-1009.

- LARSEN, I. L. & THORSTENSEN, R. T. 2020. The influence of steel fibres on compressive and tensile strength of ultra high performance concrete: A review. *Construction and Building Materials*, 256.
- LÓPEZ-CARREÑO, R.-D., CARRASCÓN, S., AGUADO, A. & PUJADAS, P. 2020. Mechanical Connectors to Enhance the Interfacial Debonding of Concrete Overlays. *Applied Sciences*, 10.
- LUO, S. 2002. *Evaluations of concrete overlays for bridge deck applications*. Master of Science in Civil Engineering, West Virginia University.
- MA, J., ORGASS, M., DEHN, F., SCHMIDT, D. & TUE, N. Comparative investigations on ultra-high performance concrete with and without coarse aggregates. International Symposium on Ultra High Performance Concrete, Kassel, Germany, 2004. 205-212.
- MA, J. & SCHNEIDER, H. J. L. A. C. E. R. 2002. Properties of ultra-high-performance concrete. 7, 25-32.
- MANDAL, D., DUTTA, B. K. & PANIGRAHI, S. C. 2008. Effect of copper and nickel coating on short steel fiber reinforcement on microstructure and mechanical properties of aluminium matrix composites. *Materials Science and Engineering: A*, 492, 346-352.
- MCDONAGH, M. D. & FODEN, A. J. 2016. Benefits of Ultra-High Performance Concrete for the Rehabilitation of the Pulaski Skyway. *First International Interactive Symposium on UHPC*, 1-9.
- MISHRA, O. & SINGH, S. P. 2019. An overview of microstructural and material properties of ultra-high-performance concrete. *Journal of Sustainable Cement-Based Materials*, 8, 97-143.
- MOHSEN A. ISSA, P. E., M.ASCE, ALHASSAN, M. A. & SHABILA, H. I. 2007. Low-Cycle Fatigue Testing of High-Performance Concrete Bonded Overlay–Bridge Deck Slab Systems. *Journal of bridge engineering © ASCE*, 419-428.
- MUÑOZ, C. & ÁNGEL, M. 2012. *Compatibility of ultra high performance concrete as repair material : bond characterization with concrete under different loading scenarios*.
- NEWTSON, C. & WELDON, B. 2018. Bridge Deck Overlays Using Ultra-High Performance Concrete. 8&63.
- PASETTO, M. & GIACOMELLO, G. 2014. Experimental Analysis of Waterproofing Polymeric Pavements for Concrete Bridge Decks. *International Journal on Pavement Engineering & Asphalt Technology*, 15.
- PEREZ, F., BISSONNETTE, B., GAGNÉ, R. J. M. & STRUCTURES 2009. Parameters affecting the debonding risk of bonded overlays used on reinforced concrete slab subjected to flexural loading. 42, 645-662.
- RESPLENDINO, J. State of the art of design and construction of UHPFRC structures in France. Proceedings of Hipermat-3rd International Symposium on UHPC and Nanotechnology for Construction Materials, 2012. 27-41.
- RICHARD, P. & CHEYREZY, M. 1994. Composition of Reactive Powder Concretes *Pergamon*, 25, 1501-1511.
- SADEK, H., TOLEDO, W., DAVILA, L., AL-BASHA, A., NEWTSON, C. & WELDON, B. 2019. Shrinkage in Ultra-High Performance Concrete Overlays on Concrete Bridge Decks. *MATEC Web of Conferences*, 271.
- SAVINO, V., LANZONI, L., TARANTINO, A. M. & VIVIANI, M. 2020. A cohesive FE model for simulating the cracking/debonding pattern of composite NSC-HPFRC/UHPFRC members. *Construction and Building Materials*, 258.
- SCHIEßL, P., MAZANEC, O. & LOWKE, D. 2007. SCC and UHPC—Effect of mixing technology on fresh concrete properties. *Advances in construction materials 2007*. Springer.
- SCHMIDT, M. & FEHLING, E. 2004. *Ultra high performance concrete (UHPC) : proceedings of the International Symposium on Ultra High Performance Concrete, Kassel, Germany, September 13-15, 2004*, Kassel, Kassel University Press.

- SHANN, S. V. 2012. *Application of ultra high performance concrete (UHPC) as a thin-bonded overlay for concrete bridge decks*. Michigan Technological University.
- SHARMA, R., JANG, J. G. & BANSAL, P. P. 2022. A comprehensive review on effects of mineral admixtures and fibers on engineering properties of ultra-high-performance concrete,. *Journal of Building Engineering*, 45.
- SRITHARAN, S. & AALETI, S. 2017. Investigation of A Suitable Shear Friction Interface Between UHPC and Normal Strength Concrete for Bridge Deck Applications. *Bridge Engineering Center and Institute for Transportation Iowa State University*, 10, 10-65.
- SRITHARAN, S., BRISTOW, B. & PERRY, V. Characterizing an ultra-high performance material for bridge applications under extreme loads. Proceedings of the 3rd International Symposium on High Performance Concrete, Orlando, FL, 2003.
- SRITHARAN, S., DOIRON, G., BIERWAGEN, D., KEIERLEBER, B. & ABU-HAWASH, A. 2018. First Application of UHPC Bridge Deck Overlay in North America. *Transportation Research Record: Journal of the Transportation Research Board*, 2672, 40-47.
- STEFANIUK, H. L. 2020. *The Behaviour of Ultra-High-Performance Concrete in Precast Concrete Bridge Deck Connections*. Master Of Science, University of Manitoba.
- STIEL, T., KARIHALOO, B. L. & FEHLING, E. Effect of casting direction on the mechanical properties of CARDIFRC. International Symposium on Ultra High Performance, 2004. 481-493.
- SU, Y., LUO, B., LUO, Z., HUANG, H., LI, J. & WANG, D. J. M. 2022. Effect of Accelerators on the Workability, Strength, and Microstructure of Ultra-High-Performance Concrete. 15, 159.
- SUN, Z. 2004. *Evaluation of Concrete Bridge Deck Overlays*. Master of Science in Civil Engineering, West Virginia University.
- TADROS, M. K. & PE, A. S. building BLOCKS.
- TADROS, M. K., SEVENKER, A. & BERRY, R. 2019. Ultra-High-Performance Concrete. *Structure magazine*.
- TAYEH, B. A., ABU BAKAR, B. H. & MEGAT JOHARI, M. A. 2012. Characterization of the interfacial bond between old concrete substrate and ultra high performance fiber concrete repair composite. *Materials and Structures*, 46, 743-753.
- TENG, L., VALIPOUR, M. & KHAYAT, K. H. 2021. Design and performance of low shrinkage UHPC for thin bonded bridge deck overlay. *Cement and Concrete Composites*, 118.
- WEIßE, D. & HOLSCHMACHER, K. J. L. A. C. E. R. 2003. Some aspects about the bond of reinforcement in ultra high strength concrete. 8, 251-63.
- WIBOWO, H. & SRITHARAN, S. 2018. Use of Ultra-High-Performance Concrete for Bridge Deck Overlays. *Bridge Engineering Center and Institute for Transportation Iowa State University*, 683, 1-48.
- WU, C., LI, J. & SU, Y. D. 2018. *Development of ultra-high performance concrete against blasts: from materials to structures*, Woodhead Publishing.
- WU, Z., SHI, C., HE, W. & WU, L. 2016. Effects of steel fiber content and shape on mechanical properties of ultra high performance concrete. *Construction and Building Materials*, 103, 8-14.
- YANG, Q., ZHANG, S., HUANG, S., HE, Y. J. C. & RESEARCH, C. 2000. Effect of ground quartz sand on properties of high-strength concrete in the steam-autoclaved curing. 30, 1993-1998.
- ZHANG, Y., ZHANG, C., ZHU, Y., CAO, J. & SHAO, X. 2020a. An experimental study: various influence factors affecting interfacial shear performance of UHPC-NSC. *Construction and Building Materials*, 236.
- ZHANG, Y., ZHU, P., WANG, X. & WU, J. 2020b. Shear properties of the interface between ultra-high performance concrete and normal strength concrete. *Construction and Building Materials*, 248.

- ZHANG, Y., ZHU, Y., YESETA, M., MENG, D., SHAO, X., DANG, Q. & CHEN, G. 2019. Flexural behaviors and capacity prediction on damaged reinforcement concrete (RC) bridge deck strengthened by ultra-high performance concrete (UHPC) layer. *Construction and Building Materials*, 215, 347-359.
- ZHU, Y., ZHANG, Y., HUSSEIN, H. H., LIU, J. & CHEN, G. 2020. Experimental study and theoretical prediction on shrinkage-induced restrained stresses in UHPC-RC composites under normal curing and steam curing. *Cement and Concrete Composites*, 110.
- ZINGAILA, T., AUGONIS, M., ŠERELIS, E., KELPŠA, Š., MARTINAVIČIUS, D. J. J. O. S. A. & ENGINEERING, C. 2016. Influence of heat treatment regimes on mechanical properties of NSC-UHPC composite members. 14, 51-59.
- ZOLLO, R. F. 1996. Fiber-reinforced Concrete: an Overview after 30 Years of Development 19, 107-122.



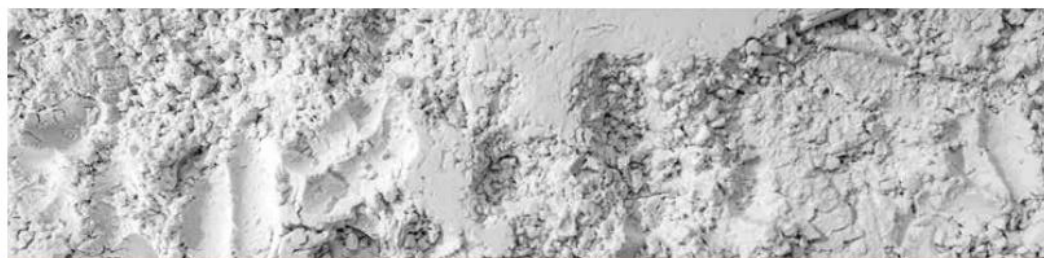
# APPENDIX A

## 1. SILICA FUME

### Concrete Admixtures - Cement Replacements

#### ECA MICROSILICA-D

Densified Silica Fume Powder



#### Product Description

ECA MICROSILICA-D is a dry densified silica fume powder designed to increase concrete compressive and flexural strength, reduce permeability, increase durability and improve hydraulic abrasion/erosion resistance. ECA MICROSILICA-D improves concrete through two mechanisms. The extremely fine silica fume particles are able to fill the microscopic voids between the cement particles, creating a less permeable structure. In addition, the silica fume reacts with the free calcium hydroxide within the concrete to form additional calcium silicate hydrate (glue), producing a tighter paste-to- aggregate bond. ECA MICROSILICA-D can be used to consistently produce high strength concrete with locally available materials and existing methods. It may also be used in precast and prestressed applications where high early strengths are required. The addition of ECA MICROSILICA-D also produces concrete with increased water tightness and dramatically reduced permeability compared to conventional mixes. Reduced permeability is an important advantage in slowing the intrusion of chloride where corrosion of reinforcing steel is a potential problem. Examples are parking garages, bridge decks and concrete in a marine environment. ECA MICROSILICA-D also enhances the durability of concrete against aggressive chemical attack and in hydraulic abrasion/erosion applications.

#### Advantages

- Reduces permeability.
- Enhances durability against aggressive chemical attack.
- Improved resistance to abrasion.
- Reduces the intrusion of chloride.
- Compressive strength increase.

#### Typical Properties

Appearance: Ultra-fine amorphous light to dark grey, colored powder  
Specific Gravity:  $2.25 \pm 15\%$  at  $20^{\circ}\text{C}$   
Sulphate Content:  $<1.0\%$  as S03  
Air Entrainment: Nil.  
Bulk Density:  $\geq 650$  kg/m<sup>3</sup>  
SiO<sub>2</sub> Content: 90 % min  
Freezing Point: N.A

#### Compatibility

With cements: ECA MICROSILICA-D can be used with all types of Portland Cements, including cement replacement materials. For use with special cements we recommend that you consult European Concrete Additives.  
With Other Admixtures: ECA MICROSILICA-D is compatible with all conventional water reducers, superplasticizer, set retarders and EUNICOR DCI Corrosion Inhibitor. Only non-chloride set accelerators may be used with ECA MICROSILICA-D concrete. All admixtures must be added separately to assure their prescribed performance. Trial mixtures and pretesting of concrete are recommended to optimize dosage rates, and ensure ultimate performance.

#### Addition Rates Range

2% - 15% (w/w) by weight of cement ECA MICROSILICA-D dosage rates will vary based on the requirements of the application. When used to improve compressive strength, ECA MICROSILICA-D is dosed at a level of 8% - 10% by weight of total cementitious material. Dosages as low as 2% - 4% of ECA MICROSILICA-D may be used to improve the rheology of mixtures. Normally a dosage of EUNICEM SP6 of 1% v/w total cementitious material is used in combination with ECA MICROSILICA-D. It is strongly

recommended that trial mixtures be made several weeks before construction start up. This will allow the concrete producer an opportunity to determine the proper batching sequence and amounts of other admixtures needed in order to deliver the required concrete mixture to the site. A trial mixture will also help determine whether the construction practices will allow the concrete to meet a specified performance. European Concrete Additives experience with this product can help the concrete producer deliver a satisfactory product regardless of the mix proportions. ECA MICROSILICA-D is supplied bagged and ready for use. The method of addition of ECA MICROSILICA-D is important as it is vital that Complete, uniform dispersion is achieved. ECA MICROSILICA-D is best added after the course aggregates and water, and given an extended mix prior to the addition of fines and cement. ECA MICROSILICA-D is always used in combination with a Superplasticizer as the water demand for a concrete containing ECA MICROSILICA -D is increased. ECA MICROSILICA-D will reduce the surface bleed water of concrete in large applications. Good Practice for curing concrete must be followed to ensure that problems occurring due to decreased bleeding are minimized.

#### **Effects of Overdosing**

Will normally produce a decrease in workability and a reduction in setting time. The hardened properties of the concrete may be enhanced, but only if the concrete is thoroughly mixed.

#### **Dispensing**

ECA MICROSILICA-D is a powder product, and requires manual dispensing techniques. It is recommended that you consult European Concrete Additives should dispensing of the product become problematic.

#### **Packaging**

ECA MICROSILICA-D is available in 25 kg bags. Manual dispensing by tearing the bags is the normal method. A simple dust mask should be used when dispensing the bagged product.

#### **Storage**

Bagged ECA MICROSILICA-D should be stored in a dry, protected area.

#### **Health and Safety**

See ECA MICROSILICA-D Safety Data Sheet or consult European Concrete Additives.

#### **Technical Service**

The Technical Service department of European Concrete Additives is available to assist you in the correct use of our products and its resources are at your disposal entirely without obligation.

#### **Contact Information**

Al-Faiha for Engineering Products  
techsupport@alfaihaengineering.com  
www.alfaihaengineering.com

## 2. GROUT

### PRODUCT DATA SHEET

# SikaGrout®-212

## FLOWABLE SHRINKAGE COMPENSATED CEMENTITIOUS GROUT

### PRODUCT DESCRIPTION

SikaGrout®-212 is a one part flowable shrinkage compensated cementitious grout. Meets the requirements of Class R4 of BS EN 1504-3 & BS EN 1504-6.

### USES

- General purpose grouting
- Under stanchion plates
- Filling cavities, voids, gaps and recesses
- Concrete repairs
- Machine & base plates
- For exterior and interior use
- Steel reinforcement anchoring

### CHARACTERISTICS / ADVANTAGES

- Excellent flow properties
- Pre batched for quality
- Just add water
- Compatible with Sika® FerroGard® corrosion inhibitors
- High compressive strength gain
- Easy to mix and apply
- Contains no chloride admixtures
- Overcoatable with Sika reprofiling/levelling mortars and coatings
- Low shrinkage
- Generally more durable than equivalent class of concrete
- Does not segregate or bleed
- Fire rating and protection properties comparable to concrete
- Can be pumped or poured
- Good mechanical properties
- Grouting thickness between 10-75 mm

### PRODUCT INFORMATION

<b>Chemical Base</b>	Cement, selected fillers and aggregates, special additive
<b>Packaging</b>	25 kg bags
<b>Appearance / Colour</b>	Grey powder
<b>Shelf Life</b>	6 months from date of production if stored properly.
<b>Storage Conditions</b>	in dry conditions in undamaged and unopened original sealed packaging.
<b>Density</b>	~ 2300 kgm <sup>3</sup> (wet density)

Product Data Sheet  
SikaGrout®-212  
September 2017, Version 01.01  
020201010010000002

## TECHNICAL INFORMATION

Compressive Strength	Ambient temperature: +20°C			
	1 day	7 days	28 days	R4 Requirements
	~ 25 - 30 N/mm <sup>2</sup>	~ 60 - 65 N/mm <sup>2</sup>	~ 65 - 70 N/mm <sup>2</sup>	> 45 N/mm <sup>2</sup>
Flexural Strength	~ 10 N/mm <sup>2</sup> (28 days)			(EN 196)
Tensile Strength	~ 3.6 N/mm <sup>2</sup> (28 days)			
Pull-Out Resistance	Displacement < 0.6mm at load of 75KN (Wet & Dry)			(EN 1881)
Expansion	0.25 – 0.50%			
Electrical Resistivity	~ 7.3			(Wenner Test)

## APPLICATION INFORMATION

Ambient Air Temperature	+5°C min. / +30°C max.
Substrate Temperature	+5°C min. / +30°C max.

## APPLICATION INSTRUCTIONS

### SUBSTRATE QUALITY / PRE-TREATMENT

*Concrete, mortar, stone:* Surfaces must be sound, thoroughly clean, free from ice, oils, grease, standing water and any loose or friable particles and any other surface contaminants.  
The concrete "pull off" (tensile) strength should be > 1.0 MPa.

*Steel, iron:* Clean, free from oil or grease, rust and scale etc.

*Shutter/Formwork:* All formwork should be of adequate strength, treated with release agent and sealed to prevent leakage. Sealing can be achieved by using Sikaflex® -11FC+ sealant beneath or around formwork and between joints. Ensure formwork includes outlets for extraction of the pre-soaking water. A header box/hopper should be constructed on one side of the formwork so that a grout head of 150-200 mm can be maintained during the grouting operation. The substrate should be prepared by suitable mechanical preparation techniques such as high pressure water jetting, breakers, blastcleaning, scabblers, etc. The concrete substrates should be pre-soaked with clean water continuously for 2 - 6 hours to ensure a saturated surface dry condition throughout the operation. Immediately before pouring grout, remove all excess or standing water from within any formwork, cavities or pockets.

### MIXING

Place the water into a forced action grout mixer or in a clean drum. Slowly add complete bag of SikaGrout® 212 into the water and continuously mix for 2 minutes in mixer to achieve a uniform and lump free consistency. Alternatively use a slow speed drill (200-500 rpm) and helical mixer.  
Dependent on the desired consistency and flow prop-

erties, the mixing ratio can be adjusted.

Measure the appropriate amount of water to achieve the desired grout consistency given in the table below. Heat water if necessary to achieve a temperature between 15-20°C.

### Water addition rate per 25 kg bag

Pourable consistency	2.3 – 3.9 litres
Flowable consistency	2.3 – 3.9 litres

### APPLICATION

Pour the mixed grout into the header box/hopper ensuring continuous grout flow during the complete grouting operation to avoid trapping air. Use steel banding or chains to assist flow where necessary. For large volume placement, grout pumps are recommended.

### CURING TREATMENT

After the grout has initially hardened, remove formwork and trim edges while concrete is 'green'. Cure all exposed grout surfaces using Sikafloor® ProSeal. In cold weather apply heat blankets to maintain a constant temperature.

### CLEANING OF TOOLS

Clean all tools and application equipment with water immediately after use. Hardened/cured material can only be mechanically removed.

### LIMITATIONS

- Do not exceed water addition
- Not to be used for patch repair works
- Do not use vibrating pokers
- Use only on clean, sound substrate
- Do not apply when there is a risk of frost
- Pour or pump from one side only
- Keep exposed surfaces to a minimum

## VALUE BASE

All technical data stated in this Product Data Sheet are based on laboratory tests. Actual measured data may vary due to circumstances beyond our control.

## LOCAL RESTRICTIONS

Please note that as a result of specific local regulations the performance of this product may vary from country to country. Please consult the local Product Data Sheet for the exact description of the application fields.

## ECOLOGY, HEALTH AND SAFETY

For information and advice on the safe handling, storage and disposal of chemical products, users shall refer to the most recent Safety Data Sheet (SDS) containing physical, ecological, toxicological and other safety-related data.

## LEGAL NOTES

The information, and, in particular, the recommendations relating to the application and end-use of Sika products, are given in good faith based on Sika's current knowledge and experience of the products when properly stored, handled and applied under normal conditions in accordance with Sika's recommendations. In practice, the differences in materials, substrates and actual site conditions are such that no warranty in respect of merchantability or of fitness for a particular purpose, nor any liability arising out of any legal relationship whatsoever, can be inferred either from this information, or from any written recommendations, or from any other advice offered. The user of the product must test the product's suitability for the intended application and purpose. Sika reserves the right to change the properties of its products. The proprietary rights of third parties must be observed. All orders are accepted subject to our current terms of sale and delivery. Users must always refer to the most recent issue of the local Product Data Sheet for the product concerned, copies of which will be supplied on request.

### SIKA LIMITED

#### Watchmead

Welwyn Garden City  
Hertfordshire, AL7 1BQ  
Tel: 01707 394444  
Web: [www.sika.co.uk](http://www.sika.co.uk)  
Twitter: @SikaLimited

### SIKA IRELAND LIMITED

#### Ballymun Industrial Estate

Ballymun  
Dublin 11, Ireland  
Tel: +353 1 862 0709  
Web: [www.sika.ie](http://www.sika.ie)  
Twitter: @SikaIreland



### 3. STEEL FIBER

## HONGTU STEEL FIBER Product



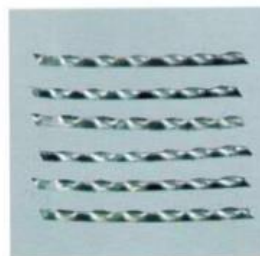
#### Micro steel fiber:

- Material: low carbon steel wire, copper coated
- Diameter: 0.2mm -- 0.25mm
- Length: 12mm - 14mm
- Tensile strength: >2850Mpa
- Feature: Excellent tensile, bending and shearing strength, resistance against cracking, impact and fatigue.
- Use: It is widely used for buildings, road surface, bridges, tunnels, airport road surface, water conservancy projects, military engineering, and all kinds of building products.



#### Straight steel fiber:

- Material: low carbon steel wire or stainless steel
- Diameter: 0.4mm - 1.0mm
- Length: meet your requirements
- Tensile strength >1000Mpa
- Feature: excellent tensile, high tenacity, against cracking, impact and fatigue
- Uses: highway road surface, tunnel, building, airport road surface and so on.




#### Wavy steel fiber:

- Wavy steel fiber:
- Material: Cold-draw steel wire
- Tensile Strength: 750 Mpa - 1200Mpa
- Fiber Length: 20mm, 25mm, 30mm, 40mm, 60 mm
- Conformance: ASTM A 820/ A 820 M
- Widely used in
  - 1) construction bridges
  - 2) thin roof engineering
  - 3) highway etc.

## 4. SUPERPLASTICIZERS

- **Hyperplast PC800M**



# Hyperplast PC800M

New generation hyperplasticising admixture for extended slump retention and low sensitivity to bleeding

### Description

Hyperplast PC800M is a new generation hyperplasticiser for concrete, based on polycarboxylic polymers with long chains specially designed to produce concrete with extensive workability.

This effect can be used to produce low viscosity concrete for mid-to-high scale projects or when pumping concrete over long distances is required.

### Applications

- ▲ Under water micro concrete repair and grouting.
- ▲ For high levels of concrete pumping.
- ▲ Suitable for long distances with extended slump retention.
- ▲ Low viscosity concrete with Enhanced compressive strength.
- ▲ Structures with congested reinforcement.
- ▲ Pre-stressed concrete.
- ▲ Improved cohesion allows for use in mass concrete pours and piling.
- ▲ Producing concrete capable of maintaining its flow for 3 hours.
- ▲ For producing concrete with low sensitivity to bleeding.

### Compatibility

Hyperplast PC800M is suitable to use with all types of Portland cement and cement replacement materials. Hyperplast PC800M is compatible with other DCP admixtures used in the same concrete mix.

If more than one type of admixture will be used in the concrete mix, they must be dispensed to the concrete separately.

### Standards

Hyperplast PC800M complies with ASTM C494, Type G.

### Method of Use

Hyperplast PC800M should be added to the concrete with the mixing water to achieve optimum performance.

An automatic dispenser should be used to dispense the correct quantity of Hyperplast PC800M to the concrete mix.

### Technical Properties @ 27°C:

Colour:	Light yellow
Specific gravity:	1.07 ± 0.02
pH:	5 - 7

### Dosage

The recommended dosage of Hyperplast PC800M is 0.5 - 3.5 litre per 100 kg of cementitious materials in the mix, including GGBFS, PFA or microsilica.

Representative trials should be conducted to determine the optimum dosage of Hyperplast PC800M to meet the performance requirements by using the materials and conditions in actual use.

### Effects of Over Dosage

Overdosage of Hyperplast PC800M will cause the following:

- ▲ Increase in workability.

Ultimate concrete strength will not be adversely affected and will generally be increased provided that proper concrete curing is maintained.

### Cleaning

Clean Hyperplast PC800M with fresh cold water.

### Packaging

Hyperplast PC800M is available in 25 litre jerrycan, 210 litre drums and 1000 litre bulk supply.

### Storage

Hyperplast PC800M has a shelf life of 12 months from date of manufacture if stored at temperatures between 2°C and 50°C.

If these conditions are exceeded, contact DCP Technical Department for advice.

# Hyperplast PC800M

## Cautions

### Health and Safety

Hyperplast PC800M is not classified as a hazardous material. Hyperplast PC800M should not come into contact with skin and eyes.  
In case of contact with eyes, immediately flush with plenty of water and seek medical attention.

For further information, refer to the Material Safety Data sheet.

### Fire

Hyperplast PC800M is nonflammable.

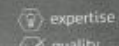
## More from Don Construction Products

A wide range of construction chemical products are manufactured by DCP which include:

- ▲ Concrete admixtures.
- ▲ Surface treatments
- ▲ Grouts and anchors.
- ▲ Concrete repair.
- ▲ Flooring systems.
- ▲ Protective coatings.
- ▲ Sealants.
- ▲ Waterproofing.
- ▲ Adhesives.
- ▲ Tile adhesives and grouts.
- ▲ Building products.
- ▲ Structural strengthening.

**Note:**

We endeavour to ensure that any information, advice or recommendation we may give in product literature is accurate and correct. However, because we have no control over where and how products are applied, we cannot accept any liability arising from the use of the products.



01-0459-A-20



- **Sika ViscoCrete**

## PRODUCT DATA SHEET

# Sika® ViscoCrete®-5930 L IQ

### HIGH RANGE WATER REDUCING ADMIXTURE

#### DESCRIPTION

Sika® ViscoCrete®-5930 L IQ is a High range water reducing and super plasticizing admixture for Concrete & Mortar utilizing Sika's 'ViscoCrete®' polycarboxylate polymer technology ( 3rd Generation ) .

#### USES

Sika® ViscoCrete®-5930 L IQ is mainly used for the following applications:

- 1- Concrete Containing GGBS , Micro Silica , Fly ash , .... Etc.
- 2- Production of Ready Mixed Concrete, High performance Concrete .
- 3- Impermeable & dense Concrete with smooth surface , Water tight mix design proportion must be considered.
- 4- Production of Self-compacting Concrete ( SCC ) , SCC mix design proportion must be considered.
- 5- Production of complex & fine elements such as Slabs , Foundations , Walls , Beams & Columns even through congested reinforcement .

#### CHARACTERISTICS / ADVANTAGES

Sika® ViscoCrete®-5930 L IQ is a powerful superplasticizer which acts through several different mechanisms including surface adsorption and sterically effects separating the cementitious binder particles. The following advantages properties are achieved:

- 1- High water reduction, resulting in high density, high strength and reduced permeability
- 2- Superior plasticizing effect, resulting in improved flow, placing and compaction characteristics
- 3- Reduced shrinkage during curing and reduced creep when hardened .
- 4- Chloride Free thus; no corrosion effect on steel.
- 5- Reduced rate of carbonation of the Concrete .
- 6- NO need for vibration , thus NO noise pollution .
- 7- Suitable for Winter conditions .

#### APPROVALS / CERTIFICATES

Sika® ViscoCrete®-5930 L IQ meets the requirements of ASTM C-494 Types F.

## PRODUCT INFORMATION

<b>Composition</b>	Aqueous solution of modified polycarboxylates
<b>Packaging</b>	Bulk Deliveries 1000 Kgs IBC 20 kg Pail
<b>Appearance / Colour</b>	Brownish liquid
<b>Shelf life</b>	12 months from date of production if stored properly in undamaged unopened, original sealed packaging.
<b>Storage conditions</b>	In dry conditions at temperatures between +5°C and +35°C. Protect from direct sunlight. It requires recirculation when held in storage for extended periods.
<b>Specific gravity</b>	1.085 ± ( 0.01 ) g/cm <sup>3</sup>
<b>pH-Value</b>	4 - 6
<b>Total chloride ion content</b>	Nil

## TECHNICAL INFORMATION

<b>Concreting guidance</b>	The standard rules of good concreting practice, concerning production and placing, are to be followed. Laboratory trials shall be carried out before concreting on site, especially when using a new mix design or producing new concrete components. Fresh concrete must be cured properly and curing applied as early as possible.
----------------------------	--

## APPLICATION INFORMATION

<b>Recommended dosage</b>	Recommended dosage for concrete: 1- For plastic Concrete ( 0.2 - 0.8 % ) by weight of Binder ( 200 - 800 gm ) for 100 kg cement . 2- For Flow & Self Compacting Concrete ( 0.8 - 1.8 % ) by weight of Binder ( 800 - 1800 gm ) for 100 kg cement . 3- Optimum dosage should be determined by site trials. When adjusting the consistency, high water reduction property of the admixture must be taken in consideration , excessive water addition must be prevented .
<b>Compatibility</b>	Sika® ViscoCrete®-5930 L IQ can be used in conjunction with : 1- SikaFiber® 2- Sika®PlastoCrete-N 3- Sika®Antifreeze 4- SikaRapid® 5- SikaRetarder® All admixtures must be added separately. Trials are always recommended before combining products . For additional information, please contact Sika technical personnel.
<b>Dispensing</b>	Sika® ViscoCrete®-5930 L IQ is added to the gauging water or added with it into the concrete mixer. To take advantage of the high water reduction, a wet mixing time, which is depending on the mixing conditions and mixer performance, of at least 2 mins. per cubic meter after the admixture addition is recommended. Sika® ViscoCrete®-5930 L IQ shall not be added to dry cement.
<b>Restrictions</b>	Over dosage effect An over dosage of Sika® ViscoCrete®-5930 L IQ with water excess will cause the following : 1- Increase of air entrainment . 2- Bleeding or Segregation .

## **BASIS OF PRODUCT DATA**

All technical data stated in this Product Data Sheet are based on laboratory tests. Actual measured data may vary due to circumstances beyond our control.

## **IMPORTANT CONSIDERATIONS**

When using Sika® ViscoCrete®-5930 L IQ the following points should be taken in consideration :

- 1- A suitable mix design has to be taken into account and local material sources shall be trialed.
- 2- Do not use with naphthalene based admixtures.

## **ECOLOGY, HEALTH AND SAFETY**

For information and advice on the safe handling, storage and disposal of chemical products, users shall refer to the most recent Safety Data Sheet (SDS) containing physical, ecological, toxicological and other safety-related data.

## **APPLICATION INSTRUCTIONS**

Application Method / Tools :

The standard rules of good concreting practice , concerning production as well as placing are to be followed , refer to relevant standards . Fresh Concrete must be cured properly .

Cleaning of tools :

Clean all tools & application equipment with water immediately after use .

Hardened / Cured material can only be mechanically removed .

## **LOCAL RESTRICTIONS**

Please note that as a result of specific local regulations the declared data for this product may vary from country to country. Please consult the local Product Data Sheet for the exact product data.

## **LEGAL NOTES**

The information, and, in particular, the recommendations relating to the application and end-use of Sika products, are given in good faith based on Sika's current knowledge and experience of the products when properly stored, handled and applied under normal conditions in accordance with Sika's recommendations. In practice, the differences in materials, substrates and actual site conditions are such that no warranty in respect of merchantability or of fitness for a particular purpose, nor any liability arising out of any legal relationship whatsoever, can be inferred either

from this information, or from any written recommendations, or from any other advice offered. The user of the product must test the product's suitability for the intended application and purpose. Sika reserves the right to change the properties of its products. The proprietary rights of third parties must be observed. All orders are accepted subject to our current terms of sale and delivery. Users must always refer to the most recent issue of the local Product Data Sheet for the product concerned, copies of which will be supplied on request.

## 5. Strain Gauge

- 80 mm - Conc.

NAME	STRAIN GAUGE
TYPE	BE120-80AA-X-3.5cm (80 x 3)
OHMS	119.7±0.1
GAGE FACTOR	2.08±1%
LOT NO.	2018-12-1-11
GRADE	A
QUANTITY	100 PCS
INSPECTOR	J-05 C-05
MANUFACTURER	HT SENSOR TECHNOLOGY CO., LTD

## 6. Composite structure stress strain distribution derivation

- For NSC:

$$\frac{\varepsilon_{cu}}{C_b} = \frac{\varepsilon_y}{d - C_b}$$

$$C_b = \left( \frac{\varepsilon_{cu}}{\varepsilon_{cu} + \varepsilon_y} \right) d \dots\dots\dots \text{Eq. A1}$$

$$\rho_b = 0.85\beta_1 \frac{f'_c}{f_y} \frac{\varepsilon_{cu}}{\varepsilon_{cu} + \varepsilon_y} \dots\dots\dots \text{Eq. A2}$$

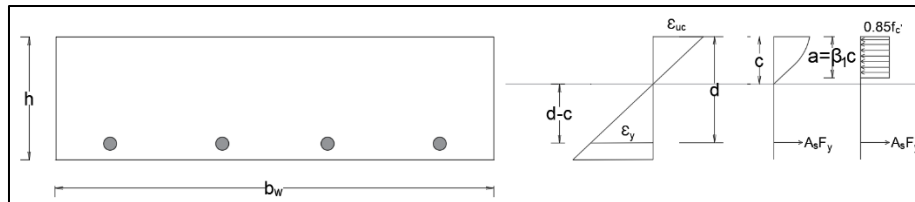


Figure A-1: Stress strain distribution for NSC

- UHPC+NSC

- If  $C \leq h_H$

$$\rho_b = 0.85\beta_1 \frac{f'_c}{f_y} \frac{\varepsilon_{cuH}}{\varepsilon_{cuH} + \varepsilon_y} \dots\dots\dots \text{Eq. A3}$$

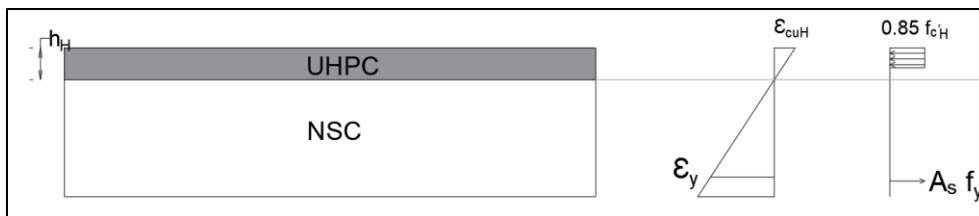


Figure A-2: Stress strain distribution for composite structure  $C \leq h_H$

○ If  $C > h_H$

$$\varepsilon_{cH} = \varepsilon_{cuH}$$

$$\varepsilon_{cN} = \frac{C - h_H}{C} \varepsilon_{cuH}$$

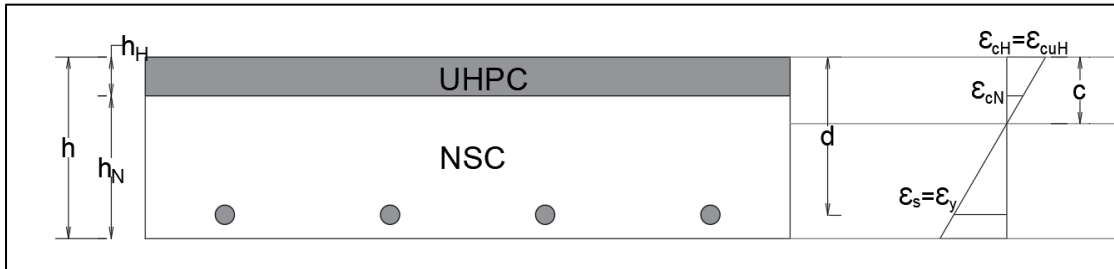


Figure A-3: Stress strain distribution for composite structure  $C > h_H$

(Sum.  $F_x = 0$ ) For high value of  $\varepsilon_{cuH}$ ,  $\varepsilon_{cN}$  may be exceed  $\varepsilon_{cuN}$ , then take the  $\varepsilon_{cN} = \varepsilon_{cuN} = 0.003$ . in this case the stress distribution become:

$$0.85 f'_{cH} b_w h_H + 0.85 f'_{cN} b_w (a - h_H) = A_s f_y$$

$$A_s = \rho_b b_w d$$

$$a = \beta_1 C_b = \beta_1 \left( \frac{\varepsilon_{cuH}}{\varepsilon_{cuH} + \varepsilon_y} \right) d$$

$$0.85 f'_{cH} b_w h_H + 0.85 f'_{cN} b_w \left[ \beta_1 \left( \frac{\varepsilon_{cuH}}{\varepsilon_{cuH} + \varepsilon_y} \right) d - h_H \right] = \rho_b b_w d f_y$$

$$\rho_b = 0.85 \left( \frac{f'_{cH}}{f_y} \right) \left( \frac{h_H}{d} \right) + 0.85 \left( \frac{f'_{cN}}{f_y} \right) \left[ \beta_1 \left( \frac{\varepsilon_{cuH}}{\varepsilon_{cuH} + \varepsilon_y} \right) - \frac{h_H}{d} \right] \dots \dots \dots \text{Eq. A4}$$

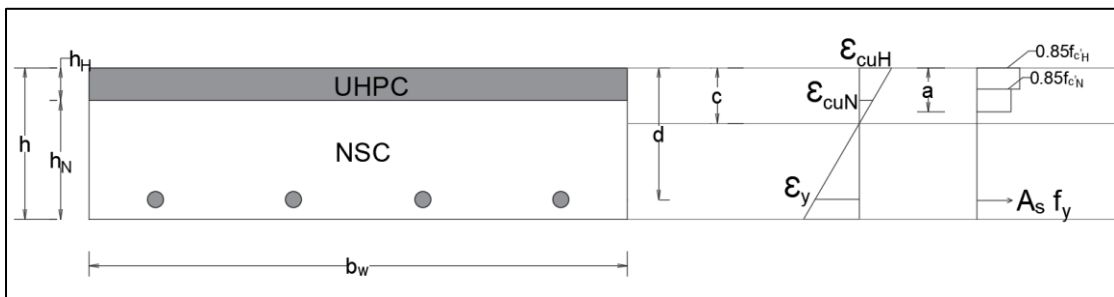


Figure A-4: Stress strain distribution for composite structure  $C > h_H$  and  $\varepsilon_{cN} = \varepsilon_{cuN}$

## APPENDIX B

Table (B-1): The experimental database of Bridge and Slab overlay with UHPC

Ref.	No.	Substrate							Overlay				Failure Region	Result
		L (mm)	Cross Section		Substrate Material & Strength (MPa)	Rf. Ratio %	fy (MPa)	Surface Preparation (mm)	Overlay Material & Strength (MPa)	Thickness (mm)	fy (MPa)	Rf. Ratio %		
			b (mm)	H (mm)										
(Luo, 2002)	1	127	127	38	NSC fc'42	0	0	Rough + Latex based slurry with extra water	LMC fc'47	38	0	0	Substrate Failure	17.92 kN Maximum failure load
	2	127	127	38	NSC fc'42	0	0	Rough + Latex based slurry with extra water	MMC fc'57	38	0	0	Substrate Failure	10.18 kN Maximum failure load & 1.82 MPa Maximum shear strength
	3	127	127	38	NSC fc'42	0	0	Rough + Latex based slurry with extra water	MMC-FA fc'49	38	0	0	Substrate Failure	13.23 kN Maximum failure load & 2.41 MPa Maximum

														shear strength
	4	127	127	38	NSC fc'42	0	0	Rough + Latex based slurry with extra water	FR.C fc'61	38	0	0	Substrate Failure	11.54 kN Maximum failure load & 2.1 MPa Maximum shear strength
(Habel, 2004)	5	-	100 0	152	NSC fc'40	0.9	50 0	$\frac{1}{2}$ Roughness of Contact Zone	UHPC fc'150	50	50 0	2	Substrate Failure	Strengthening Detail alone
(Buitelaar et al., 2004)	6	-	-	-	Steel Bridge Deck	0	-	Epoxy with Silica Aggregate	HPC fc'117	50	0	0	Interface Failure	2.96 MPa Bond strength
	7	-	-	-	Steel Bridge Deck	0	-	Epoxy with Hyperit Aggregate	HPC fc'117	50	0	0	Interface Failure	4.81 MPa Bond strength
	8	-	-	-	Steel Bridge Deck	0	-	Weld Mesh Reinforcement	HPC fc'117	50	-	-	Undesirable Local Peak Stress	-
(Mohsen A. Issa et al., 2007)	9	850 0	180 0	200	Precast C.	-	-	Epoxy	LMC fc'47	25	0	0	Overlay Failure	-
	10	850 0	180 0	200	Precast C.	-	-	Epoxy	MSC fc'51	25	0	0	Overlay Failure	-



	11	850 0	180 0	200	Precast C.	-	-	Sandblast	LMC fc'47	25	0	0	Substrate Failure	2.1 MPa Bond strength
	12	850 0	180 0	200	Precast C.	-	-	Sandblast	MSC fc'51	25	0	0	Substrate Failure	2.3 MPa Bond strength
(Perez et al., 2009)	13	300 0	100 0	200	NSC fc'45	-	-	Scarification	CFC fc'55	80	-	-	Substrate Failure	2.60 MPa Direct shear strength
	14	300 0	100 0	200	NSC fc'45	-	-	Sandblast	CFC fc'55	80	-	-	Substrate Failure	2.42 MPa Direct shear strength
	15	300 0	100 0	200	NSC fc'45	-	-	Jackhammer + Sandblast	CFC fc'55	80	-	-	Interface Failure	1.81 MPa Direct shear strength
	16	300 0	100 0	200	NSC fc'45	-	-	High Pressure Water Jet	CFC fc'55	80	-	-	Substrate Failure	2.71 MPa Direct shear strength
(Shann, 2012)	17	300 0	100 0	150	NSC fc'30	-	-	Assume Full Bond	UHPC fc'117	25	0	0	Clarified in 2.4.1&2. 5.2	0.09 MPa Debonding stress & 0.48 MPa Interface shear stress
	18	300 0	100 0	250	NSC fc'30	-	-	Assume Full Bond	UHPC fc'117	25	0	0	Clarified in	0.04 MPa Debonding

													2.4.1&2.5.2	stress & 0.17 MPa Interface shear stress
	19	300 0	100 0	200	NSC fc'30	-	-	Assume Full Bond	UHPC fc'117	6.3	0	0	-	0.03 MPa Debonding stress & 0.16 MPa Interface shear stress
	20	300 0	100 0	200	NSC fc'30	-	-	Assume Full Bond	UHPC fc'117	12. 7	0	0	-	0.05 MPa Debonding stress & 0.25 MPa Interface shear stress
	21	300 0	100 0	200	NSC fc'30	-	-	Assume Full Bond	UHPC fc'117	19	0	0	-	0.055 MPa Debonding stress & 0.33 MPa Interface shear stress
	22	300 0	100 0	200	NSC fc'30	-	-	Assume Full Bond	UHPC fc'117	25	0	0	-	0.06 MPa Debonding stress & 0.37 MPa Interface

														shear stress
	23	300 0	100 0	200	NSC fc'30	-	-	Assume Full Bond	UHPC fc'117	50	0	0	-	0.08 MPa Debonding stress & 0.48 MPa Interface shear stress
(Tayeh et al., 2012)	24	100	100	150	NSC fc'38	0	0	No Roughness	UHPC fc'170	15 0	0	0	Substrate Failure + partial interface failure	169 kN Max. force & 8.5 MPa Shear stress
	25	100	100	150	NSC fc'38	0	0	Sandblast	UHPC fc'170	15 0	0	0	Substrate Failure	343 kN Max. force & 17.17 MPa Shear stress
	26	100	100	150	NSC fc'38	0	0	Wire Brush	UHPC fc'170	15 0	0	0	Substrate Failure + partial interface failure	232 kN Max. force & 11.65 MPa Shear stress
	27	100	100	150	NSC fc'38	0	0	Drilled Hole	UHPC fc'170	15 0	0	0	Substrate Failure + partial interface failure	221 kN Max. force & 11.1 MPa Shear stress
	28	100	100	150	NSC fc'38	0	0	Horizontal Groove	UHPC fc'170	15 0	0	0	Substrate Failure + partial	277 kN Max. force & 13.89

													interface failure	MPa Shear stress
(Muñoz and Ángel, 2012)	29	393.7	100	38.1	NSC fc'31	0	0	Smooth -0.6 mm depth	UHPC-Ductal production	38.1	0	0	Substrate Failure + partial interface failure	3.84 MPa Indirect tensile strength
	30	393.7	100	38.1	NSC fc'31	0	0	Chipped - 0.92 mm depth	UHPC-Ductal production	38.1	0	0	Substrate Failure + partial interface failure	4.28 MPa Indirect tensile strength
	31	393.7	100	38.1	NSC fc'31	0	0	Brush - 0.7 mm depth	UHPC-Ductal production	38.1	0	0	Substrate Failure + partial interface failure	3.33 MPa Indirect tensile strength
	32	393.7	100	38.1	NSC fc'31	0	0	Sandblast - 1.06 mm depth	UHPC-Ductal production	38.1	0	0	Substrate Failure + partial interface failure	3.77 MPa Indirect tensile strength
	33	393.7	100	38.1	NSC fc'31	0	0	Groove	UHPC-Ductal production	38.1	0	0	Substrate Failure + partial interface failure	5.72 MPa Indirect tensile strength
(Hussein et al., 2016)	34	-	75	75	NSC fc'41	0	0	Smooth	UHPC fc'158.5	75	0	0	Substrate Failure + partial	13.22 kN Max. force & 3.02

													interface failure	MPa Shear stress
	35	-	75	75	NSC fc'41	0	0	Sandblast	UHPC fc'158.5	75	0	0	Substrate Failure + partial interface failure	21.48 kN Max. force & 5.01 MPa Shear stress
	36	-	75	75	NSC fc'41	0	0	Rough	UHPC fc'158.5	75	0	0	Substrate Failure	24.24 kN Max. force & 5.63 MPa Shear stress
(Bao et al., 2017)	37	450	200	25	NSC fc'50	-	-	Calcium hydroxide	UHPC fc'124	25	0	0	Interface Failure	1.31 MPa Bond strength
(Sritharan and Aaleti, 2017)	38	240 0	609 .6	203 .2	NSC fc'31.3	0.6 27	-	Smooth	UHPC fc'106.8	30	0	0	Substrate Failure + Partial Interface Failure	311.3 kN Ultimate load & 71.17 (kN.m)/m Ultimate moment
	39	240 0	609 .6	203 .2	NSC fc'31.3	0.6 27	-	Inclined Groove - 1.26 mm depth	UHPC fc'106.8	30	0	0	Substrate Failure	311.3 kN Ultimate load & 71.17 (kN.m)/m Ultimate moment

	40	240 0	609 .6	203 .2	NSC fc'31.3	0.6 27	-	Inclined Groove -3 mm depth	UHPC fc'106.8	30	0	0	Substrate Failure	311.3 kN Ultimate load & 71.17 (kN.m)/m Ultimate moment
	41	240 0	609 .6	203 .2	NSC fc'31.3	0.6 27	-	Inclined Groove – 5 mm depth	UHPC fc'106.8	30	0	0	Substrate Failure	311.3 kN Ultimate load & 71.17 (kN.m)/m Ultimate moment
(Wibowo and Sritharan, 2018)	42	240 0	240 0	203 .2	NSC fc'45	0.6 25	51 7	Horizontal Groove	UHPC fc'117	38	51 7	-	Substrate Failure	273.92 kN Ultimate load & 124.5 (kN.m)/m Ultimate moment
(Sritharan et al., 2018)	43	-	900 0	-	Old B.D.	-	-	Rough + Groove with Bridge Length	UHPC fc'124	38	-	-	Substrate Failure	1.51 MPa Bond Strength
(Newtson and Weldon, 2018)	44	900	900	101 .6	NSC fc'36	0.6 16	42 0	Rough – 2 mm depth	UHPC fc'123	25. 4	0	0	Control Specime n	39.9 kN Ultimate Load
	45	900	900	101 .6	NSC fc'36	1.1 02	42 0	Rough – 2 mm depth	UHPC fc'123	25. 4	0	0	Low Shrinkag e	39.9 kN Ultimate Load

	46	900	900	152.4	NSC fc'36	0.66	420	Rough – 2 mm depth	UHPC fc'123	25.4	0	0	Great Shrinkage	-
	47	300	150	150	NSC fc'36	0	0	Lightly Ground - 0.05 mm depth	UHPC fc'118.8	47.6	0	0	-	7.1 MPa Shear Stress
	48	300	150	150	NSC fc'36	0	0	Horizontal Groove – depth 0.9 mm	UHPC fc'118.8	47.6	0	0	-	12 MPa Shear Stress
	49	300	150	150	NSC fc'36	0	0	Cross Hatch – depth 1.6 mm	UHPC fc'118.8	47.6	0	0	-	12 MPa Shear Stress
	50	300	150	150	NSC fc'36	0	0	Diagonal Groove – depth 1.6 mm	UHPC fc'118.8	47.6	0	0	-	11.4 MPa Shear Stress
	51	300	150	150	NSC fc'36	0	0	Vertical Groove – depth 1.6 mm	UHPC fc'118.8	47.6	0	0	-	9.8 MPa Shear Stress
	52	300	150	150	NSC fc'36	0	0	Rough – depth 2.8 mm	UHPC fc'118.8	47.6	0	0	-	19.8 MPa Shear Stress
(Lapi et al., 2018)	53	2300	2300	150	NSC fc'32	1.84	-	Rough	Bonded Reinforced Concrete Overlay fc'36	60	-	1.3	Interface Failure	580 kN Punching strength

	54	230 0	230 0	150	NSC fc'34	1.8 4	-	Rough + Cement Grout	Bonded Reinforced Concrete Overlay fc'37	60	-	1.3	Interface Failure	590 kN Punching strength
	55	230 0	230 0	150	NSC fc'26	1.8 4	-	Rough + Dowel	Bonded Reinforced Concrete Overlay fc'34	60	-	1.3	Punching full cross section	568 kN Punching strength
	56	230 0	230 0	150	NSC fc'25	1.8 4	-	Rough + Cement Grout + Dowel	Bonded Reinforced Concrete Overlay fc'39	60	-	1.3	Punching full cross section	550 kN Punching strength
(Graybeal and Haber, 2018)	57	305 00	853 0	430	NSC	-	-	Scarification	LMC-fy3.8	38	-	-	Interface Failure	1.8 MPa Peak Tensile Stress
	58	305 00	853 0	430	NSC	-	-	Scarification	UHPC-fy5.7	38	-	-	Interface Failure	0.8 MPa Peak Tensile Stress
	59	305 00	853 0	430	NSC	-	-	Hydrodemol ition	LMC-fy3.8	38	-	-	Interface Failure	3 MPa Peak Tensile Stress
	60	305 00	853 0	430	NSC	-	-	Hydrodemol ition	UHPC-fy5.7	38	-	-	Substrate Failure	3.4 MPa Peak Tensile Stress
	61	305 00	853 0	430	UHPC Fy5.7	-	-	Scarification	LMC-fy3.8	38	-	-	Overlay Failure	3.4 MPa Peak



															Tensile Stress
	62	305 00	853 0	430	UHPC Fy5.7	-	-	Scarification	UHPC-fy5.7	38	-	-	Interface Failure	3.4 MPa Peak Tensile Stress	
	63	305 00	853 0	430	UHPC Fy5.7	-	-	Hydrodemolition	LMC-fy3.8	38	-	-	Overlay Failure	3.2 MPa Peak Tensile Stress	
	64	305 00	853 0	430	UHPC Fy5.7	-	-	Hydrodemolition	UHPC-fy5.7	38	-	-	Interface Failure	4.5 MPa Peak Tensile Stress	
(Sadek et al., 2019)	65	274 0	810	203	NSC fc'32	-	-	Broom Finish – depth 2 mm	UHPC fc'107	-	0	0	Substrate Failure + Interface Failure	320 kN Ultimate load	
	66	274 0	810	203	NSC fc'32	-	-	Rough – depth 3 mm	UHPC fc'107	-	0	0	Substrate Failure	320 kN Ultimate load	
	67	274 0	810	203	NSC fc'32	-	-	Rough – depth 6 mm	UHPC fc'107	-	0	0	Substrate Failure	347 kN Ultimate load	
(Zhang et al., 2019)	68	320 0	200 0	280	NSC fc'60.2	0.7 29	40 0	Rough + Post Installed Stud	UHPC fc'140	50	40 0	4.1 6	Substrate Failure	1295 kN Ultimate load & 970 (kN.m)/m Ultimate moment	

(López-Carreño et al., 2020)	69	260 0	180 0	310	Asphalt Concrete Pavement	0	0	Steel Anchor	Conventional Concrete + Polyolefin fiber fc'50	10 0	0	0	Excessive Shrinkage	4 kN Pull- off test result
	70	260 0	180 0	310	Asphalt Concrete Pavement	0	0	Rough by Replacement	Conventional Concrete + Polyolefin fiber fc'50	10 0	0	0	Produce Crack	2.5 kN Pull-off test result
	71	260 0	180 0	310	Asphalt Concrete Pavement	0	0	Rough by Replacement + Bent Rebar	C.C.+P.F fc'50	10 0	0	0	High Structural Performance	4.5 kN Pull-off test result
(Zhang et al., 2020b)	72	300	300	410	NSC fc'30	0.6 5	45 3	Low Roughness – depth 1.78 mm	UHPC fc'128.2	50	45 3	3.6	Interface Failure	472 kN Ultimate load
	73	300	300	410	NSC fc'50	0.6 5	45 3	Low Roughness - depth 2.12 mm	UHPC fc'128.2	50	45 3	3.6	Substrate Failure + Partial Interface Failure	808.75 kN Ultimate load
	74	300	300	410	NSC fc'50	0.6 5	45 3	High Roughness – depth 4.56 mm	UHPC fc'128.2	50	45 3	3.6	Substrate Failure	1040 kN Ultimate load

	75	300	300	410	NSC fc'50	0.6 5	45 3	Ep.Rb-4.14	UHPC fc'128.2	50	45 3	3.6	Substrate Failure	1153 kN Ultimate load
	76	300	300	410	NSC fc'50	0.6 5	45 3	Grooved Joint	UHPC fc'128.2	50	45 3	3.6	Substrate Failure	877.5 kN Ultimate load
	77	300	300	410	NSC fc'50	0.6 5	45 3	Drilled Hole	UHPC fc'128.2	50	45 3	3.6	Interface Failure	777.5 kN Ultimate load
	78	300	300	410	NSC fc'50	0.6 5	45 3	Post Installed Stud	UHPC fc'128.2	50	45 3	3.6	Substrate Failure	1218.5 kN Ultimate load
(Savino et al., 2020)	79	114 0	820	200	NSC fc'59	-	-	High Roughness	UHPFRC fc'147	50	-	-	Substrate Failure	Fx vs. slip/debon ding 20kN vs. 0.025mm
	80	114 0	820	200	NSC fc'59	-	-	High Roughness	HPFR.C fc'78	50	-	-	Interface Failure	Fx vs. slip/debon ding 36kN vs. 0.025mm
(Zhu et al., 2020)	81	600	600	280	NSC fc'60	0.2 05	-	Rough – depth (1-4) mm	UHPC fc'140	50	-	4.1 8	Substrate Failure	8.4 MPa Maximum shear stress
(Freeseman et al., 2020)	82	300	300	80	-	-	-	Rough	Epoxy	9.5	0	0	Interface Failure	-

	83	300	300	45	-	-	-	Rough	Low Slump Dense Concrete	40	0	0	Interface Failure	-
(Zhang et al., 2020a)	84	200	200	250	NSC fc'30	0.5 23	-	Rough – depth 2 mm	UHPC fc'135.5	50	-	2.5 1	Substrate Failure + Partial Interface Failure	237.7 kN Ultimate load
	85	200	200	250	NSC fc'40	0.5 23	-	Rough – depth 2 mm	UHPC fc'135.5	50	-	2.5 1	Substrate Failure + Partial Interface Failure	277.3 kN Ultimate load
	86	200	200	250	NSC fc'50	0.5 23	-	Rough – depth 2 mm	UHPC fc'135.5	50	-	2.5 1	Substrate Failure	351 kN Ultimate load
	87	200	200	250	NSC fc'50	0.5 23	-	Drilled Hole – 30 mm depth & 0.12 mm diameter	UHPC fc'135.5	50	-	2.5 1	Substrate Failure + Partial Interface Failure	356 kN Ultimate load
	88	200	200	250	NSC fc'50	0.5 23	-	Grooved Joint – 10 mm width & 10 mm depth	UHPC fc'135.5	50	-	2.5 1	Substrate Failure + Partial Interface Failure	338.67 kN Ultimate load
	89	200	200	250	NSC fc'50	0.5 23	-	Post Installed Stud	UHPC fc'135.5	50	-	2.5 1	Substrate Failure + Partial Interface Failure	341.67 kN Ultimate load

	90	200	200	250	NSC fc'50	0.5 23	-	Smooth	UHPC fc'135.5	50	-	2.5 1	Substrate Failure + Partial Interface Failure	216 kN Ultimate load
(Teng et al., 2021)	91	200 0	100 0	150	NSC fc'37	-	-	Rough	CC fc'37	38	0	0	Interface Failure	1.5 MPa bond strength
	92	200 0	100 0	150	NSC fc'37	-	-	Rough	CC fc'37	50	0	0	Interface Failure	1.2 MPa bond strength
	93	200 0	100 0	150	NSC fc'37	-	-	Rough	LMC fc'46	25	0	0	Interface Failure	2.1 MPa bond strength
	94	200 0	100 0	150	NSC fc'37	-	-	Rough	LMC fc'46	38	0	0	Interface Failure	1.7 MPa bond strength
	95	200 0	100 0	150	NSC fc'37	-	-	Rough	LMC fc'46	50	0	0	Interface Failure	1.5 MPa bond strength
	96	200 0	100 0	150	NSC fc'37	-	-	Rough	G50 fc'111	38	0	0	Substrate Failure	1.9 MPa bond strength
	97	200 0	100 0	150	NSC fc'37	-	-	Rough	LWS35 fc'134	38	0	0	Substrate Failure	2.1 MPa bond strength
	98	200 0	100 0	150	NSC fc'37	-	-	Rough	EA5LWS35 fc'120	25	0	0	Substrate Failure	2.5 MPa bond strength

	99	200 0	100 0	150	NSC fc'37	-	-	Rough	EA5LWS36 fc'120	38	0	0	Substrate Failure	2.7 MPa bond strength
	10 0	200 0	100 0	150	NSC fc'37	-	-	Rough	EA10LWS35 fc'105	25	0	0	Substrate Failure	2.3 MPa bond strength
	10 1	200 0	100 0	150	NSC fc'37	-	-	Rough	EA10LWS36 fc'105	38	0	0	Substrate Failure	2.4 MPa bond strength
	10 2	200 0	100 0	150	NSC fc'37	-	-	Rough	EA10LWS37f c'105	50	0	0	Substrate Failure	2.7 MPa bond strength
	10 3	200 0	100 0	150	NSC fc'37	-	-	Rough	EA10LWS35- 3.25 fc'120	25	0	0	Substrate Failure	2.5 MPa bond strength
	10 4	200 0	100 0	150	NSC fc'37	-	-	Rough	EA10LWS35- 3.26 fc'120	38	0	0	Substrate Failure	2.6 MPa bond strength
	10 5	200 0	100 0	150	NSC fc'37	-	-	Rough	EA10LWS35- 3.27 fc'120	50	0	0	Substrate Failure	2.2 MPa bond strength

## پوخته

له دوو سدهی رابردوودا کونکریتی (Ultra-High Performance Concrete (UHPC) ده رکهوتووه، جوړیکي تارادهیک نوییه له کونکریت که تاییهتمندی میکانیکی زور باشی هیه و له کونکریتی ناسایی باشره و له هندیک حالهتدا رکابری پولا دهکن. تاییهتمندییه سرهکیهکانی UHPC که له کونکریتی بههیزکراوی ناسایی جیای دهکاتوه بریتییه له؛ باشرهونی هیزی پهستان، هیزی کیشکردن، زیادکردنی ریشالی پولا؛ تاییهتمندی مانهوه و سهقامگیری دريژخایه به کونکریت دههخشیت. تاییهتمندییه میکانیکیهکانی UHPC ریگه به بهسه بچووکتر و تهکنتر و سووکترهکان ددهن بو ئهوهی دیزاین بکریت لهکاتیکدا هیز دهپاریزیت یان باشره دهکریت.

کاری تاقیکاری بو ئهه لیکولینهوهیه پیکدیت له سهکردن و تاقیکردنهوهی حهفده (17) قالبی کونکریتی بههیزکراوی تهخت (140\*500\*1500) ملیم که به سادیهی پشتگیری دهکریت، له ریگهی باری دوو هیلییهوه به دريژایی ناراستهی کورتهکوه باردهکریت و تاقیدهکریتوه، بو لیکولینهوه له بههیزی و ههلسوکهوتی کونکریتی بههیزکراو به UHPC.

ئهو گوراوه سرهکیانهی که لهه لیکولینهوهیهدا لیکولینهوهیان لهسر کراوه بریتی بوون له؛ نهستووری سرپوش (20-50) ملیم، سرپوشی UHPC بههیزکراو به ریژهی بههیزکردن (0-1.31) %، رووکار نهخشهکان (زبر، چهقی ناسویی، چهقی راست، چهقی پاقلوهی و چهقی لار)، هیزی پهستانی مادهی ژیرخان (20-40) MPa، ههلسنگاندنی سی جوړه ماده بو بهکارهینانی سرپوش (UHPC و HPC, NSC) و زیادکردنی پهیوهستکری میکانیکی به نهخشی رووکاری زبر ههلسنگیندرا (سفرتا سی ریز لهنگریک یان سی ریز برغی).

ئههجامهکان ناماژهیان بهوه کرد که قالبی ناویته به بهکارهینانی سرپوشی UHPC دهتوانیت هیزی کوتایی دوو هینده بکات به بهراورد لهگهل سرپوشی HPC. چینه تهکهکهی UHPC وهک رووکاری لهبرکردن تهمنی پیکهاتهی ههبوو زیاد دهکات و دوو جار تیچووی چاککردنهوه کم دهکاتوه به بهراورد لهگهل HPC. ههروهه زیادکردنی چینیکی شیشی جیگیرکراو له چینهکهی UHPC مهیلی نهوهی هیه که فشاری برین له رووکارهکدا و فشاری ناسایی له سرپوشی UHPC به ریژهی نزیکهی 30% ریکبختهوه. جگه لهوش، له کوتاییدا بههیزی زیاد دهکات لهگهل زیادبوونی پلهی زبری رووکار له نیوان دوو چین له کونکریت، و دهتوانریت پهیوهندییهکی گونجاو لهگهل ههموو رووکارهکاندا بهدهست بهینریت. هیزی کوتایی

زیاد دهکات لهگه‌ل زیادبوونی هیزی پهستان له ژیرخاندا بههوی تایبته‌مندی لکانندی و یه‌گرتوویی له رووکاره‌که‌دا. بو تهخته‌ی سه‌کو‌ی پرد که به UHPC داپوشراوه شیوازی شکست به‌ریوه‌ده‌چیت له ریگه‌ی ژیرخانه‌که‌وه له کاتیکدا هیزی به‌ستنه‌وه‌ی گونجاو دابین ده‌کریت له‌لایهن ناماده‌کردنی رووکاریکی باش، نه‌گه‌رنا، وردکردنی کونکریتی سه‌روه و دابه‌شکردنی پیکه‌اته‌که‌ی له‌گه‌ل HPC و NSC رووده‌دن. سه‌روه‌ها نه‌جامی تاقیکردنه‌وه‌کان نامازمیان به‌وه کردوه که زیادکردنی په‌یوه‌ستکری میکانیکی له‌گه‌ل ناماده‌کردنی رووکاری زبر ده‌بیته هوی زیادبوونی هیز به ریژه‌ی 50 %.

له‌گه‌ل به‌کاره‌ینانی سه‌ریوشی UHPC ، تایبته‌مندی‌یه‌کانی تهخته‌که به‌ته‌واوه‌تی به‌رز ده‌بیته‌وه، جه‌مانه‌وه‌ی ناوه‌ندی به ریژه‌ی نزیکه‌ی 50% زیاد دهکات به به‌راورد له‌گه‌ل HPC. شکستی سه‌ریوش هرگیز له‌گه‌ل سه‌ریوشی UHPC روونادات. په‌ستانی کونکریته‌که و په‌ستانه‌کانی کیشکردن به ریژه‌یه‌کی به‌رچاو کم ده‌بنه‌وه بو هه‌مان ناستی بار. سه‌ریوشی UHPC به ناماده‌کردنی دروستی رووکار ده‌بیته هوی ئه‌وه‌ی قالبی ناوخته به شیوه‌ی یه‌کپارجه‌یی ره‌فتار بکات و و باری شکست به ژیرخانه‌که‌دا تیپه‌ریت.

شیکاری ناماری له‌سه‌ر سه‌د و پینج تهخته و پرد له بیست و پینج نامازمدا پشکنینیان بو کراوه، له نه‌جامدا هاوکیشه‌ی پیشبینی پیشنیار کرا به یارمه‌تی به‌رنامه‌ی SPSS. سه‌روه‌ها شیکاری تیوری له‌سه‌ر بنه‌مای حیساب‌کردنی دیزاینی T-Beam به‌کاره‌ینر ابو پیشبینی‌کردنی نه‌جامه‌کان. له کو‌تاییدا ناماری نه‌جامه‌کان به‌راورد کران له‌گه‌ل نه‌جامه تاقیکاریه‌کان و ده‌رکوت که هاوکیشه‌ی پیشبینی‌کردن نه‌جامه باشته‌رکانی به‌خشی به به‌راورد له‌گه‌ل تیوری هاوکیشه‌که به‌هوی له‌سه‌دا به‌های که‌متر له ریژه‌ی جیاوازی و به‌های به‌رزتری په‌یوه‌ندی هوکار.





زانكۆی پۆلیته کینیکی ههولیر

---

ERBIL POLYTECHNIC UNIVERSITY